

Epithelial CCR2 promotes breast cancer progression directly and indirectly thru crosstalk with  
microenvironment populations

© 2018

Gage Adam Brummer

Submitted to the graduate degree program in Pathology and the Graduate Faculty of the  
University of Kansas in partial fulfillment of the requirements for the degree of Doctor of  
Philosophy.

---

Chair: Nikki Cheng, PhD

---

Timothy Fields, MD, PhD

---

Fariba Behbod, PhD

---

Fang Fan, MD, PhD

---

Tomoo Iwakuma, PhD

Date Defended: May 2, 2019

The dissertation committee for Gage Adam Brummer certifies that this is  
the approved version of the following dissertation:

Epithelial CCR2 promotes breast cancer progression directly and indirectly thru crosstalk with  
microenvironment populations

---

Chair: Nikki Cheng, PhD

Date Approved: May 17<sup>th</sup>, 2019

## Abstract

The presence of immune cells within a tumor is often a good prognostic indicator, but in breast cancer the presence of tumor-promoting macrophages within the tumor predicts poor prognosis. The current model by which macrophages promote tumor progression is that tumor cells secrete chemokines to recruit the macrophages to the tumor microenvironment, which then promote vascularization and invasion of the tumor cells. The most important chemokine in this process is CCL2 (also called monocyte-chemoattract protein 1). CCL2 is a chemotactic cytokine secreted by all cell types after injury or inflammation, and by carcinoma cells. Macrophages and monocytes express CCR2, the receptor for CCL2, through which they receive this chemotactic signal. Expression of CCR2 correlates with poor prognosis and advanced disease in breast cancer. The role CCR2 expression by cancer cells is unclear, as most studies have focused on the effects of macrophage CCR2 signaling in breast cancer. These studies show that CCR2 signaling promotes tumor-cell growth and invasion directly, and indirectly by affecting the tumor microenvironment to increase CCL2 levels and decrease levels of an immune-stimulating and tumor-suppressing molecule, CD154. CCR2-expressing tumors rely on the suppression of CD154 to support the tumor-promoting macrophage phenotype. Inhibiting CCR2 signaling in tumor cells significantly alters macrophage recruitment and tumor-promoting phenotype, resulting in decreased tumor growth and invasion. Here I present a novel mechanism where tumoral CCR2 signaling orchestrates M2 macrophage polarization, angiogenesis, and suppression of CD8<sup>+</sup> T cells to promote growth and invasion in breast cancers, with potential applications to immunotherapeutic regimens.

## **Acknowledgments**

To all of those who supported me throughout my studies:

Mom, Dad, Cade, Reid, Laura, Ashley, Sam, the Wetzels and Bichelmeyers

To those who have guided my journey:

Gary, Chris, Brian, Neal, Tim, Nikki

None of this work would be possible without you. Thank you all for believing in me, tolerating me, and supporting me along the way.

## Table of Contents

Abstract.....	iii
Acknowledgments.....	iv
Table of Contents .....	v
List of Figures .....	xi
List of Abbreviations .....	xiv
Chapter 1: Introduction.....	1
Clinical Overview .....	2
Biology of Breast Cancer.....	2
Mechanisms and Measures of Progression .....	3
Proliferation .....	3
Angiogenesis.....	4
Migration and invasion .....	4
Avoiding Apoptosis and survival.....	5
Stem cell renewal .....	6
Animal models: Understanding breast cancer .....	7
Classifying Breast Cancer Subtypes .....	8
Clinicopathologic subtyping.....	9
Receptor expression subtypes .....	10
Intrinsic molecular subtypes .....	10
Clinical relevance of tumor subtypes.....	11
Treating breast cancer .....	12

Surgical interventions .....	12
Chemotherapy .....	12
Targeted therapies .....	12
Immunotherapies.....	12
The Tumor Microenvironment .....	13
Tumor Microenvironment: An overview .....	13
Lymphocytes.....	14
Macrophages .....	15
Macrophages: a dichotomy revealed.....	16
Fibroblasts in breast cancer.....	18
Targeting the tumor microenvironment .....	19
Cytokines, chemokines, and their receptors.....	20
Direct effects of CD154 on solid carcinoma cells .....	24
Effects of CD154 on macrophages in the tumor Microenvironment.....	25
Effects of CD154 on T cells in Tumor Microenvironment.....	26
Effects of CD154 on other tumor microenvironment cell types .....	28
Tumor-promoting Microenvironment: CCL2/CCR2 Signaling .....	29
CCL2 – overview .....	29
Role of tumor-secreted CCL2 in breast cancer .....	29
Tumor cells secrete CCL2 to recruit tumor-promoting macrophages .....	30
Tumoral CCL2 enhances angiogenesis through macrophage dependent mechanisms.....	30
Therapeutic potential of CCL2-targeted therapies.....	31
CCR2 and breast cancer .....	32

Scientific question.....	34
Chapter 2: The role of CCL2/CCR2 suppressing CD154 expression on in vitro measures of cancer cell progression.....	36
Introduction.....	37
Materials and Methods.....	40
Cell culture.....	40
Generation of CD154 shRNA lentivirus.....	40
siRNA/plasmid reagents .....	41
Preparation of Ca-TAT complexes .....	41
3D cell culture.....	42
ELISA .....	42
Animal care and surgery .....	43
Tissue embedding .....	43
Histology/immunohistochemistry/immunofluorescence .....	44
Quantification of tumor-necrosis .....	45
Scoring of tumor invasion.....	46
Flow cytometry .....	47
Mammosphere assay.....	48
Statistical analysis.....	49
Results.....	50
Discussion.....	61
Chapter 3: Chemokine Signaling Facilitates Early-stage Breast Cancer Survival and Invasion through Fibroblast-dependent Mechanisms.....	64

Introduction:.....	65
Materials and Methods.....	67
Cell culture.....	67
Lentiviral transduction .....	67
Gene deletion by clustered regularly interspaced short palindromic repeats.....	68
ELISA .....	69
MIND model.....	69
Subrenal graft.....	69
DAB immunostaining.....	70
Immunofluorescence.....	71
Image quantification .....	71
Scoring of tumor invasion.....	72
Flow cytometry .....	73
Fibroblast proliferation assay.....	73
Statistical analysis.....	73
Results.....	75
CCR2 overexpression in SUM225 cells enhances DCIS progression .....	75
Knockdown or knockout of CCR2 in DCIS.com cells inhibits DCIS progression .....	79
CCL2 from DCIS fibroblasts is important for CCR2 mediated breast cancer survival and invasion.....	91
CCL2/CCR2 mediated invasion is associated with increased ALDHA11 and decreased HTRA2 expression.....	101
Discussion.....	106

Chapter 4: CCR2 signaling in breast carcinoma cells enhances tumor growth and invasion by coordinating cytokine-dependent crosstalk with tumor microenvironment .....	110
Introduction.....	111
Materials and Methods:.....	114
Animal care and surgery .....	114
Cell culture.....	114
siRNA and gRNA .....	115
Preparation of Ca-TAT complexes .....	115
Generation of conditioned media.....	116
Wound closure assay.....	116
Flow cytometry .....	116
Histology/Immunohistochemistry.....	117
CD154 ELISA.....	118
Macrophage infiltration assay.....	119
Live imaging co-culture assays.....	119
Ethics statements.....	120
Datamining.....	120
Statistical analysis .....	121
Results.....	122
Delivery of CCR2 siRNAs complexed to Ca-TAT peptides decreases mammary tumor growth and invasion .....	122
CCR2 targeting of carcinoma cells reduces M2 macrophage recruitment, associated with decreased angiogenesis and increased cytotoxic T cell infiltration .....	126

Intratumoral depletion of CCR2 increases expression of CD154.....	130
CD154 antagonizes CCR2 synergism to mediate tumor-cell proliferation and migration.	132
CCR2 promotes endothelial recruitment and budding is independent of CD154.....	135
Tumoral CCR2 enhances macrophage recruitment, M2 polarization associated with increased invasiveness and proliferation in co-culture assays .....	137
Epithelial CCR2 expression affects macrophage-mediated proliferation and migration of cancer cells .....	138
CD154 expression is a marker for favorable prognosis in breast cancers and correlates inversely with CCR2 expression in human breast tissue .....	141
Discussion.....	145
Chapter 5: Discussion .....	150
Summary of Results .....	151
Critical Review and Proposed Solutions.....	154
Perspective .....	158
References.....	163
Appendix.....	178
Overview of cancer and nomenclature.....	178
Normal breast structure and function.....	179
Pathogenesis of Breast Cancer.....	180
Benign diseases .....	180
Initiating a malignancy: hyperplasia .....	181
Malignancy: early growth and invasion.....	182
Metastasis: spreading to distant organs.....	182

## List of Figures

Figure 1 - Delivery of CCL2 siRNA via TAT nanoparticles significantly decreases the invasiveness of MDA-231 tumors in NOD-SCID mice .....	50
Figure 2 - CCL2 knockdown leads to increased CD154 expression in multiple human cell lines.. .....	52
Figure 3 - Efficiency of knockdown of CCL2 and CD154 by enzyme-linked immunosorbant assay of conditioned media from MDA-231 cells. ....	54
Figure 4 - The effect of CD154 on proliferation and migration of MDA-231 CCL2 KD cells....	56
Figure 5 - CD154 knockdown increases the survival of MDA-MB-231 cells in the presence of both 1 and 10 uM doses of doxorubicin over 24 hours.....	57
Figure 6 - CD154 levels correlate with mammosphere formation in MDA-231 cells. ....	59
Figure 7 - Effect of CD154 knockdown on formation of MCF10A mammospheres. ....	60
Figure 8 - CCR2 overexpression in SUM225 breast cancer cells enhances invasiveness...78	78
Figure 9 - shRNA mediated CCR2 knockdown in DCIS.com breast cancer cells inhibits invasive progression.....	81
Figure 10 - Collagen and laminin expression in DCIS.com MIND lesions. ....	82
Figure 11 - Knockout of CCR2 in DCIS.com cells significantly decreases tumor growth and invasion in the MIND model. ....	83
Figure 12 - Effect of CCR2 overexpression and knockdown on stromal reactivity. ....	85
Figure 13 - CCR2 overexpression in SUM225 MIND xenografts increases the levels of CCL2 expressing fibroblasts.....	87
Figure 14 - CCR2 shRNA knockdown in DCIS.com MIND xenografts reduces the levels of CCL2 expressing fibroblasts.....	89

Figure 15 - CCR2 knockdown alone does not significantly affect progression of DCIS.com breast cancer cells. ....	92
Figure 16 - CCR2 knockdown in DCIS.com cells inhibits fibroblast-mediated cancer progression.....	95
Figure 17 - CCR2 shRNA knockdown in DCIS.com MIND xenografts reduces the levels of CCL2 expressing fibroblasts.....	97
Figure 18 - CCL2 derived from DCIS fibroblasts is important for progression of DCIS.com breast cancer cells. ....	100
Figure 19 - CCL2 treatment of DCIS.com breast cancer cells increase ALDH1 and decreases HTRA2 expression.....	101
Figure 20 - Effect of CCR2 overexpression on ALDH1 and HTRA2 expression in SUM225 MIND xenografts.....	102
Figure 21- CCL2/CCR2 mediated DCIS progression is associated with increased ALDH1 and decreased HTRA2 expression.....	106
Figure 22 - CCR2 deficiency in DCIS.com breast cancer cells does not affect fibroblast growth .....	109
Figure 23 Ca-TAT complexes are preferentially taken up in PyVmT mammary tumor tissues. ....	122
Figure 24 Effect of intratumoral injections of TAT-Ca <sup>2+</sup> nanoparticles complexed with CCR2 siRNA on tumor growth, cellular proliferation, and apoptosis.....	124
Figure 25 - Delivery of CCR2 siRNA complexes inhibit tumor angiogenesis and enhances CD8 <sup>+</sup> T cell levels.....	127

Figure 26 - CCR2 siRNA upregulates CD154, but not CCL2, in human and mouse tumor-cell lines. ....	130
Figure 27 CCR2 has expression-level effects on proliferation and migration in murine and human breast cancer cells. ....	133
Figure 28 - CD154 neutralization and CCL2 rescues endothelial cell recruitment inhibited by CCR2 deficiency, but not endothelial sprouting, in mammary carcinoma cells.....	136
Figure 29 - CD154 rescues macrophage recruitment in CCR2 deficient mammary carcinoma cells. ....	139
Figure 30 - CCR2 expression in breast tissues inversely correlates with CD154, a marker associated with favorable survival in breast cancer patients.....	144
Figure 31 Regression-free survival of patients based on CD154, CD40 expression by subtype. ....	143
Figure 32 - Expression of CD40LG mRNA in human tissue samples correlates inversely with invasive stage and metastatic spread.....	142
Figure 33 - Mechanism for CCR2 to promote breast cancer progression through suppressing tumoral expression of CD154. ....	161
Figure 34- Normal architecture of the breast and pathogenesis of invasive ductal carcinoma...	179

### List of Abbreviations

AALAC	Assessment and Accreditation of Laboratory Animal Care
ADH	Atypical ductal hyperplasia
ANOVA	Analysis of variance test
APC	Antigen-presenting cells
BSA	Bovine serum albumin
CNS	Central nervous system
CRISPR	Clustered regularly interspersed short palindromic repeats
CTL	Cytotoxic T cell
DAB -	3,3'-Diaminobenzidine
DAPI -	4',6-diamidino-2-phenylindole
DCIS	Ductal carcinoma <i>in situ</i>
DMEM –	Dulbecco's modification of Eagle's medium
DMFS	Distance Metastasis Free Survival
EDTA	Ethylenediaminetetraacetic acid
EGFR	epidermal growth factor receptor
ELISA	enzyme-linked immunosorbent assay
ER	Estrogen receptor
FACS	flow-assorted cell sorting
FasL –	Fas ligand
FDA –	Federal Drug Administration
FVB –	Friend leukemia virus-B

GFP –	Green fluorescent protein
H&E –	Hematoxylin and eosin
HGF –	Hepatocyte growth factor
HR	Hazard ratios
IACUC -	Institutional Animal Care and Use Committee
IDC	Invasive ductal carcinoma
IgD –	Immunoglobulin D
IgG –	immunoglobulin G
IgM –	Immunoglobulin M
IHC -	Immunohistochemistry
IRB	Institutional Review Board
KLH	Keyhole limpet hemocyanin
KUMC	University of Kansas Medical Center
LPS	Lipopolysaccharide
MAPK	Mitogen-activated protein kinase
MHC	Major histocompatibility complex class
MIND –	Mammary Intraductal
MMP	matrix metalloprotease
MMTV	murine mammary tumor virus
MOM	Mouse on Mouse
MTS	(3-(4,5-dimethylthiazol-2-yl)-5-(3-carboxymethoxyphenyl)-2-(4-sulfophenyl)-2H-tetrazolium)
NEB	New England Biolabs

NFAT –	nuclear factor
NFkB -	nuclear factor kappa-light-chain-enhancer of activated B cells)
NIH –	National institutes of health
NK	Natural killer
PBS –	phosphate buffered saline
PCNA	Proliferating Cell Nuclear Antigen
PCR –	polymerase chain reaction
PDGF –	platelet-derived growth factor
PES -	polyethersulfone
PNK -	Polynucleotide 5'-hydroxyl-kinase
PR	Progesterone receptor
PyVmT	polyoma middle T
RNA	ribonucleic acid
RT	Radiation therapy
SEER	Surveillance, Epidemiology, and End Results program
SEM	Standard error of the mean
SMA	Smooth muscle actin
TAT	Trans-activator of transcription protein
TCR	T cell receptor
TDCF	Tumor-derived chemotactic factor
TNBC	Triple-negative breast cancer
TNF	Tumor necrosis factor
TNM	Tumor, node, metastasis staging system

VEGF                      Vascular endothelial growth factor

WT                      Wild-type

## Chapter 1: Introduction

## Clinical Overview

Women in the United States have a 1 in 8 chance of developing breast cancer in their lifetime. Breast cancer is the most common form of cancer in women, and is second only to lung cancer in mortality, or the number of people who die from that disease each year. Estimates predict 40,000 women will die of breast cancer in 2019. Despite major advances in breast cancer screening and the development of better therapeutic regimens, the survival rate for patients that present with distant spread or patients with recurrent breast cancer have only marginally improved. One reason for this is that breast cancer is a complex disease, and the mechanisms by which it progresses from early to late disease are not similar between all patients. The diverse mutational backgrounds of tumor cells and diversity in tumor microenvironments between tumors make predicting the behavior of any tumor difficult. Herein lies the major charge of cancer researchers today – to understand the various mechanisms by which tumors progress, and to utilize those findings to predict patient outcomes, modify current treatment regimens, and identify targets for developing new therapies.

## Biology of Breast Cancer

The first known report of a tumor was written on papyrus between 2500 and 1600 BC in Ancient Egypt, and is believed to report surgical removal of a breast tumor [1]. Many physicians and scientists devoted their careers to understanding and treating cancer, with many paradigm shifts and fundamental steps being made along the way. While earlier scientists theorized that tumors could be caused by anything from bad humors to remnant blastocysts residing in our tissues, we now understand that tumors are derived from mutated normal cells. A brief overview of cancer pathogenesis and the terminology utilized in the following manuscript can be found in Appendix: Overview of cancer and nomenclature

## Mechanisms and Measures of Progression

Cancer cells resist many of the genomic and systemic protections in place to prevent neoplastic growth. A seminal paper highlighted these six fundamental mechanisms by which cancer cells circumvent these safeguards which apply to all malignant neoplasms, called the hallmarks of cancer [2]. They describe that a neoplastic cell must: proliferate in the absence of mitogenic stimuli, be unresponsive to growth suppressive stimuli, prevent pre-programmed apoptotic signaling, sustain limitless potential for replication, recruit blood vessels for nutrients, and invade beyond their structural boundaries.

Understanding the cellular and molecular mechanisms by which normal epithelium becomes invasive neoplasms is the basis for the field of cancer research. By understanding the molecular mechanisms by which tumors form, invade, grow, and spread, we can better understand how to prevent those processes through therapeutic intervention. This section will describe the cellular and molecular mechanisms of tumor progression and means of interrogating them in the laboratory.

### **Proliferation**

Tumors grow as most living tissues do, through taking in nutrients, building macromolecules for cellular proliferation, and subsequently undergoing cellular division. Signaling pathways that promote these functions are called mitogenic pathways, for which the canonical pathway mitogen-activated protein kinase (MAPK) pathway. Cellular proliferation can be measured by counting the growth of cells over several days, using redox substrates to measure the number of

live spectrophotometrically, but more accurate methods involve staining the nuclei for cellular markers of proliferation such as proliferating cell nuclear antigen (PCNA) or Ki67.

### **Angiogenesis**

During development, intricate vascular networks form to deliver freshly oxygenated blood from the great vessels of the heart to the gas-exchanging capillaries present throughout the body.

Capillaries also allow the diffusion of macromolecular building blocks necessary for energy production and protein synthesis, as well as various serum proteins that regulate the growth of tissues. With the exception of neonatal and embryonic neoplasms, tumors develop long after this vascular network has been established. As a result, tumors must recruit blood vessels through various mechanisms. The most commonly used proteins to measure angiogenesis include VEGF and PDGF, which are secreted by various cell types to induce endothelial recruitment and subsequent vascularization.

### **Migration and invasion**

Cellular migration can be measured either individually or collectively as a mass. The most common technique to measure migration of cells involves making a uniform wound in a confluent monolayer of cells in 2-dimensional culture; an image is captured when the scratch is made and serial images are taken at application-specific time intervals thereafter. Migration is quantified by the change in the area of the wound or the distance from wound edges along the length of the wound.

Assessing invasion requires a three-dimensional scaffold. The most biologically relevant scaffold is *in vivo* tissue, where tumor tissues are excised and imaged in the same way biopsies

are taken and assessed for extent of invasion in human disease. In breast cancer, the MIND model most accurately recapitulates the natural barriers to invasion. In vitro models attempt to recreate a three-dimensional scaffold that closely resembles the molecular and physical characteristics of native tissue. The most commonly used scaffolds for this include mixing basement membrane components such as collagen II and collagen IV, fibronectin, laminin, entactin, and various proteoglycans at prespecified ratios. By suspending cells in this mixture while it is liquid, and quickly curing the protein gel through pH manipulation or heat-induced polymerization, the end product is a biologically relevant scaffold that contains uniformly interspersed cancer cells. Invasion can be quantified by live cell imaging of cellular movements, or by taking images at set end points and quantifying the length of cellular processes extending into the tissue.

### **Avoiding Apoptosis and survival**

In addition to undergoing autonomous growth, tumor cells must also constantly resist cell death as a result of chemotherapy or pro-apoptotic signaling. Normal cells are programmed to self-destruct when they sense that DNA damage, organellar damage, or viral infection has occurred. If cells sense mitotic damage at either of the cell cycle checkpoints, p53 or Rb will prevent cell cycle from progressing. If the damage is too severe, a programmed cell suicide program is initiated, in which Bcl2 family proteins recruit caspase enzymes to destabilize the mitochondria, flooding the cytoplasm with calcium, leading to activation of multiple proteases and nucleases that ultimately cause an organized self-destruction of cell. Cancer cells avoid this by mutating the proteins critical for the checkpoints to control proliferation, or by overexpressing antiapoptotic proteins. The most common method of examining apoptosis is measurement of

cleaved caspase 3, which has benefits over other methods because it stains for a downstream product of apoptosis initiation, rather than measuring cell death in general.

### **Stem cell renewal**

Cancer stem cells (cancer stem cells) represent a tiny fraction of a tumor population, but are responsible for some tumors ability to lay dormant for decades and successfully metastasis thereafter. Cancer stem cells (CSCs) are defined as cells that are capable of generating a tumor that is phenotypically similar to its parent tumor; has the ability to self-renew by maintaining pluripotency even after multiple rounds of cellular division, and generation of daughter cells with proliferative capacity but without self-renewal capacity[3]. The search for cancer stem cells in breast cancer has focused on identifying cellular markers that enrich populations for self-renewing stem cells. One of the earliest stem cell populations in breast cancer is the CD44(high)/CD24(low) group, which was identified after phenotypically sorting primary breast cancer cells from 10 patients and injecting them into immunocompromised mice[4]. Cells isolated from this population show enhanced metastatic and invasive potential [5]. By screening for the expression of proteins that are present in both progenitor populations and subsequently transplanted populations, ALDH1 was also identified as a marker for stem cell renewal[6]. CD24/CD44 staining is often done by flow cytometry, as it allows for high throughput analysis and gating of the stem cell population. Aldehyde dehydrogenase activity assays can function similarly, where high activity of ALDH1 results in a fluorescent or luminescent product to form intracellularly, which can be subsequently imaged. It is thought that by targeting these cancer stem cells directly, the ability of a tumor to grow or recur will be greatly diminished.

### **Animal models: Understanding breast cancer**

Through the use of various animal models of breast cancer, effects of intervention can be analyzed at any step in the disease process. By using immune-compromised mice, studies on immune-independent mechanisms can be investigated, and human cell lines can be engrafted without rejection. By utilizing immune-competent models, cell lines of the same genetic background must be used to avoid rejection, but immune-tumor interactions can be studied.

Described below are the models used in these studies:

Subrenal capsule model - Mammary carcinoma cells grafted in the subrenal capsule form tumors similarly to orthotopic injection [7, 8]. Unlike injecting into the stroma-rich mammary gland, the subrenal capsule space is devoid of fibroblasts and is immunologically privileged, enabling us to determine the relative contribution of co-grafted fibroblasts without interference from host stroma.

Orthotopic injections – As a major goal of animal studies is to recreate as close to a human model of disease as possible, it is necessary to recreate as close as possible the pathogenesis of normal disease. Many mouse models of cancer have been developed with this necessity in mind, and attempt to inject cancer cells into their structure of origin. In breast cancer, the most often used orthotopic model involves injecting cancer cells directly into the mammary fat pad. While this model produces tumors that are located within the mammary gland, as the previous chapter alludes, it bypasses formation, transformation, early growth and invasion, and jumps directly to invasive disease. For this reason, a superior model that more relevantly mimics breast cancer progression was developed.

Closer to the clinic: the MIND model - The Mammary Intraductal (MIND) model of breast cancer was developed in 2009 to more closely the pathogenesis of IDC as an orthotopic model than fat pad injection [9]. Fat pad injection bypasses the invasive phase of cancer progression and allows the tumor direct access to the stroma and vasculature. Intraductal injection, on the other hand, more accurately recapitulates the natural process of invasive disease development, where the lesion first fills the lumen of the duct and then may or may not invade past the myoepithelial layer into the surrounding stroma. Recent studies have shown that the MIND model more accurately replicates the metastatic homing of breast carcinoma cells and maintains the molecular subtype of xenografts better than fat pad injections [10]. For these reasons, this study will utilize the MIND model to more accurately assay the effects that CCL2/CCR2 signaling has on tumor progression.

### Classifying Breast Cancer Subtypes

The treatment plan and outcomes for patients with breast cancer can vary widely, with some tumors needing nothing more than annual monitoring and others extensive surgical, radiologic, and pharmacologic interventions. This clinical variety is a product of the heterogeneity of IDC on a molecular level. To better predict the outcome and treatments necessary for a patient, classification systems were developed to find subtypes and the behaviors and vulnerabilities of those subtypes. Increasingly sophisticated methods have developed over the years, and a major research goal in breast cancer research is finding better therapeutic targets

and prognostic predictors. to the identification of receptor subtypes by IHC and in-situ hybridization, to the more detailed genetic approaches that have developed most recently.

**Clinicopathologic subtyping** – Once diagnosed, breast cancer is subdivided and described by 3 major measures: the histologic subtype, the grade of the cancer cells, and the clinical stage of the cancer. Histologic subtyping is decided by pathologists by microscopic examination of tumor tissue. Pathologists classify tumors by their epithelial origin as ductal or lobular, and by whether the basement membrane is intact. If the lesions are contained within the basement membrane, it is called *in situ* (in its original place<sup>1</sup>). If the carcinoma cells have compromised the basement membrane and entered the surrounding stroma, they are invasive. Invasive lobular carcinomas are less aggressive than IDCs Ductal carcinoma accounts for over 80% of invasive carcinomas of the breast, and 85% of *in situ* breast carcinomas (DCIS). IDC can be subclassified as tubular, mucinous, or medullary based on appearance. Ductal carcinoma variants usually predict good prognosis, as they are usually more differentiated than other carcinomas.

The level of differentiation, or how closely the carcinoma cells resemble the cells and structures of origin, is what dictates tumor grade. Grading is scored on a scale of I-IV, with I being well-differentiated and IV being poorly differentiated. The anatomic characteristics of the tumor dictate the TNM staging, which stands for tumor (size and spread), nodal involvement, and metastasis. This staging system has been used to document tumors for decades and shows has a high value when predicting prognosis. This system does not, however, take into the underlying molecular diversity that anatomical observation cannot provide.

---

<sup>1</sup> Merriam Webster Dictionary, s.v. “In situ”

### **Receptor expression subtypes**

The existence of receptor status subtypes is due to the development of estrogen-antagonizing therapy and Her2 antagonizing therapies. This simple classification scheme is still relevant today, and is part of the standard diagnostic workup for breast cancer patients. In order for estrogen-targeted or Her2-targeted therapies to have any efficacy, the cancer cells must express the receptor corresponding that therapy. The efficacy of these targeted therapies justifies the use of this basic subtyping for nearly all patients at diagnosis. Tumors are simply referred to as ER-positive, Her2-positive, or triple-negative if they have no receptor expression. For patients with triple-negative disease, the only systemic therapy available for all patients is chemotherapy.

### **Intrinsic molecular subtypes**

Prior to 2000, prognostic clinical attributes and receptor expression dictated tumor treatment and classification. In the last two-decades, however, advances in gene expression analysis enabled researchers to classify tumors at the molecular level, revealing intrinsic molecular profiles that better predict tumor behavior and treatment response.

The breakthrough study in this new field of molecular profiling utilized gene expression analysis from 65 samples derived from 42 patients. Hierarchical clustering analysis revealed 4 specific subtypes of breast cancer based on their expression of genes associated with tumor phenotypes [11]. These subtypes clustered closely with receptor subtype – luminal epithelial ER+, Her2-overexpressing, basal-like (triple-negative), and normal breast (largely grouping with ER+ breast cancers). In 2001, these findings were reproduced as 78 additional tumor samples also expressed one of these distinct gene sets [12]. This study also identified a subclass for the luminal group, termed “luminal A” and “luminal B”. The fidelity of these subtypes was

demonstrated in 2003, when independent gene expression data from 117 tumors also found these 5 distinct subtypes.[13]

In 2009, a new classification was developed that combined hierarchical expression clustering with copy number analysis to identify 10 distinct subtypes by integrative clustering [14]. They applied this approach to 1992 tumor samples and found ten distinct subtypes utilizing an integrative clustering algorithm; these subtypes were aptly named IntClust 1-10. The IntClusts map closely to the expression of hormone receptors, but the complex subtypes allow more accurate predictions of prognoses and therapeutic efficacy.

### **Clinical relevance of tumor subtypes**

Tumor classification systems are developed to predict tumor behavior and improve patient outcomes. Receptor classification dictates whether or not a patient would benefit from estrogen antagonizing therapies or Her2-targeted treatments, and combined with clinicopathologic data can predict patient prognosis as well. However, intrinsic subtyping revealed the range of tumor phenotypes that can exist within ER+, Her2+, or triple-negative breast cancers. However, the detailed genetic profiling performed to develop these classification systems is not yet clinically feasible. To overcome this barrier, several groups and companies have developed truncated gene sets that accurately predict intrinsic subtype. The PAM50 gene set, consisting of 50 genes that cluster most strongly with receptor status, has shown clinically useful in predicting both patient outcome and response to chemotherapy, and is currently used to guide treatment decisions for patients[15]. The clinical utility of molecular subtypes is still being realized, but it has and as a result, therapeutic options and goals[16].

## Treating breast cancer

**Surgical interventions** – The first therapy for breast cancer (and many other cancers) was surgical removal of the tumor, often resulting in complete removal of the breast. Surgical options today are still front-line therapy for surgically resectable disease, and the development of breast-conserving therapy has decreased the trauma associated with breast disease.

**Radiation therapy**– Radiation therapy (RT) is a commonly used modality for more advanced breast cancers. For women with positive nodal status, radiation therapy improves survival outcomes compared to women who do not receive RT. [17]

**Chemotherapy** – The use of chemotherapeutics as an adjuvant therapy in breast cancer has long been commonplace for more advanced breast cancer patients. For years it was the only systemic medication class available for triple-negative or basal-like breast cancers. Chemotherapeutics are cytotoxic agents that target cancer cells based on their increased metabolic needs and proliferative rate compared to normal tissues. Recently, the use of chemotherapy + endocrine therapy in ER+ breast cancer was shown to be noninferior to endocrine therapy alone in patients with node-negative disease.

**Targeted therapies** – For patients with ER+ breast cancer, estrogen-antagonizing therapies are effective. Estrogen is targeted either by direct competition of estrogen with the site, or through aromatase inhibiting drugs that inhibit the peripheral conversion of hormones to estrogen. For patients with Her2+ tumors, growth-factor-receptor-targeting antibodies have been a breakthrough, providing significant clinical relief compared to chemotherapeutics.

**Immunotherapies** – While writing this dissertation, the first targeted immunotherapy has been approved for the treatment of advanced triple-negative breast cancer. Based on findings from the

Impassion trial (trial NCT02425891), there was a 3 month increase in median progression free survival, with a hazard ratio of 0.48 to 0.77 for patients in the anti-PDL1 arm of the trial. This is the first immunotherapeutic approved by the FDA for bresat cancer.

## The Tumor Microenvironment

### **Tumor Microenvironment: An overview**

Once thought of as a mass of rapidly proliferating cancer cells, the tumor is now known to harbor a diverse population of cells. Tumors are a heterogenous mixture of cancer cells, fibroblasts, immune cells, endothelial cells forming blood vessels, platelets, erythrocytes, adipocytes, and neurons. The phenotype of these various cells dictates tumor behavior and disease progression. Non-tumor cells in the microenvironment can produce tumor-promoting and tumor-suppressing effects. For example, macrophages express pro-inflammatory cytokines and contribute to a cytotoxic response if activated by IFN- $\gamma$  (termed M1 macrophages). However, if activated by IL-4, these same macrophages will express cytokines and growth factors to promote wound healing and repair (termed M2 macrophages) [18]. The accumulation of M2 macrophages facilitates angiogenesis and metastasis, and predicts poor outcome in breast, lung, and ovarian cancer patients [19].

Tumor cells are thought to influence their microenvironment through complex interactions with stromal cells via cell-surface receptor expression and secretion of proteins such as cytokines and growth factors; however, these mechanisms are still poorly understood. Understanding the mechanisms by which certain tumor recruit tumor-promoting

microenvironments could enable therapies that target the tumor as a whole, rather than the tumor cells alone.

## **Lymphocytes**

The immune system protects the body's various organ systems from harm, and can remember previously encountered threats. The 2 major classes of lymphocytes are T lymphocytes and B-lymphocytes. The most common lymphocytes are CD4<sup>+</sup> helper T cells and cytotoxic CD8<sup>+</sup> cells, though many other cell types do exist. Cytotoxic CD8<sup>+</sup> T cells (CTLs) and natural killer cells (NK cells) monitor somatic cells for mutations and malignancy by scanning for abnormal proteins. T lymphocytes function to survey the circulation and tissues for abnormal or foreign proteins via their T cell receptors (TCRs), a protein that is unique for each T-lymphocyte and designed to recognize a specific antigen.

CD4<sup>+</sup> T cells are the helpers of the immune system, and more specifically, they assist T cells and B cells in receiving the correct signaling required to proliferate, activate, and perform their cytotoxic functions. Many of their functions occur in conjunction with antigen-presenting cells, such as dendritic cells, to help cytotoxic T cells recognize their antigens being presented. CD4<sup>+</sup> T cells are classified into Th1 and Th2 subclasses, which are functionally distinct. Th1 cells promote a cytotoxic T cell response that is important for anti-tumor immunity, whereas Th2 cells promote a humoral immune response that favors B cell activation and M2 macrophage polarization[20]. The Th1 subtype express IL-2 and IFN-gamma. IL-2 stimulates T cell activation and can overcome checkpoint inhibition by PDL1, while IFN-gamma stimulates M1 macrophage activation and antigen presentation [21]. The Th2 subtype expresses IL-4, IL-6, and

IL-10 to promote M2 macrophage polarization, inhibit CTL function, and generate T regulatory cells.

CTLs recognize and kill non-self cell types, including bacteria, virally-infected cells, and tumor cells, if their TCR recognizes an antigen presented by MHC-I molecules. CTLs must receive a co-stimulatory signal from the cell presenting the antigen or a CD4<sup>+</sup> T cell in order to activate. Of interest, CD40-CD154 is a co-stimulatory pair of molecules. CD154 on the surface of CD4<sup>+</sup> helper T cells helps maintain the survival of memory cytotoxic T cells. CD154 can be cleaved to a soluble form, which is also capable of providing co-stimulation of CTLs independently of an antigen-presenting cell or CD4<sup>+</sup> T cells[22]. If a T cell both recognizes MHC-bound antigens and receives a co-stimulatory signal, they induce cellular death of that target cell by forming pores in their membrane and injecting them with hydrolytic enzymes.

CD19<sup>+</sup> B cells secrete immunoglobulins upon recognition of their antigen, which mainly function to clear acellular toxins and contaminants from the blood and mucosa. As most durable anti-tumor immune responses require recognition of a cytoplasmic antigen, B cells have not been as well studied as CTLs in immune surveillance.

## **Macrophages**

Macrophages are a highly heterogeneous population that are widely distributed throughout the body. Macrophages are a critical part of the innate and adaptive immune system. In the innate immune response, they phagocytose debris and pathogens non-specifically by recognizing bacterial and viral molecular patterns via toll-like receptors. They facilitate adaptive immunity by presenting antigens to lymphocytes via their MHC class II molecules. They are recruited to sites of inflammation and injury via chemokine receptors including CCR2. At the site of injury

or inflammation, they coordinate the recruitment and activity of effector cells. Primary deficiencies of macrophages are rare in humans [23].

Monocytes, precursor cells to mature macrophages, circulate in the blood. Monocytes originate from common myeloid progenitor cells in the bone marrow, which also produce dendritic cells and osteoclasts, upon stimulation with granulocyte-macrophage colony stimulating factor (GM-CSF), macrophage-colony stimulating factor (M-CSF), and other fate-determining cytokines such as IL-3, KIT, and various tumor necrosis family molecules. These monocytes then extravasate from circulation throughout the body to become resident macrophages, where they respond non-specifically to foreign bodies (such as bacteria) or sterile-insult (trauma) to orchestrate an appropriate immune response. Once matured, macrophages terminally differentiate depending on the microenvironment of the organ/site of injury.

The role of macrophages in protecting the few organs for which they have been specifically named serve to illustrate their diverse role in regulating inflammation. Alveolar macrophages in the lung are primed to produce a strong pro-inflammatory response upon activation by foreign bodies[24], whereas in the central nervous system (CNS) their function as microglia is to maintain an anti-inflammatory microenvironment to prevent inflammatory damage to nerves[25]. Langerhans cells, mature skin macrophages, must first promote inflammation to facilitate clearance of damaged or infected tissue, and then switch to turn off the immune response and facilitate blood vessel growth and tissue remodeling.

### **Macrophages: a dichotomy revealed**

Researchers created the M1/M2 classification scheme after realizing a differential arginine metabolism by macrophages activated in a Th1 immune background versus

macrophages activated in a Th2 environment. Th1-derived macrophages are “classically activated”, and are called M1 macrophages. M1 macrophages utilize arginine to produce nitric oxide for killing of phagocytosed pathogens and malignant cells. Th2-derived macrophages are “alternatively activated,” and called M2 macrophages. M2 macrophages express arginase and produce ornithine, which is a precursor for various pro-inflammatory leukotrienes and cytokines characteristic of M2 macrophages [26]. M2 macrophages also produce a variety of cytokines that inhibit M1 phenotype and cytotoxic responses including IL-4 and IL-10.

The pro-inflammatory phenotype is known as the “classically activated” or M1 macrophage, and is characterized phenotypically by IFN-gamma receptor activation, and expression of the pro-inflammatory cytokines IL-6, TNF, and IL-1. These macrophages engulf damaged or foreign contaminants (e.g. bacteria, fungi, silica, etc.), present antigens to T- and B cells, and activate a cytotoxic adaptive immune response. Re-education back to an M1 phenotype has shown promise at both controlling the growth of tumors and increasing immune surveillance [27]. M1 macrophages express high levels of major histocompatibility complex class II (MHC II), which allows them to present antigens to T cells, as well as iNOS,

M2 macrophages, on the other hand, act to suppress the immune response and secrete pro-inflammatory and angiogenic cytokines. M2 macrophage activation occurs physiologically in response to fungal cells, parasitic infections, immune complexes, and the Th2 cytokines IL-4, IL-13, IL-10, and TGF-beta. M2 macrophages secrete large amounts of IL-10, which functions to suppress NF-kB signaling and cytokine secretion [28]. M2 macrophages also suppress antigen presentation and activation of helper T cells by downregulating M1 macrophage polarization and from a Th2 immune background[29]. M2 macrophages are the predominant subtype in breast cancer, and have been shown to facilitate angiogenesis, facilitate invasive migration thru

secretion of matrix-metallo-proteinases, and even initiate malignant invasion [30-32]. Of particular interest to the studies presented here, is that CCL2 secreted by tumor cells recruits and maintains M2 macrophages [33].

Many recent studies illustrate that macrophages do not fall discretely into one of these two categories[34]. For example, though classically an M2 macrophage marker, arginase has also been found to expressed in M1 macrophages and resident macrophages [35]. The plasticity of macrophage function led to more nuanced categorization of macrophage activation, where the M1 and M2 subtypes are further divided. In this scheme, M2 macrophages can be divided into M2a, M2b, M2c, etc. These different subgroups are defined by which immune cells and markers activate the macrophage [36]. However, this has led to significant confusion, as different research groups define these macrophages subsets differently, and has led to suggestions that macrophages be defined by the activating stimulus, such as M(IL-4) or M(IL-10) [37]. Macrophage activation and its effect on human disease is thus as evolving field, and these categorizations statuses are beyond the scope of this work (for a contemporary review, see [34]). Thus, the studies herein will focus on the most basic categorization of macrophages as M1 or M2.

### **Fibroblasts in breast cancer**

Present in most epithelial organs of the body, fibroblasts play a major role in tumor development and progression. Normally, fibroblasts maintain the architecture of organs by secreting extracellular matrix proteins such as collagen and fibronectin, and regulate epithelial growth during wound healing and development and are referred to here as normal-associated fibroblasts (NAFs). By these same mechanisms, fibroblasts in the tumor microenvironment can

promote the growth, invasion, and metastasis of cancer cells. Fibroblasts that promote tumor growth and invasiveness are termed tumor-associated fibroblasts (TAFs), and can constitute 80% of the fibroblast population within a tumor [38]. NAFs and Cancer-associated fibroblasts (CAFs) have opposing roles in tumor initiation. For example, when co-grafted with prostate cancer cells, CAFs stimulate cancer cell proliferation and growth, whereas co-grafted NAFs do not promote tumor growth[39]., How one cell type can have such diametric roles in tumor development is important to understand, because attenuating/reversing tumor-promoting phenotypes in the tumor microenvironment could lead to therapeutic responses in cancer patients.

### **Targeting the tumor microenvironment**

To stimulate or inhibit tumor development, stromal cells (i.e. fibroblasts, macrophages, etc.) must be able to interact with the cancer cells. Stromal cells do so by expressing various proteins, both membrane-bound and soluble, which interact with receptors on carcinoma cells. These proteins can stimulate or inhibit tumor-cell growth. For example, interferons secreted by dendritic cells in the tumor microenvironment induce apoptosis in cancer cells and increase their immunogenicity; but factors like FGF7 secreted from TAFs stimulate tumor growth [40, 41]. From a therapeutic standpoint, the molecules that are most interesting are those with potent effects on both the tumor cells and the microenvironment. To have the greatest anti-tumor effect, the ideal molecule would inhibit the growth of the tumor cells, polarize plastic cell types (i.e. fibroblasts, macrophages) to be tumor suppressive, and cause a sustained immune response to the cancer. A major class of proteins with these characteristics is the cytokine family.

## **Cytokines, chemokines, and their receptors**

The term cytokine describes a broad class of small 5-20kd proteins that act through receptors to send immunomodulatory signals between different cells. Within this broad class are chemokines, interleukins, tumor-necrosis factors, interferons, and lymphokines. These cytokines were classically named for their major function or source, i.e. interleukins are mainly produced by leukocytes to signal to other leukocytes; interferons are involved in antiviral responses and *interfere* with viral reproduction.

The main functions of cytokines are to maintain a balanced immune response through migratory, stimulatory, and inhibitory signals between immune cells and other normal cell types. A single cytokine can elicit vastly different responses depending on the context, as the functions of cytokines often synergize or antagonize other cytokines. The effect of cytokines on cells are redundant, wherein different cytokines can all elicit a particular response (i.e. increase T cell activation). Cytokines are also pleiotropic, meaning a single cytokine can produce a diverse range of effects on various cell types. All of these characteristics allow the relatively small number of cytokines to fine-tune the immune response based on tissue and stimulus, but also make them particularly difficult to study.

Within this broad class, the chemokine subclass is the largest with an estimated 50 ligands and over 20 receptors. Chemokines are small soluble signaling proteins with conserved cysteine residues necessary for their proper folding [42]. Chemokines are structurally named based on the location of the first 2 cysteine residues of the 4 chemokine classes: C, CC, CXC, or CX<sub>3</sub>C [43]. The X represents the number of intervening amino acids between the cysteine residues; in the case of the C class, there are only 2 residues at C and N-terminal ends of the molecule[43, 44]. Most chemokine receptors are G-protein coupled receptors (GPCRs), and

demonstrate biased agonism in their downstream signaling, which allows for a single type of receptor to activate different signaling mechanisms in a context-dependent manner [45]. The diverse outcomes of chemokine signaling is further expanded by the significant overlap in binding affinity between receptors and ligands within the class. Furthermore, chemokines can be immobilized by extracellular glycosaminoglycans, which can further modulate the intensity and character of the downstream signaling[46]. This complex network of possible signaling outcomes explains the diverse functional outcomes of chemokine binding

## Tumor-suppressing microenvironments: the role of CD154

### **CD154 and CD40 structure and function**

One molecule with these characteristics is CD154. CD154, also known as CD40L, is a 39-KD transmembrane glycoprotein in the tumor necrosis factor (TNF) superfamily. Its gene generates a 13 kB fragment that shares 80% homology with murine CD154[47, 48]. The gene for CD154 encodes a 2.3 kb transcript with 5 exons and 4 introns encoding 261 amino acids (aa's) [49]. The majority of the protein is the C-terminal extracellular portion (215 aa's), accompanied by a small transmembrane (24 aa's) and N-terminal intracellular portion (22 aa's) [49]. CD154 gene expression has been shown to be regulated by the calcium ionophore and nuclear factor of activated T cells (NFAT) in T lymphocytes, however, its regulation in other cell types is poorly understood [50] [51]. The membrane bound form of CD154 can also be cleaved to form a biologically active soluble form consisting of residues 113-261[52]. Membrane-bound CD154 is cleaved by metalloproteases upon activation of platelets and T cells, and cleavage can be inhibited by metalloproteinase inhibitor KB8301 [53]. Cleavage can occur intracellularly prior to vesicular release, or cleaved from the membrane upon binding its receptor CD40[54, 55]. Many truncation products exist for CD154, with a 38, 31, 18 and 14 kDa form being reported [56, 57].

CD154 binds its primary receptor CD40 with highest affinity, though it has also been reported to bind to integrin-family proteins [58], [59]. CD40 is a TNF-family receptor, consisting of a 151 amino acid extracellular domain, a small 22 amino acid transmembrane domain, and a cytoplasmic signaling domain of 62 amino acids. The extracellular and transmembrane domains are highly conserved between CD40 and other TNF-family receptors, but its cytoplasmic

signaling domain is unique [57, 60]. Crystal structure shows that CD154 binds to CD40 in a 3:2 ratio, which induces recruitment of TRAF proteins that facilitate signaling through various signaling cascades including p38, Erk, and JNK-dependent signaling [61].

CD154 induces apoptosis in carcinoma cells, depletes tumor-promoting stroma, and stimulates anti-tumor immune responses.. Its receptor is CD40, a 48-KD transmembrane TNF-family receptor [58]. CD154 is normally expressed on the surface of helper T cells, and CD40 is expressed highly by antigen-presenting cells (APCs). CD40 is also found on fibroblasts, endothelial cells, and epithelial cells throughout the body. When the TCR on a T cell recognizes an antigen presented by an APC, membrane-bound CD154 on the T cell engages with CD40 on the APC and provides a co-stimulatory signal. This co-stimulatory signal “licenses” the immune response, and induces proliferation and activation of the APC. B cells, dendritic cells, and macrophages are all APCs [62].

In B cells, activation of CD40 by CD154 results in immunoglobulin isotype class-switching, a process necessary in the production of monomeric antibodies. Mutations in CD154 or CD40 results in hyper-IgM syndrome in humans, where B cells are not able to switch from IgM to IgD, IgE, or IgG, which immunocompromises hosts and increases susceptibility to opportunistic infections [63]. The first hint that CD154 plays a role in cancer came from hyper-IgM patients. Indeed, patients with mutations in CD154 or CD40 have increased rates of carcinomas and sarcomas relative to the general population [63]. The role of CD154 in cancer gained much more interest when it was discovered that CD40 is expressed at high levels on the surface of many carcinoma cells[64]. Over the last 20 years, this has led to a whole field of research into the role that CD154 plays, both directly and indirectly, on the development and progression of cancer. Ongoing research indicates that CD154exerts direct inhibitory effects on

carcinoma cells themselves, and reshapes the tumor microenvironment to be more tumor suppressive. These findings are discussed below.

### **Direct effects of CD154 on solid carcinoma cells**

The presence of CD40 on the surface of many carcinoma cell lines led to investigations on the effects of CD154 treatment of these cells. Human breast tumors express CD40 at higher levels than normal ductal epithelium, making it a good target to selectively target carcinoma cells [65]. Although CD154 causes activation and proliferation of immune cells, CD154 induces growth arrest, apoptosis, and decreased motility in CD40-expressing carcinoma cells [66]. Breast cancer patients with high mRNA levels of CD154 experience longer survival; this effect is strongest in subtypes with higher propensity for metastasis [67].

CD154 can decrease the proliferation of cancer cells, and in some cases, induce their apoptosis. CD40-expressing breast cancer cells have suppressed proliferation in the presence of soluble CD154 and membrane-bound CD154, with the membrane-bound form being more potent [68]. Soluble CD154 selectively decreases the proliferation of malignant urothelial carcinoma cells, but not normal urothelial epithelium, showing a selective effect of CD154 on malignant cells. In addition, membrane-bound CD154 induces apoptosis in malignant cells, once again showing that its membrane-bound form is more active than the soluble form [69]. CD154 also has growth-inhibitory effects in ovarian, pancreatic, and cervical carcinomas [70-72].

In addition to its direct cytotoxic effects, CD154 also makes carcinoma cells more susceptible to chemotherapy and apoptosis-inducing agents. Ovarian carcinoma cells undergo apoptosis in a caspase eight and caspase-3 dependent manner in the presence of both FasL and soluble CD154 [69]. Mouse models of melanoma and neuroblastoma showed that the use of

CD40-agonistic antibodies synergized with chemotherapy in reducing tumor burden [73].

Another study found overexpressing CD154 on CD40-positive bladder, ovarian, and cervical carcinoma cells potently decreases their proliferation, and amplifies the cytotoxic effects of 5-fluoruracil, cisplatin, and mitomycin C [74]. These findings have led to combination therapies for human disease. For example, a phase I trial treating pancreatic carcinoma patients with agonistic-CD40 antibodies and gemcitabine resulted in a synergistic response. This study showed the efficacy of CD154 in treating human disease, along with several other phase I trials in cancer. These researchers found that in mouse models of pancreatic carcinoma, CD40-agonism increased cytotoxic M1 macrophages, suggesting that CD154 could re-educate resident macrophages from tumor-promoting to tumoricidal [75]. Indeed, one study shows CD154-expressing cancer cells are attacked by M1 macrophages and cytotoxic T cells [76].

### **Effects of CD154 on macrophages in the tumor Microenvironment**

Indeed, many other studies suggest that CD154 is capable of polarizing macrophages toward an M1 phenotype thus creating a hostile microenvironment for cancer cells. Monocytes incubated with 3LLSA murine lung cancer cells engineered to overexpress CD154 resulted in the production of nitric oxide, TNF-alpha and IL-12 [77]. These cytokines are associated with an M1, tumoricidal macrophage phenotype and facilitate strong cytotoxic responses. Additional studies in mice indicate that CD154-based therapies result in M1 polarization and tumoricidal responses *in vivo*. Treatment with CD40-agonistic antibodies decreases the function of T cells and NK cells in C57BL/6 mice, but prime macrophages for stimulation by LPS and polarized tumor-associated macrophages to an M1 phenotype [73].

In an orthotopic model of renal cell carcinoma, co-treatment with IL-2 and agonist anti-CD40 reduces metastasis; this is associated with decreased MMP expression in the tumor microenvironment, and a substantial polarization toward the M1 phenotype [78]. Moreover, CD40-agonistic antibodies work independently of T cells, B cells, and NK cells at delaying the progression of NXS2 neuroblastoma lesions in immune-compromised mice. Delivery of anti-CD40 increases the survival of tumor-bearing mice, and increases IL-12 expression. B16F10 melanoma and TS/A mammary adenocarcinoma cells transfected with CD154 induce an immune response in cancer cells and complete rejection of tumor cells compared to mock phage controls. Over a month later, the mice rejected control cells as well, suggesting that CD154 expression by carcinoma cells enables immune memory against that tumor [74].

These *in vitro* and *in vivo* studies show that CD154, exogenously applied or expressed on the surface of carcinoma cells, has profound effects on macrophage phenotype. The mechanism for this effect likely involves CD154-induced intratumoral cytokine expression, particularly IL-12. IL-12 then polarizes resident macrophages toward an M1 phenotype, resulting in tumor-cell death and a strong immune response. Although a few studies indicate macrophages alone respond sufficiently to affect tumor progression, the strength and durability of this immune response suggest that components of the adaptive immune system could play a role as well.

### **Effects of CD154 on T cells in Tumor Microenvironment**

Several studies indicate that CD154 is capable of stimulating a durable immune response through T cell dependent mechanisms. MB49 bladder carcinoma xenografts engineered to overexpress CD154 were rejected in immune-competent mice, but not athymic mice, suggesting a role for T cells in CD154-dependent tumor rejection. T cells are necessary for the observed

anti-tumor function of CD154, they also found that CD154 overexpression by MB49 cells results in less suppressive myeloid cells, defined as CD11b<sup>+</sup>/Gr-1<sup>high</sup>[79]. This study suggests that macrophages and T cells work synergistically to eradicate cancer cells when exposed to CD154. Whatever the mechanism of initial tumor regression, several studies have shown that long-term cancer immunity is through T cell dependent mechanisms.

Most studies which implicate T cells in CD154-induced immunity have used therapeutic, nonreplicating viruses to induce the production of CD154 on cancer cells. One study showed that murine CT-26 colon cancer cells transduced with CD154-adenovirus were eliminated in a CD8<sup>+</sup> T cell-dependent manner from mice. This anti-tumor immunity is systemic, as CD154-adenovirus injected in only one tumor site results in rejection of distant tumor sites as well. The anti-tumor immunity was durable, as CT-26 cells not overexpressing CD154 when challenged 30 days later were also rejected [80]. CD154 gene therapy also induced a long-lasting, systemic T cell response in rats injected bilaterally with RCN-9 metastatic rat liver cells. Like in the study with CT-26 cells in mice, injecting adenovirus vector-expressing CD154 into just one tumor resulted in rejection of the contralateral tumor as well [81]. The reason for the immunity observed in these tumors is likely due to increased activation of APCs by CD154, combined with a flood of tumor-associated antigens from CD154-induced tumor-cell death, resulting in robust cytotoxic T cell activation and replication [82]. These findings are promising, because they suggest that CD154 is capable of mediating a diverse and sustained immune response to cancer cells.

### *Effects of CD154 on other tumor microenvironment cell types*

The role of other tumor microenvironment cell types has been studied as well, but to a lesser degree than immune cells. In the study on pancreatic cancer in patients and mice discussed above, investigators showed that delivery of CD40-agonizing antibodies resulted in decreased collagen I content of murine pancreatic tumors [75]. Because tumor-associated fibroblasts are the main contributor of collagen type I, it can be conjectured that M1 macrophages reduce the number of TAFs or repolarize them to NAFs. CD40 is expressed on fibroblasts, and treatment of NAFs with CD154 results in increased proliferation and cellular adhesion molecule expression [83]. These studies suggest that CD154 can influence the behavior of fibroblasts, but no studies have explored how CD154 affects CAFs. More studies are needed to understand the role that CAFs play in the CD154-mediated cancer response.

Platelets are another contributor to the tumor microenvironment, and are worth investigating in the context of CD154-based therapies, because they are possibly the single largest reservoir of CD154 in the blood [84]. Upon activation, platelets express membrane-bound CD154. If activated for an extended period of time, the CD154 will be cleaved in a MMP-dependent manner to produce the less tumoricidal, soluble form of CD154 [85]. However, the role of platelet-bound CD154 is unclear, as activation of platelets and thrombosis are generally found to be beneficial to tumor cells, protecting them from immune evasion and resulting in increased metastasis, among other roles [86, 87].

## Tumor-promoting Microenvironment: CCL2/CCR2 Signaling

### **CCL2 – overview**

CCL2 is the prototypic chemokine of the CC family and the first characterized in its subclass. CCL2 is also as monocyte-chemoattractant protein 1, which usefully describes its most well-known function [88]. CCL2 has significant amino acid homology to CCL7, CCL8, CCL13, and CCL12, all of which have identical location of their cysteine residues [43]. Knockout of CCL2 or CCR2 in mice produces viable offspring with normal levels of all immune cells, but with near complete inhibition of macrophage recruitment to sites of inflammation [89]. In its physiologic role, CCL2 is secreted by many cell types in the body in response to inflammatory stimuli, and this secretion creates a chemical gradient that recruits monocytes from circulation and activates resident macrophages to initiate the immune response. CCL2 is found to be elevated in many inflammatory disorders including lupus nephritis and skin hypersensitivity reactions [90]. Though secreted by many cell types in the body, macrophages are the bodies largest source of CCL2, which is thought to enhance recruitment of additional effector cells when first respond to sites of inflammation.

### **Role of tumor-secreted CCL2 in breast cancer**

CCL2 is a small soluble cytokine that attracts circulating monocytes to tissues via chemical gradient [91]. It interacts with CCR2, a G-protein-coupled receptor, on the surface of monocytes and other immune cells. In addition to its expression on monocytes, CCR2 is also expressed on prostate and breast carcinoma cells at higher levels than normal epithelium [92, 93]. In breast cancer, it is known to attract tumor-associated macrophages, increase

angiogenesis, enrich cancer stem cells, and increase invasion and metastasis of CCR2-expressing carcinomas [94].

### **Tumor cells secrete CCL2 to recruit tumor-promoting macrophages**

Reports describing CCL2 secretion by tumor cells before CCL2 had even been described. Several papers from the 1980's describe a tumor-derived chemotactic factor that induced migration of monocytes *in vitro*. Botazzi et al first described the chemotactic properties of conditioned media from primary human and murine tumor-cell lines, and found a correlation between the magnitude of the chemotactic response and the macrophage density in the original tumors [95]. These early studies described this unknown entity as tumor-derived chemotactic factor (TDCF). The lab of Edward J. Leonard at the National Cancer Institute first cloned full-length cDNA for human CCL2 (still called MCP-1 at the time) in 1989, which led to the discovery in 1992 that TDCF and CCL2 are the same molecule, derived from the same mRNA transcript [96, 97].

### **Tumoral CCL2 enhances angiogenesis through macrophage dependent mechanisms**

Early studies investigating the influence of macrophages on tumor progression found that the macrophage content of tumors correlated with increased vascularity and significantly elevated CCL2 expression by gastric carcinoma tumors [98]. Similar correlational studies on human breast tissue revealed that CCL2 is expressed by both tumor cells and macrophages, and that CCL2 levels correlated with VEGF expression and tumor vascularity[99, 100]. Ablation of macrophages by clodronate therapy has been shown to significantly reduce tumor burden and reverse angiogenesis in rhabdomyosarcoma mouse models[101].

### **Therapeutic potential of CCL2-targeted therapies**

While CCL2 remains a therapeutic target of interest, its translation to the bedside remains controversial. CCL2 neutralizing antibodies effectively block cancer progression in some animal models[102-104], but in other models of breast cancer, where its failure is due to accumulating levels of CCL2 protein[105]. Furthermore, cessation of CCL2 antibody neutralization in animal models of breast cancers created a rebound effect, enhancing metastatic disease associated with increased tumor angiogenesis[106]. Recent studies from our lab suggested that methods to target chemokine expression, rather than antibody neutralization may be more effective at inhibiting chemokine signaling activity[105, 107].

Developing a successful immunotherapy for breast cancers have been challenging, relative to the success response rates of immunotherapy for melanomas, lung cancers and acute leukemias[108-110]. Recent clinical trials show promise for anti-PD1 or anti-PDL1 treatment in triple-negative breast cancers with an objective response rate ranging from 4-19%[111, 112]. CTLA4 inhibitors have shown even lower clinical response [113]. Relative to melanomas or lung cancers, the immune landscape of breast cancers is unique in several aspects. For one, T cell infiltration varies among luminal, HER2+ and basal-like breast cancers [114]. Breast cancers show intratumoral heterogeneity in expression of PD-L1 or CTLA4 and expression varies among subtypes[115-117], potentially limiting effectiveness of these therapies. Therapeutic vaccines, which target tumor-associated antigens such as HER2, MUC1 and carbohydrates are in development for breast cancer treatment [118-120]. However, recent clinical trials involving vaccination with Sialyl-Tn, a carbohydrate antigen in metastatic breast cancer patients showed no clinical benefit [121]. Low T cell activity in breast cancer are attributed to high levels of M2

macrophages and T regulatory cells in the local tumor microenvironment[68, 122]. Therapies that target M2 macrophage phenotype and T cell regulatory mechanisms could be used to sensitize tumors prior to checkpoint blockade.

### **CCR2 and breast cancer**

The chemokine receptor for CCL2 is CCR2, a seven-transmembrane G-coupled receptor with an extracellular N-terminal motif required to bind CCL2 and a C-terminal intracellular signaling domain. Two major isoforms exist in humans that differ by 50 units in their C-terminal domain due to alternative splicing, CCR2A and CCR2B[123]. CCR2B accounts for 90% of expressed CCR2 in humans, as it is highly expressed by macrophages and NK cells. CCR2A contains a cytoplasmic retention signal on its C-terminal domain that sequesters it to the cytoplasm[124].

CCL2 preferentially binds CCR2, although it can also bind to other receptors such as CCR4. Binding of CCL2 to CCR4 can have an immune-stimulatory effect by binding the cytotoxic T cells and recruiting them to a site of inflammation, or an immune suppressive function by binding CCR4 on regulatory T cells. Due to the conserved cysteine residues between CCL2 and its structural homologs, CCR2 can also bind to CCL7, CCL8, CCL12, and CCL13. Binding of CCL7 can stimulate monocyte recruitment from the bone marrow to metastatic niches, and binding of CCL8 stimulates the migration of colon cancer cells similarly to CCL2[125, 126].

CCL2 and CCR2 are overexpressed in multiple cancer types including: pancreatic, prostate and colon cancers and breast cancer correlating with poor patient prognosis [127, 128]. CCL2/CCR2 chemokine signaling is a critical regulator of macrophage recruitment during

wound healing and infection [129]. In breast cancer, animal models have demonstrated that CCL2 recruits CCR2<sup>+</sup> macrophages to promote tumor growth and metastasis [128, 130]. Macrophages utilize CCR2 to hone to tumors and influence angiogenesis and tumor suppression, however, the role of epithelial CCR2-signaling in tumors is not well understood. We recently found that CCR2 is overexpressed in breast cancer cells and regulates CCL2-induced cell survival and migration [93]. Tumor-cell expression of CCR2 is associated with M2 macrophage recruitment and poor prognosis, suggesting that CCR2 signaling in tumor cells likely contributes the immune phenotype observed in CCR2-high tumors, however, few studies investigate the role of epithelial CCR2 signaling in breast cancer progression.

Given the profound contribution of macrophages on tumor progression, their ability to secrete massive amounts of CCL2, and the fact that many breast cancer express high levels of CCR2, it seems likely that tumoral CCR2 signaling not only affects the tumor cells directly, but may also help to shape the tumor-promoting microenvironment around it. As evidenced by the failure of many CCL2-targeted therapies, our understanding of how CCL2/CCR2 signaling in breast cancer is incomplete. By better understanding the mechanisms by which CCR2 expression by tumor cells contributes to breast cancer progression, thru both microenvironment-independent and microenvironment-dependent mechanisms, we may be able to effectively target the CCL2/CCR2 axis in breast cancer.

### **Scientific question**

How does epithelial CCL2/CCR2 signaling in tumors promote early progression of breast cancer?

### **Hypothesis**

Based on the background information presented, I hypothesized:

Tumoral CCL2/CCR2 signaling suppresses CD154 to promote early invasion and growth in IDC, thru mechanisms that affect the tumor cells directly and thru indirect mechanisms dependent upon stromal and macrophage involvement.

## Aims

To test this hypothesis, I developed these specific aims:

Determine the role of tumor-cell-secreted CCL2 in the growth and invasion of breast tumors in the context of CD154 suppression. Specifically, characterize how tumoral CCL2 expression affects CD154 expression *in vitro*, and determine which CCL2-dependent functions are interdependent on CD154 suppression.

Determine how tumor-cell CCR2 expression affects breast cancer progression, and if this is reliant on stromal interaction, by generating human cancer cells with variable CCR2 expression and transplanting them into mouse models with no stromal interactions (subrenal grafts), fibroblast-specific interactions (subrenal grafts co-grafted with fibroblasts), and myeloid lineages (fat pad and intraductal injections of breast cancer cells into immune-compromised mice).

Determine how carcinoma CCR2 expression affects the tumor microenvironment and immune landscape of that environment. Determine which microenvironment-dependent mechanisms of CCR2 require suppression of CD154 through *in vitro* studies of both murine and human cell lines with variable CCR2 expression and rescue experiments with exogenous CCL2 supplementation or CD154 ablation by antibody neutralization.

Chapter 2: The role of CCL2/CCR2 suppressing CD154 expression on in vitro measures of cancer cell progression.

## Introduction

Major advances in screening and better understanding the underlying molecular mechanisms of breast cancer progression have greatly reduced breast cancer mortality in the past 30 years. However, the major contributors to this increased survival are enhanced early detection and refining of chemotherapeutic combinations and treatment schedules, not because of the discovery or adoption of novel therapies. One potential therapeutic target in breast cancer is CCL2, as it is significantly overexpressed the majority of invasive ductal carcinomas[96, 98, 99, 131, 132]. Tumor cells that overexpress CCL2 contribute to tumor progression through mechanisms that affect the intrinsic tumor-promoting functions of the tumor cells and indirectly by modulating the various host factors that comprise the tumor microenvironment.

Tumoral CCL2 has been shown to directly promote the proliferation, migration, invasion, and stem cell renewal of breast cancer cells in vitro [93, 133]. Ueno et al. discovered that tumor-cell levels of CCL2 correlated significantly with intratumoral macrophage levels and expression of the angiogenic factors VEGF, IL-8, TNF-alpha, and TP[99]. CCL2 polarizes macrophages to an M2 phenotype by activating CCR2 and inhibiting secretion of IL-10 (an M2-promoting interleukin), and in doing so block M1 polarization [134]. Neutralization of CCL2 in a mouse model of breast cancer metastasis effectively blocked recruitment of macrophages, inhibited metastasis, and increased survival. [103]

Despite these early promising results, systemic ablation of CCL2 incites a rebound surge of CCL2 upon therapy withdrawal. A human trial for antiCCL2 therapy in rheumatoid arthritis patients was halted prematurely because serum levels of CCL2 rose above pre-treatment levels in some patients [135]. In mice, CCL2-neutralization was also observed to paradoxically increase serum CCL2 levels, which resulted in increased angiogenesis and metastatic spread compared to

untreated mice. Another major limitation of systemic CCL2 neutralization is that it is required for normal immune functioning, including anti-tumor responses [106, 136]. As CCL2 expression by tumor cells is responsible for recruiting tumor-promoting macrophages and subsequent angiogenesis, targeting expression of CCL2 in tumor cells may be more effective than systemic neutralization.

To test this therapy, our lab recently demonstrated that by using siRNA complexed to cell-penetrating TAT nanoparticles, CCL2 was selectively downregulated in tumor cells. Targeted delivery of CCL2 siRNA by calcium-TAT nanoparticles (siCCL2) resulted in significantly decreased tumor growth and metastatic spread of MDA-231 xenografts in NOD-SCID mice, associated with decreased macrophage recruitment, angiogenesis, stem cell renewal, and proliferation of breast cancer cells [137]. Additionally, siCCL2-treatment increased necrotic cell death but had no effect on apoptosis. Stem cell populations were decreased following siCCL2 treatment, as measured by flow cytometry analysis of CD24/CD44 staining and an increased expression of ALDH1 *in vivo*, <sup>and</sup> decreased mammosphere formation during serial passage *in vitro*. Using an *in vitro* model of macrophage recruitment, we confirmed the *in vivo* findings that siCCL2 treatment of cancer cells decreases macrophage recruitment.

Given the broad range of phenotypes observed by modulating CCL2 expression, we next addressed the possibility that tumoral CCL2 may regulate other tumor-promoting or tumor-suppressing cytokines in the tumor microenvironment. We analyzed supernatants from MDA-231 cells treated with CCL2 siRNA or control siRNA complexed with TAT nanoparticles, which revealed several cytokines that were up-or-down regulated in the siCCL2 group. Of particular interest was the upregulation of CD154 in siCCL2 cells, as CD154 is known to antagonize many of the mechanisms by which CCL2 promotes tumor progression.

The goal of the following studies is to assess the possibility that some of the tumor-promoting functions of CCL2 are attributable to decreased CD154 levels. Through various *in vitro* methods described below, a novel regulatory mechanism by which tumor cells inhibit tumor-suppressive CD154 thru autocrine production of CCL2.

## Materials and Methods

### Cell culture

MCF10A and MDA-MB-231 cells were obtained from American Tissue Culture Collection. Cancer associated fibroblasts were isolated from invasive breast ductal carcinoma and characterized in previous studies [95, 96]. DCIS.com cells were generously provided by Fariba Behbod, PharmD, Ph.D. (University of Kansas Medical Center). Raw 264.7 mcherry cells were generously provided by George Veilhauer, Ph.D (University of Kansas Medical Center, Kansas City, KS). All cell lines were cultured on plastic in DMEM media containing 10% FBS with 0.1% amphotericin, 1% penicillin-streptomycin (cat no. 30-004-CI, Cellgro).

### Generation of CD154 shRNA lentivirus –

Knockdown plasmids for CD154 were generated by cloning the following sequences into the pSico-Efla-mCherry-Puro plasmid (Addgene plasmid #31845). Oligos were ordered from ADT using standard desalting in the following manner

Sequence 1-(5)TxxxxxxxxxxxTTCAAGAGAxxxxxxxxxxxxxxxxxxxxxxTTTTTTG (3) and

Sequence 2- (5)GATCCAAAAAxxxxxxxxxxxxxxxxTCTCTTGAAxxxxxxxxxxxxxxxxxxxA (3)

Using the following shRNA target sequences:

5-TTGGCAAGTTATCTGCTGT-3

5- GGGTGGGCTTAACCGCTGT-3

5-TCACAAAGCCTTCAAAGT-3

5-AGAACTGACTAGCAACGGC-3

5-GAAGACTCCCAGCGTCAGC-3

Where the shRNA target sequence goes into the 5' stretch of x's, and the reverse complement of that sequence goes into the second set of x's of Sequence 1 and 2. This allows a blunt-sticky cloning method to be used. pSico was digested by HpaI and BamHI @ 2 units/ug pSico using a double digest in NEB Buffer four with 100 ug/ml BSA at 37C for 1 hour. The resulting DNA was purified with a silicon column kit from Promega. Oligos were annealed simultaneously with PNK enzyme and 10 mM ATP utilizing the following temperature protocol: 37C 30min; 95C 3min; for 80 cycles decrease temperature by 0.5C with 30s cycle length. Annealed, phosphorylated oligos were then individually ligated at a 5:1 ratio of oligomer to HpaI/BamHI digested pSico overnight at room temperature. Because HpaI site is destroyed upon successful ligation, ten units HpaI were added to the ligation mixture to prevent transformation of bacteria by recircularized pSico vector using chemically competent DH5alpha cells and a 45 second 40-degree heat shock protocol. Clones were selected from positively inserted dish and resultant plasmid was sequenced to ensure proper ligation and sequence fidelity.

### **siRNA/plasmid reagents**

Sense and anti-sense oligonucleotides were synthesized and annealed by GE Dharmacon. The following siRNA targeting sequences were designed: enhanced green fluorescent protein (eGFP) as a negative control: 5'-GCUGACCCUGAAGUUCAUC-3' [97], huCCL2si1: 5'-ACCUGCUGUUAUAACUUCA-3', huCCL2si2: 5'-CAGCAAGUGUCCC AAAGAA-3'.

### **Preparation of Ca-TAT complexes**

The following formula was used to determine the amount of TAT peptide needed for a specific N/P ratio per  $\mu\text{g}$  of DNA or siRNA:  $\mu\text{g of TAT} = 0.446 * (\text{N/P ratio}) + 0.116$ . For example, complexing 2.346  $\mu\text{g}$  of TAT per 1  $\mu\text{g}$  of DNA or siRNA would yield N/P=5. To prepare complexes, TAT peptides were mixed with siRNA or pDNA in 45  $\mu\text{l}$  sterile deionized

water containing: 37.5 mM, 75 mM or 112.5 mM CaCl<sub>2</sub>. The solution was pipetted vigorously for 20 times and incubated on ice for 20 minutes. For 2D and 3D cell culture studies and mammosphere assays, cells were incubated directly with the complexes for 24 hours before media replacement. For *in vivo* studies, 25 µl of 10 % glucose was added to the complexes, and diluted with PBS to a total volume of 100 µl before use.

### **3D cell culture**

In each well of a 24 well plate, 100,000 breast cancer cells were embedded in 200 µl rat tail collagen (BD Pharmingen) using methods adapted from previous studies [98]. Briefly, the pH of 2 mg/ml of stock collagen was adjusted by mixing at a 4:1 ratio with setting solution comprised of: 1X EBSS, 75 mM NaOH, and 290 mM NaHCO<sub>3</sub>. Breast cancer cells were detached from the plate by trypsinization, quenched, counted by hemocytometer, and pelleted by centrifugation. 100,000 cells were mixed thoroughly with 250 µL collagen solution and pipetted directly in each well, and incubated at 37C for 30 minutes for polymerization of collagen. Cells were incubated in 1 ml of DMEM/10% FBS for 24 hours prior to transfection.

### **ELISA**

For each well in a 24 well plate, 40,000 cells were seeded in a monolayer or 100,000 cells were seeded in collagen for 24 hours in DMEM/10% FBS. To generate conditioned medium, cells were washed in PBS and incubated in serum-free DMEM for 24 hours in 500 µl volume per well. Conditioned media generated from indicated cell lines were subject to ELISA specific to human CCL2 (cat no.900-M31, Peprotech), VEGF (cat no. 900-K10, Peprotech) or IL-6 (cat no. 900-K16, Peprotech). Samples were analyzed according to manufacturer protocol. Reactions were catalyzed using tetramethylbenzidine substrate (cat no. 34028, Pierce) according to

manufacturer's instructions. Absorbance was read at OD 450 nM using a BioTek Microplate Reader.

### **Animal care and surgery**

Female athymic Foxn1<sup>nu/nu</sup> mice, 6-8 weeks old (Balb/c background) were purchased from Envigo, Inc. Animals were maintained at the University of Kansas Medical Center, in accordance with the Association for Assessment and Accreditation of Laboratory Animal Care (AALAC). All animal experiments were performed at the University of Kansas Medical Center under an approved IACUC. 250,000 human carcinoma-associated fibroblasts were embedded with 100,000 MDA-MB-231 cells in 50  $\mu$ l of collagen rat tail collagen I (BD Pharmingen), using methods previously described [40]. One collagen plugs was transplanted into each mouse, in the #4-5 inguinal mammary glands. When the tumors reached 0.5 cm in diameter, 10  $\mu$ g (100  $\mu$ l) of Ca-TAT/control or Ca-TAT/CCL2 siRNA nanoparticles were injected into the primary tumor in four different areas of the tumor, using a 27-gauge needle. Each mouse received a total of three injections of Ca-TAT/siRNA complexes. Animals were monitored twice weekly for tumor formation by palpation and measurement by caliper. Animals were euthanized 30 days post-transplantation, when control tumors reached maximum allowable tumor size, approximately 1.5 cm<sup>3</sup> (Figure 2A).

### **Tissue embedding**

Tissues were fixed in 10 % neutral formalin buffer for 24 hours. Tissues were embedded in wax as described [98]. Briefly, tissues were dehydrated in a series of alcohols: 70, 90, 100% ethanols for 1 hour each. Tissues were further dehydrated in isopropanol for 1 hour, 50:50 ratio of isopropanol: paraffin wax at 60°C for 1 hour and then in wax at 60°C overnight. Tissues were

placed into the wax containing molds and allowed to harden at room temperature. Tissues were then processed for histological analysis.

### **Histology/immunohistochemistry/immunofluorescence**

Wax embedded sections were sectioned at five micron thickness onto 1 mm glass slides, dewaxed and rehydrated as described [98]. For H&E stain, slides were incubated in Harris's hematoxylin for 2 minutes and eosin for 2 minutes prior to dehydration and mounting in Cytoseal. For immunostaining, tissue sections were subjected to antigen retrieval through heating in low pressure in sodium citrate buffer pH 6.0 for 2 minutes. Slides were washed in PBS, and endogenous peroxidases were quenched in PBS containing 60 % methanol and 3% H<sub>2</sub>O<sub>2</sub>. Samples were blocked in PBS containing 3% fetal bovine serum for 1 hour, and incubated with primary antibodies (1:100) to: cleaved caspase-3 Asp 175 (cat no. 9579, Cell Signaling Technology), HMGB1 (cat no.6393, Cell Signaling Technology), LC3B (cat no. L10382, Life Technologies), VWF8 (cat no. Ab7356, Millipore), arginase I (cat no. sc20150, Santa Cruz Biotechnology) or VEGF (cat no. sc-152, Santa Cruz Biotechnology) overnight at 4°C. Slides were washed in PBS 3 times, incubated with secondary rabbit biotinylated antibodies at 1:1000 dilution (cat no. BA-5000, Vector Labs) for 2 hours, conjugated with streptavidin peroxidase (cat no. PK-4000, Vector Labs) and incubated with DAB substrate (cat no. K346711, Dako). For detection of PCNA or IL-6 endogenous mouse immunoglobulins were first incubating with blocking reagents from the Mouse on Mouse kit (cat no. BMK-2202, Vector Laboratories), according to commercial protocol. Slides were incubated with PCNA antibodies (cat no. sc25280, Santa Cruz Biotechnology) or IL-6 antibodies (cat no. MAB-2061m RnD Systems) at a 1:100 for 1 hour and then incubated with secondary mouse biotinylated antibodies from the MOM kit at a 1:250 dilution for 1 hour. For detection of CD24, slides were incubated with

antibodies at a 1:100 (cat no. 561777 BD Pharmingen), and detected with secondary rat-biotinylated antibodies (cat no. BA-9401, Vector Laboratories) at a 1:1000 dilution. Sections were counterstained with Harris' hematoxylin for 1 minute, dehydrated and mounted with Cytoseal. Because tumor sections were of various sizes, it was determined that four fields could be captured consistently among tumor samples, while enabling a good representation of the tumor. Therefore, 4 random fields per section, with two sections per sample, were captured at 10x magnification using a Motic AE 31 microscope with Infinity2-1c color digital camera. DAB staining was quantified by pixel density analysis, normalized to total tumor area, using an Image J software protocol (NIH) described in previous studies [98-101].

For immunofluorescence, sections were incubated at 1:100 dilution of antibodies to Cytokeratin 5 (CK5, cat no. XM-26, ThermoFisher ) and Calsequestrin (cat no. SC-28274, Santa Cruz Biotechnologies) overnight at 4°C, conjugated with anti-rabbit-Alexa-568 and anti-mouse-Alexa-488 at a 1:500 dilution for 2 hours. Sections were washed in PBS, counterstained with DAPI and mounted with PBS/glycerol.

### **Quantification of tumor-necrosis**

To quantify the extent of necrosis in breast tumor xenografts, tumor tissues were sectioned at five different depths, approximately 50 microns apart. 3 sections from each depth were placed on a slide and stained by H&E. Sections were imaged at 4x magnification, at 2-3 fields per section to capture the whole tissue section. Software analysis for necrotic areas in breast tissues was performed using methods adapted from previous studies [96]. Images were first imported into Adobe Photoshop. Color and exposure of images were normalized using auto-contrast. Necrotic areas were selected using a lasso tool, copied to a new window and saved a separate file. Images were opened in Image J software (NIH), and converted to grey scale.

Background pixels resulting from luminosity of bright field images were removed by threshold adjustment. Images were the subject to particle analysis. Necrotic areas and total areas were expressed as particle area values of arbitrary units. Values representing necrotic areas were normalized to values representing total tissue section.

### **Scoring of tumor invasion**

To quantify the extent of tumor invasion into muscle tissue, tumor tissues were sectioned at three different depths approximately 50 microns apart. Three serial sections from each depth were placed on each slide and stained by H&E. The muscle tissue was distinguished by a striated appearance that was strongly positive for eosin stain. Each section from each sample was scored for extent of invasion by analysis of slides at 4x and 10x magnification. Three different individuals in blinded studies used a numerical scoring system. 0 indicated no to low invasion, characterized by no or a few tumor viable cells present in muscle tissue, or the presence of necrotic tumor cells in muscle tissue; the border between muscle and tumor tissue was well-defined. 1 indicated some tumor-cell invasion, characterized by viable tumor cells present in muscle tissue; the border between muscle and tumor tissue was less defined. 2 indicated high invasion characterized by extensive number of tumor cells in muscle tissue; tumor was embedded in muscle, and the border between muscle tissue and tumor undefined.

### **Quantitation of lung metastases**

Metastatic nodules in lung tissues were detected and quantified using hematoxylin staining approach of lung tissues, as previously described in previous studies [99]. Briefly, tissues were dehydrated a series of alcohols: 70, 90, 100% ethanols for 1 hour each and cleared in xylene overnight. Tissues were rehydrated in decreasing series of ethanols, flushed with running tap water for 15 minutes and then stained with Gill's hematoxylin for 10 minutes. Lung

tissues were flushed with water for 5 minutes, de-stained in 1 % HCl for 20 minutes, and then incubated in tap water overnight. Tissues were partially dehydrated in 70% ethanol for 1 hour. Metastatic lesions throughout the lung tissue were visually identified by hematoxylin staining as round shaped nodules under bright field/phase contrast microscopy using a Motic AE31 inverted microscope (Motic AE31). Metastatic nodules were manually scored in the lung tissues. The presence of metastases was confirmed by paraffin embedding of whole tissue, and H&E stain of lung sections.

### **Flow cytometry**

For adherent cells in culture, cells were first detached from plastic by washing in PBS twice, and incubation in 3 mM EDTA at 37°C for 10-15 minutes. Cells were washed with 10 ml of complete medium twice, fixed in 10 % neutral formalin buffer for 10 minutes at room temperature and washed with PBS twice to remove traces of formalin. For tumor tissues, tissues were washed in PBS, and digested into single cell suspensions with collagenase I and trypsin for 4 hours at 37°C, as described in previous studies [21, 102-104]. Tumor-cell suspensions were fixed in 10% NBF for overnight at 4C, and then washed with PBS twice to remove traces of formalin. Cells were permeabilized with 0.1 % Triton-X 100 in a 37°C water bath for 15 minutes, and washed in PBS twice. Samples were incubated with the following antibodies at 1:50 dilutions, overnight on ice in PBS containing 2% BSA: CD24- PE (cat no.555428, BD Pharmingen), CD11b-APC-Cy7 (cat. no 557657, BD Pharmingen), murine CCL2 (cat no. 1784, Santa Cruz Biotechnology), human CCL2 (cat no. sc1304, Santa Cruz Biotechnology) Ki67 (cat no. Sc15402, Santa Cruz Biotechnology), HMGB1 (cat no. 6893, Cell Signaling Technology) or LC3B (cat no. L10382, Invitrogen). Samples were incubated with anti-Fsp1 at a dilution of 1:3 (cat no. ab75550, Abcam). Murine CCL2 and human CCL2 were detected by secondary goat

antibodies conjugated to Alexa-488 (1:500) in PBS for 1 hour on ice, covered in foil. Fsp1, Ki67, HMGB1, LC3B were detected by secondary rabbit antibodies conjugated to Alexa-647 at a 1:500 dilution on ice for 1 hour. Cells were washed with PBS three times prior to analysis. Samples were analyzed on a LSRII flow cytometer, normalized to secondary antibody only controls.

### **Mammosphere assay**

30,000 cells were seeded in low-attachment six well plates (Corning) in 3 ml of DMEM/10% FBS. 48 hours after plating, cells were transfected with Ca-TAT complexed to three ug of control, huCCL2si1 or huCCLsi2 siRNAs. After an additional 5 days in culture, mammospheres were collected in 15 ml conical tubes, pelleted, and disassociated using 20 mM Trypsin/2 mM EDTA solution for 7 minutes at 37C. Cells were pelleted and replated for 48 hours before re-transfection with Ca-TAT/siRNA complexes. Images were captured using the EVOS FL auto-every 7 days of plating. Mammospheres were counted using Image J software.

### **3D macrophage infiltration assay**

MMD fluidic devices were fabricated by MetaBioscience LLC (Overland Park, KS). For each chamber device, 100,000 breast cancer cells were embedded in 250 µl rat tail collagen (BD Pharmingen), as described for 3D cultures. Devices were placed in six well dishes. 1 ml of DMEM/10% FBS was pipetted into the device and incubated overnight. After overnight incubation of the devices, 500,000 Raw 264.7 mcherry cells were counted and resuspended into 2.5 ml of DMEM/10% FBS for each device. Devices were twisted open and cells were pipetted into each well, outside of the device. Devices were imaged daily at 10x magnification using an EVOS FL Auto-Imaging System (Invitrogen) for up to 48 hours. The number of macrophages were measured by quantification of fluorescence using methods previously described [98].

**Statistical analysis**

All experiments were repeated a minimum of three times. Data are expressed as mean+ standard error of the mean (SEM) Statistical analysis was determined using Two-Tailed T-test or ANOVA with Bonferonni's post-hoc comparisons using GraphPad Software. Significance was determined by  $p < 0.05$ . \* $p < 0.05$ , \*\* $p < 0.01$ , \*\*\* $p < 0.0001$ , n.s=not significant or  $p > 0.05$ .

## Results

To ensure that the *in vitro* results were replicable *in vivo*, siCCL2 and control tumors were immunostained for CD154. Immunohistochemical staining for CD154 confirmed that siCCL2 treatment increases CD154 expression compared to siCTRL-treated tumors (Figure 1). CD154 expression appeared to be both membranous and cytoplasmic, but not nuclear.

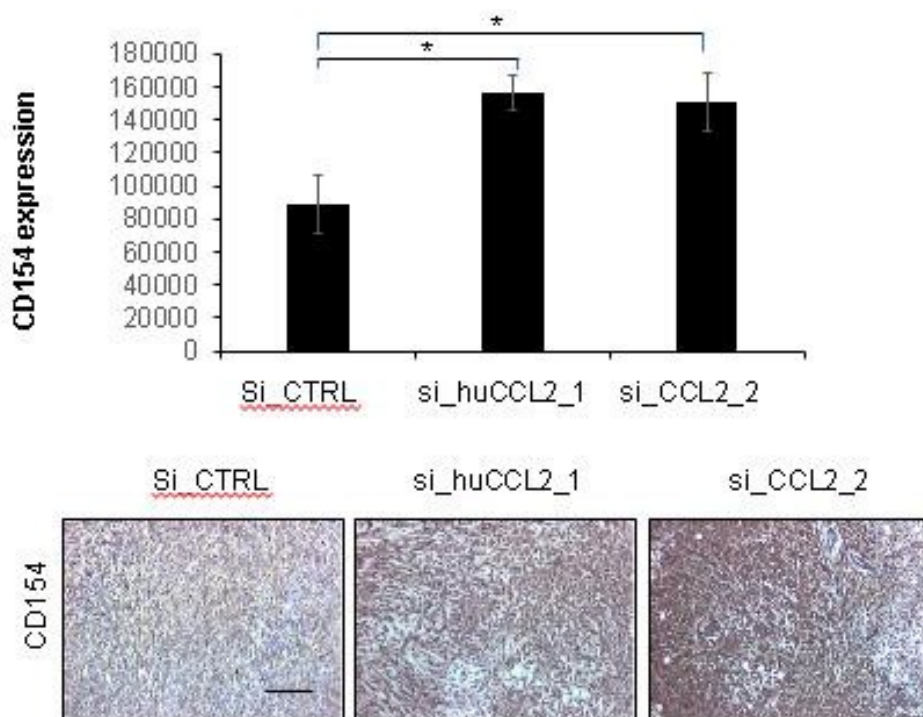


Figure 1 - Delivery of CCL2 siRNA via TAT nanoparticles significantly decreases the invasiveness of MDA-231 tumors in NOD-SCID mice. Top – quantification of positive staining, scale bar in arbitrary units of pixels of DAB normalized to total tumor area. Lower – representative images from each group. Scale bar = 200  $\mu$ m. N= 6 tumors per group. Significance determined by student's T test, \*  $p < 0.05$ .

To further confirm the cytokine array results, I generated stable knockdown of CCL2 in MDA-231, DCIS.com, and CA1D cells. ELISA analysis revealed significantly reduced CCL2 expression in MDA-231 (- Figure 2A), DCIS.com (Figure 2B), and CA1D cells (not shown) with CCL2 KD compared to control shRNA expressing cells. CCL2 depletion increases CD154 expression in CCL2 KD cell lines by Western blot and ELISA (- C-E). MDA-231 cells express nearly undetectable levels of CD154, and addition of CCL2 to either parental or control shRNA cell lines has no significant effect (data not shown). However, CCL2 KD significantly upregulates CD154 expression in MDA-231 cells, and exogenous CCL2 brings CD154 levels back to undetectable levels (- E). These data suggest that CCL2 suppresses CD154 in a number of human cell lines, both *in vitro* and in an immune-compromised model of breast cancer.

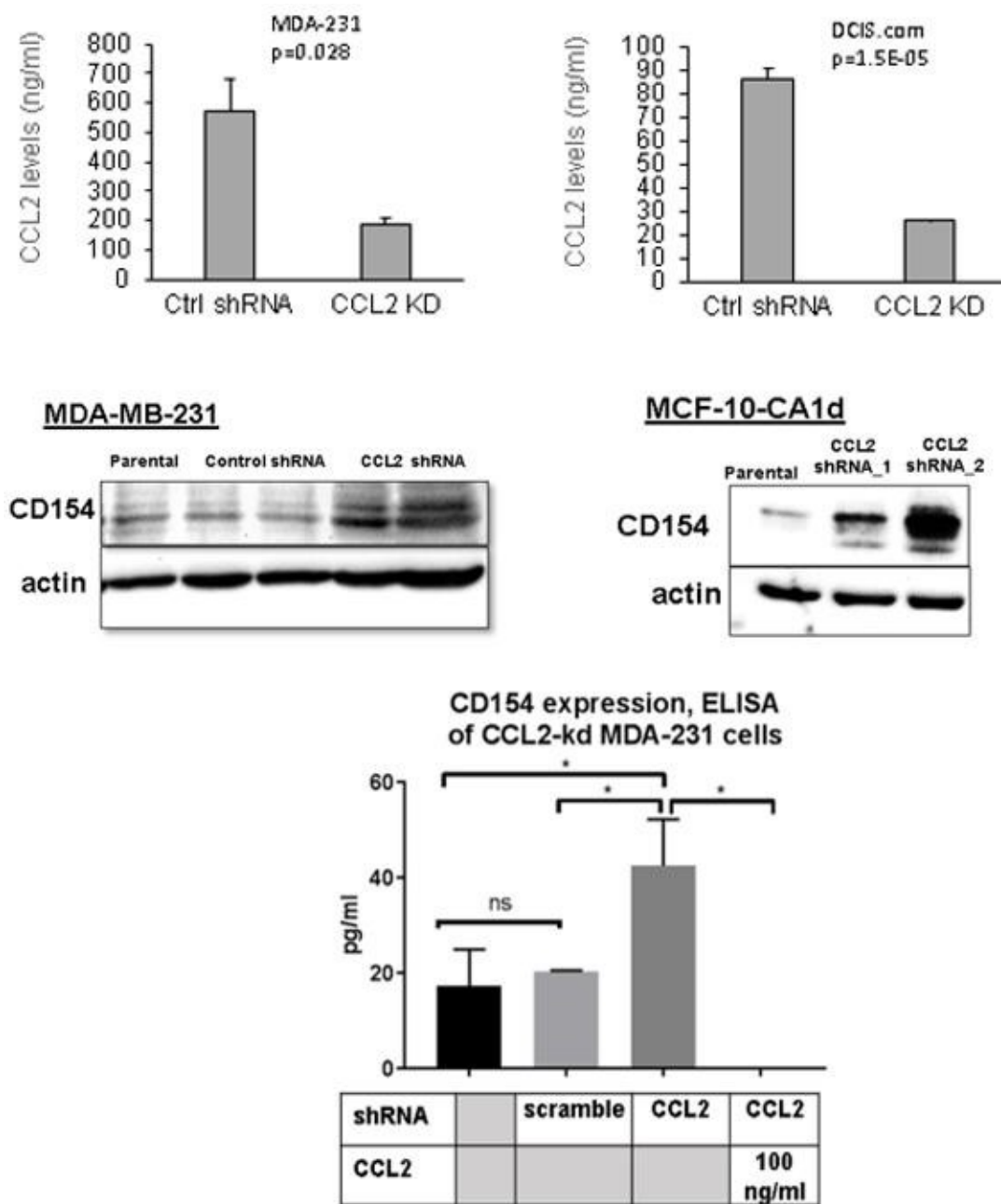


Figure 2 - CCL2 knockdown leads to increased CD154 expression in multiple human cell lines. A&B) CCL2 expression of 24 hour-conditioned media from MDA-231 and DCIS.com cells by ELISA. C&D) Western blot analysis of CD154 expression by MDA-231 and CA1D cells with CCL2 KD. E) Expression of soluble CD154 by ELISA in MDA-231 cells. breSignificance determined by student's T test, \* p<0.05.

To investigate whether any known tumor-promoting phenotype promoted by CCL2 was dependent on the suppression of CD154, I next cloned three shRNA sequences against CD154 into a pSico vector tagged with mCherry. The pGipz vector used to generate CCL2 KD cells contain a ribosomal entry site and GFP tag, and by using an mCherry vector for CD154 KD, successful dual transfectants could be visualized by two-channel fluorescent microscopy (Figure 3A). The CD154\_3 and CD154\_5 shRNA sequences most effectively reduced CD154 expression; CD154 knockdown did not affect CCL2 levels of either control or CCL2 KD cells (Figure 3B).

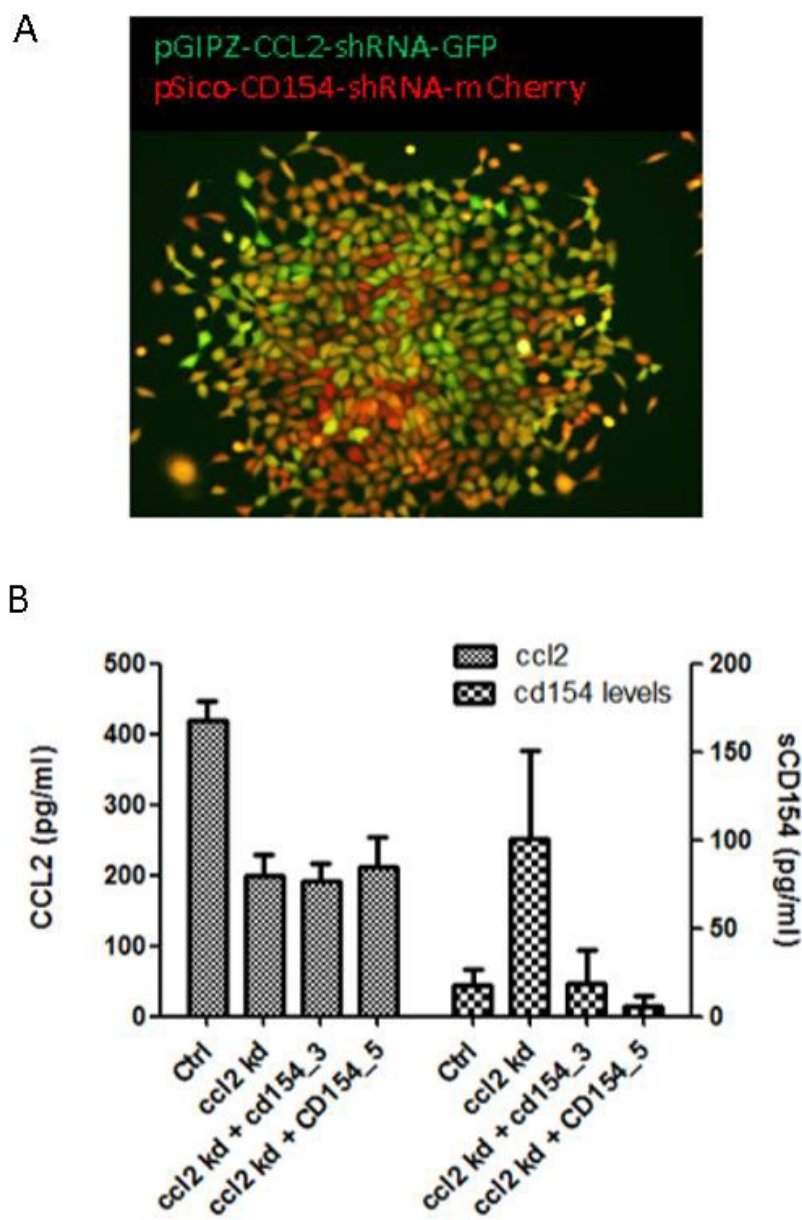


Figure 3 - Efficiency of knockdown of CCL2 and CD154 by enzyme-linked immunosorbant assay of conditioned media from MDA-231 cells. A) Representative image showing dual-transfection of cells (yellow), CCL2 KD cells (green), and CD154 KD cells (red). B) Knockdown efficiencies for CD154 and CCL2 KD cells. CCL2 levels expressed on left axis and CD154 levels expressed on right axis.

Enhanced migration of tumor cells is one of the most robust direct effects of CCL2 secreted by tumor cells. Though CD154 has been shown to decrease the migration of colon cancer cells, no studies have investigated the ability of CD154 to inhibit migration or invasion in breast cancer cells. Consistent with earlier findings, CCL2 KD decreases migration of MDA-231 cells by wound closure, and suppression of CD154 levels by antibody neutralization or shRNA knockdown rescues the migratory phenotype (Figure 4A). There were no significant effects of either CCL2 KD or antiCD154 on proliferation (Figure 4B). These data suggest that CCL2 enhances the migration of tumor cells in a CD154-dependent manner, and that neither have an effect on proliferation in MDA231 cells.

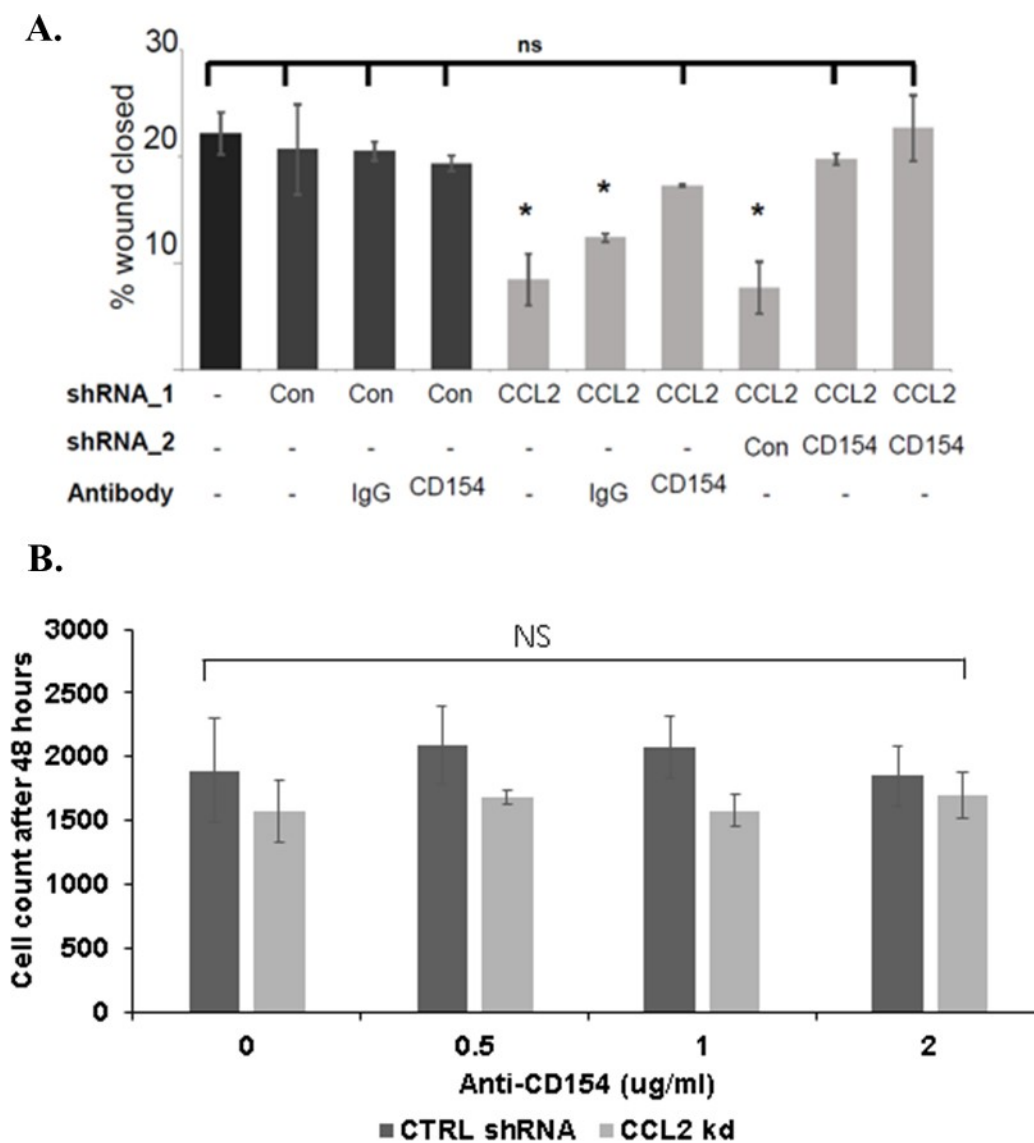


Figure 4 - The effect of CD154 on proliferation and migration of MDA-231 CCL2 KD cells. A) Migration of MDA-231 cells in the context of CCL2 KD and CD154 suppression as measured by wound closure assay. B) Proliferation of MDA-231 cells with CCL2 KD treated with varying levels of CD154 neutralizing antibodies. Number represent cell counts after 24 hours from a starting population of 1000 cells.

Previous studies show CCL2 increases the survival of 4T1, PyVmT, and MDA-231 cells in the presence of chemotherapeutics [93]. Using the dual CCL2/CD154 knockdown cells, we found that CD154 knockdown increases the survival of CCL2 KD MDA-231 cells at both a high and low dose of doxorubicin, a chemotherapeutic commonly used to treat breast cancer (Figure 5).

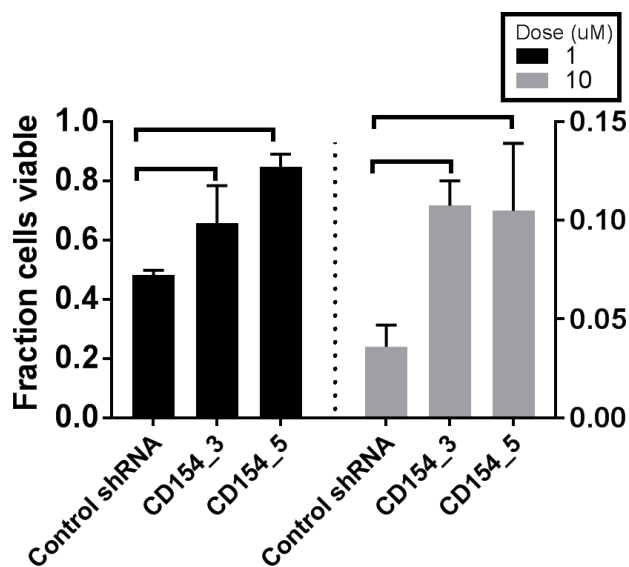


Figure 5 - CD154 knockdown increases the survival of MDA-MB-231 cells in the presence of both 1 and 10 uM doses of doxorubicin over 24 hours.

Viability measured by MTS assay relative to untreated parental MDA-MB-231 cells. N=3 experiments with duplicate readings, \* denotes  $p < 0.05$ .

Treatment of MDA-231 tumors with siCCL2 significantly reduced stem cell population markers CD24, CD44, and ALDH1 *in vivo*, and siCCL2 treated MDA-231 cells decreased stem cell renewal as measured by serial mammosphere formation assay *in vitro*. We investigated the role of CD154 suppression in these CCL2-mediated processes through serial mammosphere formation assay, which quantifies changes in the percentage of a cellular population that are self-renewing stem cells. We found that CD154 neutralization of CCL2 KD cells rescues the self-renewing stem cell population after two generations of serial passage (Figure 6). To further investigate this phenotype, we knocked down CD154 in MCF10A cells, a normal breast epithelial cell line that expresses low levels of CCL2 and CCR2 at basal levels. Immunoblot showed significant reduction in CD154 expression relative to actin (Figure 7A). CD154 KD significantly increased the number of mammospheres formed after 2 passages (Figure 7B). Interestingly, due loss of vector expression or incomplete cell sorting, a small population of untransfected cells persisted and formed mammospheres in the three knockdown lines (denoted by small black arrows, Figure 7C). Overlay of mCherry revealed that both control and untransfected MCF10A cells formed compact, nearly perfectly spherical mammospheres, whereas the CD154 KD cells displayed undefined borders, irregular shape, and high variation in size, consistent with the morphology observed in the mammospheres of more aggressive cancer cell lines.

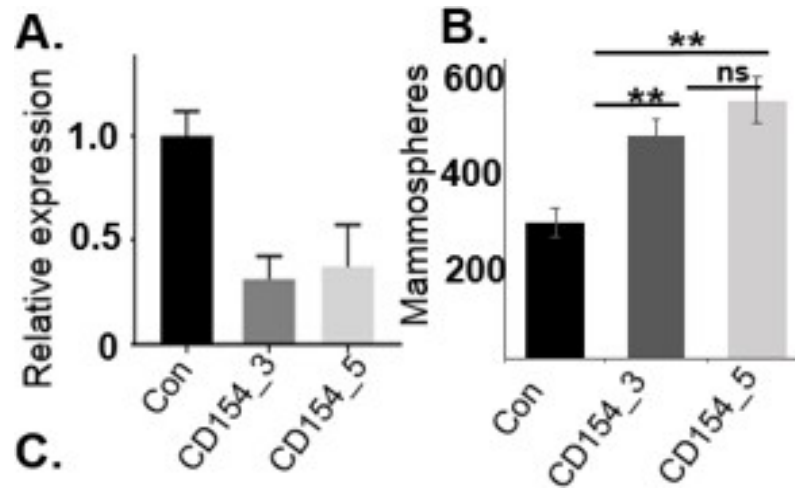


Figure 6 - CD154 levels correlate with mammosphere formation in MDA-231 cells. CCL2 KD MDA231 cells with stable CD154 KD were produced with two unique shRNA sequences lentivirally. A) Expression of CD154 was determined by Western blot and quantified in ImageJ. B) MDA231 CD154 KD cells were serially passaged in low-attachment plates to quantify number of self-renewing stem cells. Mammospheres counted after second generation. \*\*  $p < 0.005$  by Student's two-tailed T-test.

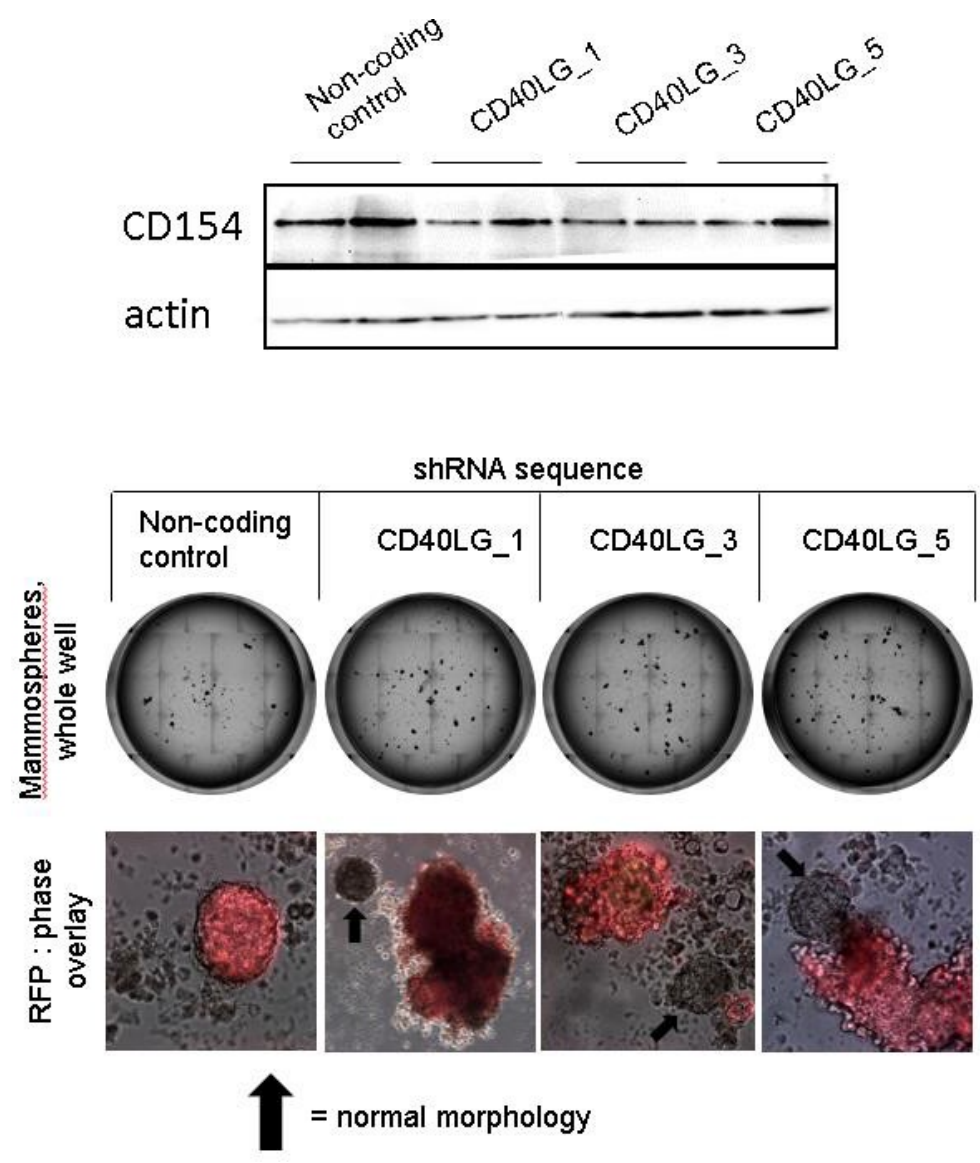


Figure 7 - Effect of CD154 knockdown on formation of MCF10A mammospheres. Top – Western blot showing the efficacy of CD154 KD in MCF10A cells by three different shRNA sequences against CD154. Bottom – representative images of mammospheres formed in 24 well plates, as well as 200x magnification of mammospheres. Red structures are transfected cells, black arrows point to untransfected mammospheres.

## Discussion

In this aim I provide evidence that CD154 has tumor-suppressive effects and that CCL2 secretion by tumor cells is inversely correlated with CD154 expression. These findings suggest that CD154 negatively regulates stem cell renewal, survival, and migration of cancer cells, and that CCL2 promotes these processes in part by suppressing expression of CD154. CD154 does not have an effect on proliferation, and though CCL2 KD did not significantly diminish proliferation, its effect was trending toward suppressing proliferation. Additionally, studies that myself and others conducted have shown that blocking expression of CCL2 *in vivo* suppresses tumor-cell proliferation, expression of cancer stem cell marker ADLH1, invasion, and metastasis, and enhances apoptosis, necrosis, and autophagy. Tumors treated with CCL2 siRNA also expressed higher levels of CD154, consistent with the *in vitro* cytokine array and studies showing increased CD154 in CCL2 KD cells. This novel mechanism by which CCL2 promotes tumor progression increases our understanding of the CCL2/CCR2 axis in breast cancer, and suggests that increasing the levels of CD154 in tumors could be especially effective in CCL2-secreting tumors.

Much work has been done to characterize the effects of CCL2 secretion by tumor cells, particularly as it relates to the recruitment of an inflammatory stroma. Some of the first studies identifying a tumor-derived chemotactic factor noted that it increased the movement of monocytes. Subsequent studies found significant correlation between CCL2 expression by tumor cells, macrophage infiltration, and blood vessel density in human breast cancers [102, 138]. Only recently has the role of autocrine/paracrine effect of CCL2 secretion been investigated, as tumor cells often express higher levels of the receptor for CCL2, CCR2. The findings here on the function of CCL2 in directly promoting tumor-cell functions is consistent

with previous studies showing that CCL2 promotes the proliferation, migration, survival and stem cell renewal of CCR2-expressing tumor cells[72, 93]. The novel finding that CCL2 and the effects it has on tumor cells is antagonized by CD154 is also consistent with known effects of CD154 on tumor cells proliferation and migration[68].

Cd154 is a well-documented immunomodulatory molecule, although its role in breast cancer progression is limited to a few studies showing that it inhibits the proliferation of CD40-expressing cancer cells by enhancing apoptotic pathways [68, 69]. Interestingly, although MDA-231 cells express CD40, we did not observe any changes in proliferation after CCL2 KD or neutralization of CD154. The original study showing this effect, showed that fixed membrane-bound CD154 and trimeric soluble CD154 was the most effective at inhibiting proliferation and inducing growth arrest. It is known that the trimeric form of CD154 is more potent in eliciting B cell activation and inhibiting tumor growth, so it is possible that the major form of CD154 expressed in MDA-231 cells as a result of CCL2 KD is the less effective monomeric form. It is also possible that CCL2 KD affects the tumor-cell expression of CD40, though studies in our lab have found that among cell lines that produce high levels of CCL2, CD40 expression is highly variable, suggesting that CD40 expression is not regulated by CCL2 levels.

The negative effect of CD154 expression on cancer stem cell renewal was significant. In both CCL2 KD MDA231 cells and MCF10A cells, both of which express low levels of CCL2 and high levels of CD154, we found that CD154 inhibition increased mammosphere formation in vitro. No studies to date have described the effect of CD154 on stem cell renewal of carcinoma cells. It is possible that CD154 suppression enhances survival and chemotherapeutic resistance by increasing the proportion of cells that are stem cells, which are known to be more resistant to chemotherapeutics than non-stem cancer cells, though our data does not directly support this.

Further studies should be conducted to elucidate the mechanism by which CD154 enhances stem cell renewal, and the extent to which the increased ratio of stem: non-stem cells contributes to cancer cell survival.

The data presented here support a model whereby CCL2 blockade in cancer cells inhibits tumor growth and invasiveness in a CD154-dependent manner. The mechanism by which CCL2 regulates CD154 is not explored. Although MDA-231 cells express CCR2 at high levels, we cannot say with certainty that CCR2 signaling is responsible for suppressing CD154, as CCL2 can bind to other chemokine receptors, notably CCR4 and CCR5. It is possible that CCL2 negatively regulates CD154 by signaling through one of these lower-affinity receptors. Future studies are planned that will examine the role of epithelial CCR2 in regulating CD154 and tumor-promoting cellular processes. This will further elucidate whether CCL2 KD produces the findings reported here by decreasing tumoral CCR2 signaling, or some other mechanism not yet explored.

In sum, CCL2 promotes tumor progression through both direct signaling to cancer cells and by inhibiting expression of a tumor-suppressive molecule, CD154. These findings suggest that CD154-enhancing therapies could be particularly useful in CCL2-secreting tumors. Tumor secretion of CCL2 directly correlates with advanced disease and poor prognosis, meaning that CD154-based therapies could be particularly useful in the population of breast cancer patients most in need of novel therapies.

Chapter 3: Chemokine Signaling Facilitates Early-stage Breast Cancer Survival and Invasion  
through Fibroblast-dependent Mechanisms

Previously published as an open access article as: Brummer, G., D. S. Acevedo, Q. Hu, M.

Portsche, W. B. Fang, M. Yao, B. Zinda, M. Myers, N. Alvarez, P. Fields, Y. Hong, F.

Behbod and N. Cheng (2018). "Chemokine Signaling Facilitates Early-Stage Breast Cancer  
Survival and Invasion through Fibroblast-Dependent Mechanisms." Mol Cancer Res 16(2):

296-308. Creative Commons License

<https://creativecommons.org/licenses/by/4.0/legalcode>.

## Introduction

DCIS is the most common form of pre-invasive breast cancer in the US, with over 50,000 cases diagnosed every year. Standard treatment for DCIS involves a combination of lumpectomy and RT [139, 140]. Yet, 10 to 35% of patients experience disease recurrence, often accompanied by IDC [141, 142], indicating that under-treatment and over-treatment remain significant concerns in patient care. Few approaches exist to evaluate prognosis of DCIS. Compared to IDC, the use of biomarkers in DCIS has not been well studied. Small or low grade lesions may still become invasive [142, 143]. ER, Her2, Ki67, p16 and Cox2 are associated with disease recurrence but not with development of invasive breast cancer [144]. Identifying key mechanisms associated with DCIS progression could lead to better prognostic factors and tailored treatments for patients with DCIS.

Chemokines are small soluble molecules (8kda), which form molecular gradients to mediate homing of immune cells to tissues during inflammation. Chemokines signal to seven-transmembrane receptors that couple to G-protein dependent and independent pathways to promote cell migration [145, 146]. CCL2/CCR2 chemokine signaling is a critical regulator of macrophage recruitment during wound healing and infection [129]. CCL2 and CCR2 are overexpressed in multiple cancer types including: pancreatic, prostate and colon cancers and breast cancer correlating with poor patient prognosis [127, 128]. In breast cancer, animal models have demonstrated that CCL2 recruits CCR2+ macrophages to promote tumor growth and metastasis [128, 130]. The CCL2/CCR2 pathway is a current therapeutic target of interest [128], but little is known about mechanisms of this pathway in cancer beyond signaling in immune cells.

We recently found that CCR2 is overexpressed in breast cancer cells and regulates CCL2-induced cell survival and migration [93], indicating a macrophage-independent role for CCL2 in breast cancer. Using a novel Mammary Intraductal injection (MIND) model of DCIS, we demonstrate that CCR2 overexpression in DCIS lesions enhances invasive progression associated with accumulation of CCL2-expressing fibroblasts. Using the subrenal capsule model, we demonstrate that fibroblasts derived from DCIS promote breast cancer survival and invasion through CCL2 dependent mechanisms. Furthermore, increased CCL2/CCR2 signaling in DCIS is associated with increased expression of ALDH1, a pro-invasive factor, and decreased expression of HTRA2, a pro-apoptotic serine protease, factors associated with poor prognosis of breast cancer patients. These studies identify a key mechanism of DCIS progression involving CCL2/CCR2 signaling between fibroblasts and breast epithelial cells, with important clinical implications.

## Materials and Methods

### Cell culture

Human fibroblasts were isolated from reduction mammoplasty or DCIS tissues obtained from the Biospecimen Core Facility at the University of Kansas Medical Center (KUMC), and immortalized by expression of human telomerase reverse transcriptase as described (16).

Fibroblasts were authenticated by expression of: platelet-derived growth factor receptor- $\alpha$  (PDGFR- $\alpha$ ), fibroblast-specific protein 1 (Fsp1), and  $\alpha$ -smooth muscle actin ( $\alpha$ -sma) and absence of pan-cytokeratin. DCIS.com cells originated from Dr. Fred Miller's laboratory (17). These cell lines were cultured in DMEM containing 10% FBS (Atlas Biologicals, catalog no. FR-0500-A), 2 mmol/L L-glutamine (Cellgro, catalog no. 25-005-CI), 100 IU/mL penicillin, and 100  $\mu$ g/mL streptomycin (Cellgro, catalog no. 10-080). SUM225 cells originated from Dr. Steven Ethier's laboratory, Medical University of South Carolina, Charleston, SC (18), and were cultured in Ham F12 media containing 10% FBS, 5  $\mu$ g/mL insulin, 1  $\mu$ g/mL cortisone, and antibiotics. Cells were passaged no longer than 6 months, and tested for mycoplasma after thawing using the MycoAlert Plus Kit (Lonza, catalog no. LT07-701).

### Lentiviral transduction

For *CCR2* overexpression, full-length *CCR2* cDNA was obtained from University of Missouri-Rolla cDNA Resource Center (clone ID no. CCR200000), and subcloned into pHAGE-CMV-MCS-IRES-zsgreen lentiviral plasmid (PLASMID, Harvard University) using *NHEI* and *XbaI* restriction sites. pHAGE empty vector was used as a vehicle control. *CCR2* and nonsilencing control shRNAs in pGFP-c-shlenti lentivirus vectors were purchased from OriGene (Catalog No. TL321181). The *CCR2* targeting sequence was: 5'-

TATTGTCATTCTCCTGAACACCTTCCAGG-3'. *CCL2* and nonsilencing control shRNAs in pGFP-c-shlenti lentivirus vectors were obtained from OriGene (catalog no. TL316716).

The *CCL2* targeting sequence (OriGene) was: 5'-

ACTTCACCAATAGGAAGATCTCAGTGCAG-3'. *CCL2* and nonsilencing control shRNAs in GIPZ shRNA lentivirus vectors were obtained from Dharmacon (catalog no. V2LHS31298).

The *CCL2* targeting sequence was: 5'-TAAGTTAGCTGCAGATTCT-3'.

To generate lentivirus, 3.33 µg of PMD2G (Addgene catalog no.12260), 6.66 µg PDPAX2 (Addgene catalog no. 12259), and 10 µg target vectors were cotransfected in HEK-293T cells using Lipofectamine 2000 (Thermo Fisher Scientific catalog no. 11668027). Medium was removed 48 hours later and used to transduce cells, which were sorted for GFP expression by FACS.

### **Gene deletion by clustered regularly interspaced short palindromic repeats**

The *CCR2* guide RNA was cloned into the pSpCAs9(BB)-2A-GFP(PX458) vector (Addgene catalog no. 48318) using *BsmBI* enzyme. The *CCR2* guide RNA sequence was: 5'-TTCACAGGGCTGTATCACATCGG-3', which targeted the exon encoding the extracellular loop between the second and third transmembrane domains of human *CCR2*. The vector was transfected into DCIS.com breast cancer cells using jetPei transfection reagent (Polyplus, catalog no. 101-01), with N/P 7.5. Forty-eight hours later, GFP-positive cells were FACS sorted, cultured as single-cell clones in 96-well plates, and expanded into 6-well plates. Genomic DNA of individual colonies was screened by PCR to detect mutant colonies. The detection primer pair spanning the *CCR2* targeting site was: 5'-ACATGCTGGTCGTCCTCATC, 3'-AAACCAGCCGAGACTTCCTG. The PCR product of the wild-type (WT) gene was 901 bp, and contained one *DdeI* enzyme digestion site to yield 231- and 670-bp fragments. Exon

excision introduced an additional *DdeI* restriction site resulting in fragment sizes of 181, 231, and 468 bp upon *DdeI* digestion.

## **ELISA**

A total of 40,000 cells/well were seeded in 24-well plates in DMEM/10% FBS for 24 hours, washed in PBS, and incubated in serum-free DMEM for 24 hours in 500  $\mu$ L/well. Conditioned media were assayed for human CCL2 by ELISA (PeproTech, catalog no. 900-M31). Reactions were catalyzed using tetramethylbenzidine substrate (catalog no. 34028, Pierce). Absorbance was read at OD<sub>450nm</sub>/L using a BioTek Microplate Reader.

## **MIND model**

NOD-SCID *IL receptor- $\gamma$ 2* null female mice 8 to 10 weeks of age were purchased from The Jackson Laboratory. MIND injections were performed as described (19). Briefly, 4,000 cells/ $\mu$ L breast epithelial cells were prepared in 50  $\mu$ L PBS containing 0.1% Trypan blue. A Y incision was made on the abdomen of mice anesthetized with ketamine/xylazine [100 mg/kg / 10 mg/kg ] to expose the 4–5 and 9–10 inguinal glands. The inguinal nipples were snipped. A 30-gauge Hamilton syringe with a blunt-ended 0.5-inch needle was used to deliver 5  $\mu$ L (20,000) cells/nipple. Skin flaps were closed with wound clips. Mice were palpated for lesions twice weekly. SUM225 injected mice were sacrificed 7 weeks post-injection. DCIS.com-injected mice were sacrificed 4 weeks post-injection.

## **Subrenal graft**

Transplantation into subrenal capsules of NOD-SCID female mice (6–8 weeks old) was performed as described (20). Briefly, 250,000 fibroblasts were resuspended with 100,000 DCIS.com cells in 50  $\mu$ L rat tail collagen I (BD Pharmingen), and cultured in DMEM/10% FBS for 24 hours. Mice were anesthetized by ketamine/xylazine, a 1 to 1.5 cm midline incision was

made in the back 3 cm from the base of the tail, and the lateral or contralateral kidney was exposed. A small incision was made in the capsule layer using forceps and small spring-loaded scissors. The graft was inserted using a glass pipette. The body wall was closed with gut absorbable sutures and the skin was closed with wound clips. Mice were monitored twice weekly and sacrificed 3 weeks post-transplantation.

### **DAB immunostaining**

Tissues were fixed in 10% neutral formalin buffer and embedded in wax as described (21). For DAB immunostaining, 5 µm sections were dewaxed and heated in ten mmol/L sodium citrate buffer pH 6.0 for 2 minutes. Endogenous peroxidases were quenched in PBS/60% methanol/3% H<sub>2</sub>O<sub>2</sub>, blocked in PBS/3% FBS, and incubated with primary antibodies (1:100) overnight at 4°C: collagen IV (Novus Biologicals NB120-6586SS), cleaved caspase-3 Asp175 (Cell Signaling Technology, catalog no. 9579), Von Willebrand Factor 8 (VWF8; Millipore, catalog no. Ab7356), PDGFR- $\alpha$  (Cell Signaling Technology, catalog no. 5241), KI67 (Santa Cruz Biotechnology, catalog no. 1307), HTRA2 (Cell Signaling Technology, catalog no. 2176), CCL2 (Santa Cruz Biotechnology, catalog no. 1304), or F4/80 (Abcam, catalog no. ab6640). Fsp1 antibodies (Abcam, catalog no. 27427) were diluted 1:3. Slides were incubated for 2 hours at 1:1,000 with: anti-rabbit-biotinylated (Vector Laboratories, catalog no. BA-5000), anti-goat biotinylated (Vector Laboratories, catalog no. BA-5000), or anti-rat-biotinylated (catalog no. BA-9401, Vector Laboratories). For laminin staining, slides were treated with 20 µg/mL Proteinase K for 1 hour at 37°C prior to incubation with 1:100 pan-specific antibodies (Novus Biologicals, catalog no. NB300-144AF700). Slides were incubated with streptavidin peroxidase (Vector Laboratories, catalog no. PK-4000), developed with 3,3'-diaminobenzidine (DAB) substrate (Dako, catalog no. K346711), counterstained with Mayer hematoxylin and mounted

with Cytoseal. PCNA (catalog no. sc25280, Santa Cruz Biotechnology) and ALDH1A1 (R & D Systems, catalog no. MAB5869) proteins were detected using the Mouse on Mouse (MOM) Kit (Vector Laboratories, catalog no. BMK-2202).

### **Immunofluorescence**

For CK/ $\alpha$ -sma costaining, slides were heated in ten mmol/L sodium citrate buffer pH 6.0 for 2 minutes. Slides were incubated with antibodies 1:100 overnight at 4°C to:  $\alpha$ -sma (Spring Biosciences, catalog no. SP171) and CK5 (Thermo Fisher Scientific, catalog no. MA5-12596) or CK19 (Thermo Fisher Scientific, catalog no. MS198). Slides were incubated for 2 hours at 1:200 with anti-rabbit-IgG-Alexa Fluor 568 (Thermo Fisher Scientific, catalog no. A10042) and anti-mouse IgG-Alexa Fluor 488 (Thermo Fisher Scientific, catalog no. A-11001). For pan-cytokeratin/phalloidin costaining, slides were heated in ten mmol/L sodium citrate pH 6.8 for 5 minutes. Slides were incubated with 1:100 Alexa Fluor 488-phalloidin (Thermo Fisher, catalog no. A12379) and anti-pan-cytokeratin (Santa Cruz Biotechnology, catalog no. 8018) overnight at 4°C, and incubated with secondary anti-mouse-Alexa Fluor 647 (Thermo Fisher Scientific, catalog no. 31571) using the MOM kit. Sections were counterstained with 4',6-diamidino-2-phenylindole, dihydrochloride (DAPI) and mounted with PBS/glycerol.

### **Image quantification**

Five random fields/section were captured at 10 $\times$  magnification using the FL-Auto-EVOS System (Invitrogen). DAB staining was quantified as described previously ([10](#)). Briefly, images were imported into Adobe Photoshop, DAB staining was selected using the Magic Wand tool, copied, and saved a separate file. Images were opened in ImageJ (NIH, Bethesda, MD), and converted to grayscale. Background pixels were removed by threshold adjustment. Images were subject to particle analysis. Positive DAB values were normalized to total area values, expressed

as arbitrary units. To quantify stromal staining, epithelial tissues were cropped out in Adobe Photoshop. DAB staining was selected in stroma, copied to a new window and saved as a separate file. Images were opened in Image J and quantified. Stromal DAB values were normalized to total stromal values.

### **Scoring of tumor invasion**

Tissues were sectioned at 3 depths approximately 50  $\mu\text{m}$  apart. Two to 3 serial sections per depth were stained. Images were captured at 4 $\times$  and 10 $\times$  magnification and scored in a blinded fashion: 1 (non-invasive), 2 (lowly-invasive), or 3 (highly-invasive). For CK/ $\alpha$ -sma CO-IF, one indicated no invasion, with intact  $\alpha$ -sma<sup>+</sup> myoepithelium and confinement of epithelial cells within the duct; 2 indicated 50% or less disappearance of the  $\alpha$ -sma surrounding the duct and/or appearance of 3 or fewer cells invading through the duct; 3 indicated more than 50%  $\alpha$ -sma disappearance, with appearance of more than 3 cells invaded through the duct and making contact with the periductal stroma. For collagen IV and laminin immunostaining: 1 indicated well-defined expression in the basement membrane; two indicated additional low-level expression in lesion; three indicated higher expression in epithelium, with poor definition between epithelium and stroma. For phalloidin/pan-cytokeratin staining, one indicated a well-defined border between tumor and kidney, with a few tumor cells invaded into kidney tissue; two indicated some tumor-cell invasion, characterized by viable tumor cells present in kidney tissue; the border between kidney and tumor tissue was less defined; and three indicated high invasion characterized by extensive number of tumor cells in kidney tissue; tumor was embedded in kidney, and the border between kidney tissue and tumor were undefined.

### **Flow cytometry**

Flow cytometry staining for CCR2 expression was conducted as described (13). Briefly, adherent cells were detached from plastic by Accutase (Thermo Fisher Scientific, catalog no. A1110501), washed in PBS, and incubated with anti-CCR2-PE for 1 hour on ice. Samples were washed in PBS three times and analyzed on a LSRII flow cytometer, normalized to unstained controls.

### **Fibroblast proliferation assay**

Fibroblasts were seeded 30,000/well in 24-well plates overnight. DCIS.com cells (500,000) were seeded in 10-cm dishes, and incubated with 5-mL serum-free DMEM for 24 hours. Fibroblasts were treated with 500  $\mu$ L of DMEM or tumor conditioned medium for 24 or 48 hours. Fibroblasts were detached through trypsinization, quenched in DMEM/10% FBS and pelleted by microcentrifugation. Fibroblasts were resuspended in 50- $\mu$ L PBS and counted by hemocytometer.

### **Statistical analysis**

Cell culture experiments were repeated a minimum of 3 times. Data are expressed as mean  $\pm$  SEM. Statistical analysis was determined using two-tailed *t* test or ANOVA with Bonferroni *post hoc* comparisons for normal distributions and Kruskal–Wallis test with Dunn *post hoc* comparison for non-Gaussian distributions. Statistical analysis was performed using GraphPad Software. Significance was determined by  $P < 0.05$  (\*,  $P < 0.05$ ; \*\*,  $P < 0.01$ ; \*\*\*,  $P < 0.0001$ ; n.s., not significant or  $P > 0.05$ ).

### **Ethics approval and consent to participate**

All animal experiments were performed at KUMC according to guidelines from the Association for AALAC. Experiments were approved by the Institutional Animal Care and Use

Committee. Patient samples were collected under approval by Institutional Review Board (IRB) at KUMC. All samples were de-identified by the Biospecimen Core, an IRB-approved facility, prior to distribution

## Results

### **CCR2 overexpression in SUM225 cells enhances DCIS progression**

In DCIS, cancer cells grow, but remain within the boundaries of ducts and lobules, which are lined by  $\alpha$ -sma<sup>+</sup> myoepithelial cells and basement membrane, structural barriers between the stroma and duct. Progression from DCIS to IDC is characterized by disappearance of the myoepithelium and appearance of invading ductal carcinoma cells into the surrounding stroma [147]. To clarify the role of epithelial CCR2 expression in DCIS progression, we utilized MIND models established through injection of SUM225 and DCIS.com breast cancer cells. SUM225 breast cancer cells are lowly-invasive, of a luminal/Her2<sup>+</sup> subtype [148]. DCIS.com breast cancer cells, a basal-like subtype, are more highly-invasive [9]. By flow cytometry, CCR2 expression was significantly lower in SUM225 cells compared to DCIS.com breast cancer cells (Figure 8A). We first examined the effects of CCR2 overexpression on progression of SUM225 lesions. By lentivirus transduction, 2 different SUM225 cell lines were generated to overexpress CCR2 (CCR2-L and CCR2-H), and compared with SUM225 cells expressing pHAGE vehicle control (Figure 8A). These cells were MIND injected into NOD-SCID mice, and examined 7 weeks post-injection, when lesions were palpable. CCR2-overexpressing xenografts showed no significant changes in mammary tissue mass compared to pHAGE control (Figure 8B).

Extent of epithelial invasion in the mammary gland or breast tissue has been determined by evaluating myoepithelial integrity through  $\alpha$ -sma expression, and examining for presence of carcinoma cells contacting the surrounding stroma [9, 149-151]. To evaluate the effects of CCR2 overexpression on ductal invasion, we co-stained for  $\alpha$ -sma to define ductal myoepithelium, and for human specific CK19 to define SUM225 cells. Lesions were scored for

invasiveness. Non-invasive lesions had intact  $\alpha$ -sma<sup>+</sup> myoepithelium, lowly-invasive lesions showed reduced -sma expression, lining the breast duct, and a few invasive cancers. Highly-invasive lesions showed minimal  $\alpha$ -sma expression and multiple invasive cancer cells. In the pHAGE controls, 21 % were non-invasive, 51% were lowly-invasive and 28% were highly-invasive. Of CCR2-L MIND lesions, 12% were non-invasive, 57% were lowly-invasive and 31% were highly-invasive. Of CCR2-H MIND lesions, 8% were non-invasive, 66% were lowly-invasive and 26% were highly-invasive (Figure 8C). The decrease in lowly-invasive lesions and increase in highly-invasive lesions indicate a shift toward invasion.

To further characterize basement membrane invasion, mammary tissues were stained for laminin and collagen IV, which are basement membrane proteins associated with invasiveness in breast cancer [152, 153]. In non-invasive lesions, laminin and collagen IV were expressed in the basement membrane and surrounding stroma. In lowly-invasive lesions, laminin and collagen IV were also detected in the epithelium, correlating with a few invading epithelial cells. In highly-invasive lesions, laminin and collagen IV expression in lesions resulted in poorly-defined borders between stroma and epithelium. Consistent with CCR2 overexpression in SUM225 cells decreased the number of lowly-invasive lesions and increased the number of highly-invasive lesions (Figure 8). CCR2 overexpression was also associated with increased cell proliferation and decreased apoptosis as indicated by Ki67 and cleaved caspase-3 staining (Figure 8D-E). These data indicate that CCR2 overexpression in SUM225 cells enhances the progression of MIND xenografts.

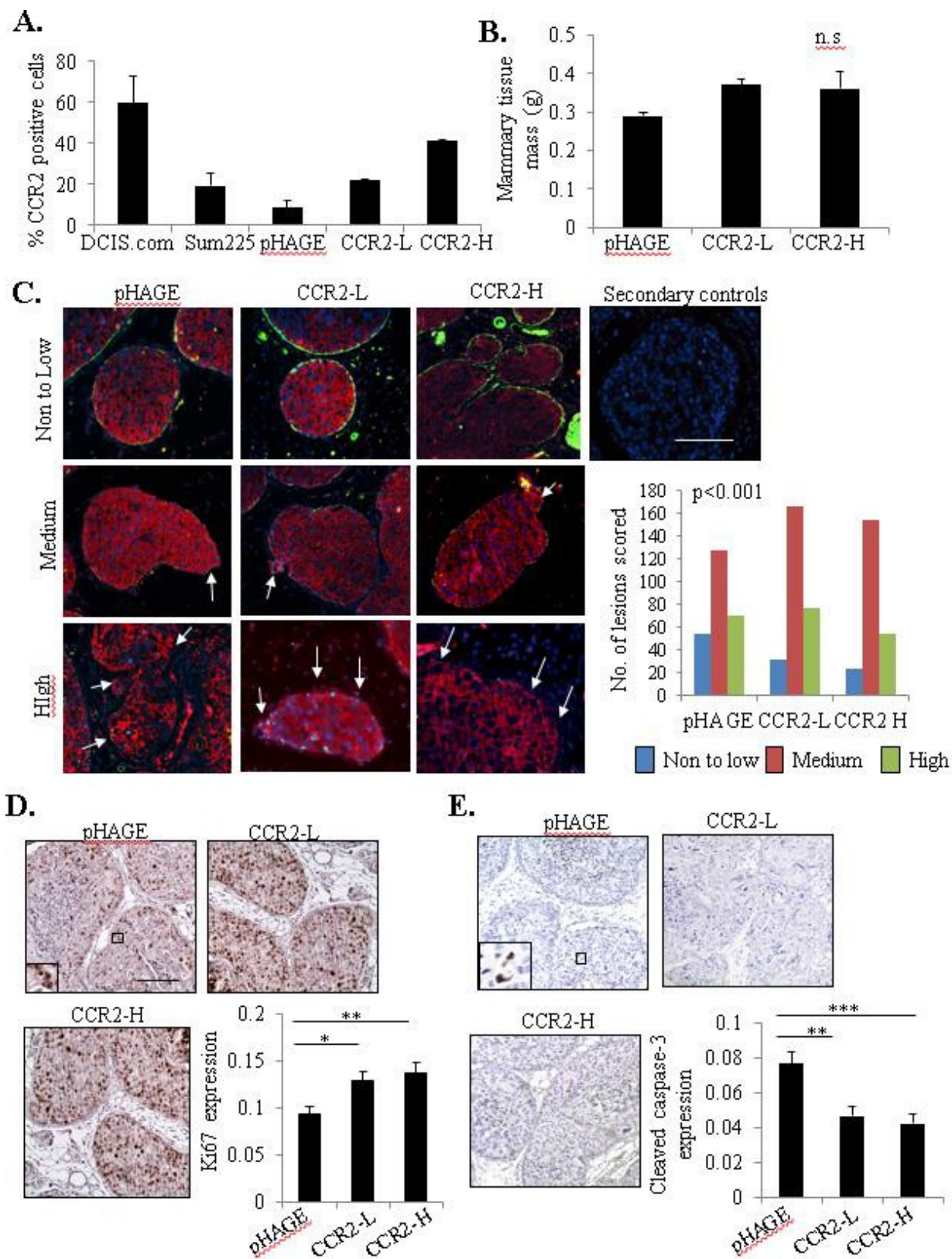


Figure 8 - CCR2 overexpression in SUM225 breast cancer cells enhances invasive progression

A. Flow cytometry analysis for CCR2 expression in parental DCIS.com or SUM225 parental cells or SUM225 cells expressing vehicle pHAGE control or CCR2 (CCR2-L, CCR2-H). Histogram analysis shown on left. Graph shows percentages of positive cells. B. Tissue mass of SUM225 MIND injected mammary glands C. SUM225 lesions were co-stained for CK-19 (red) and  $\alpha$ -sma (green), and scored for the number of invasive lesions n=252 lesions for control pHAGE, 272 lesions for CCR2-L, and 231 for CCR2-H group. Representative images are shown with secondary antibody control panel of anti-rabbit-Alexa-fluor488/anti-mouse-Alexa-fluor-568/DAPI overlay. Arrows indicate invasive foci. D-E. Image J quantification of immunostaining for Ki67 (D) or cleaved caspase-3 (E) in SUM225 lesions (arbitrary units). Arrows point to examples of positive staining. Statistical analysis was performed using One way ANOVA with Bonferonni post-hoc comparison (B, D, E) or Chi square test (C). Statistical significance was determined by  $p < 0.05$ . \* $p < 0.05$ . ns= not significant. Mean $\pm$ SEM values are shown. Scale bar=200 microns.

### **Knockdown or knockout of CCR2 in DCIS.com cells inhibits DCIS progression**

We next examined the effects of CCR2 deficiency on progression of DCIS.com lesions. Of the four shRNA sequences tested, one induced significant knockdown of CCR2 expression in DCIS.com cells (A). MIND injection of DCIS.com cells in NOD-SCID mice resulted in palpable mammary lesions at 4 weeks. CCR2 knockdown (CCR2-KD) decreased mammary tissue tumor growth compared to control shRNA expressing xenografts (Figure 9B). To examine for changes in ductal invasion, sections were CO-IF stained for  $\alpha$ -sma to identify the basement membrane and human specific CK5 to identify DCIS.com cells, and scored. These data indicate a shift toward less-invasive lesions in tumors with CCR2-KD (Figure 9C). CCR2 KD was also associated with decreased tumor-cell proliferation and increased apoptosis (Figure 9D-E).

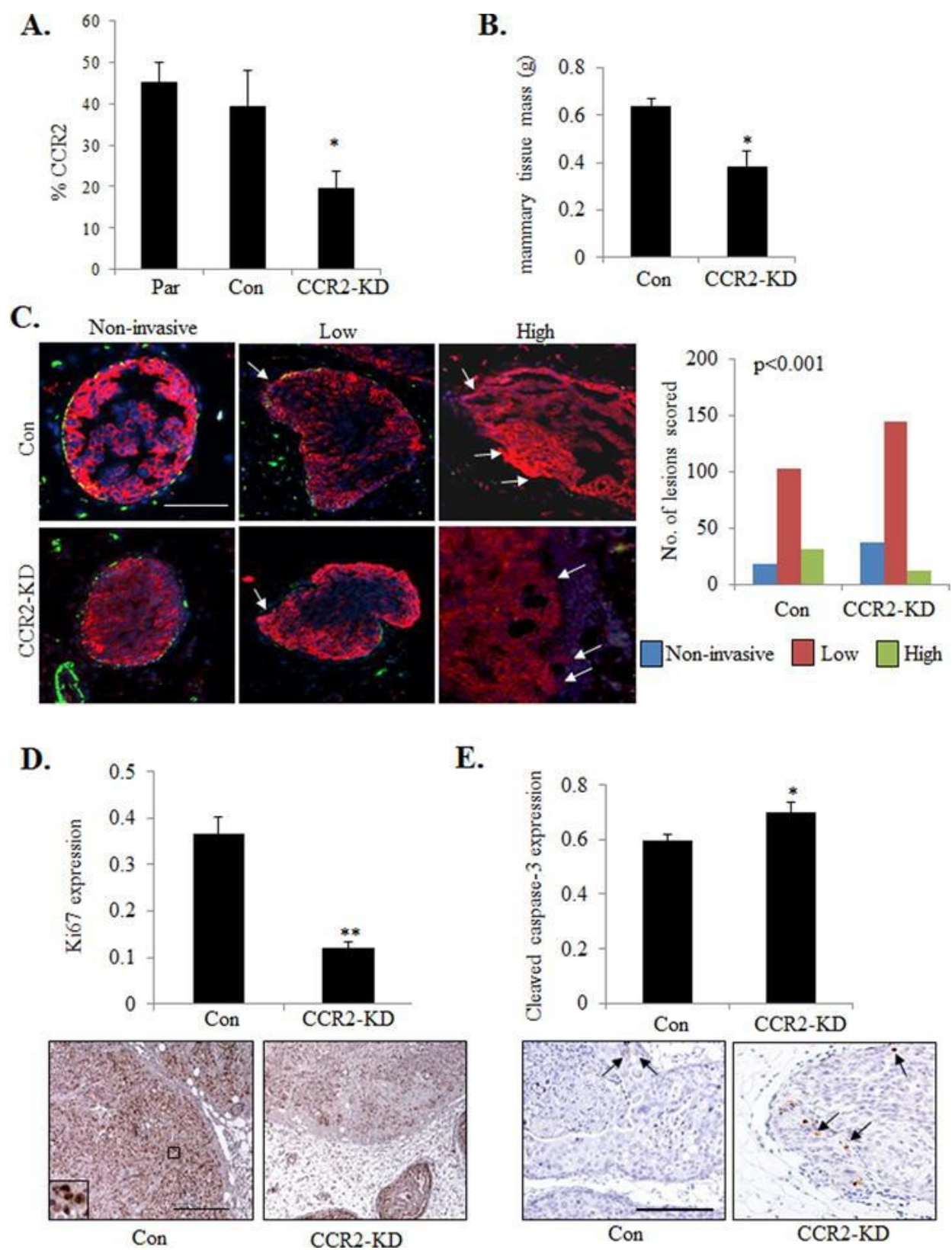


Figure 9 - shRNA mediated CCR2 knockdown in DCIS.com breast cancer cells inhibits invasive progression. **A.** Flow cytometry analysis for CCR2 expression in Parental (Par) or DCIS.com cells expressing control (Con) or CCR2 shRNA (CCR2-KD). **B.** Tissue mass of DCIS.com MIND injected mammary glands **C.** DCIS.com MIND lesions were co-stained for CK5 (red) and  $\alpha$ -sma (green) and counterstained with DAPI (blue). Representative images are shown with arrows pointing to invading tumor cells. Lesions were scored for invasiveness. n=152 lesions for control shRNA group, 193 lesions for CCR2-KD group. n=8 mice/group. **D-E.** Image J quantification of Ki67 (**D**) or cleaved caspase-3 (**E**) immunostaining in DCIS.com lesions. Arbitrary units are shown. Arrows point to examples of positive staining. Statistical analysis was performed using one-way ANOVA with Bonferonni post-hoc comparison (B, D, E) or Chi square test (C). Statistical significance was determined by  $p < 0.05$ . \* $p < 0.05$ , \*\* $p < 0.01$ . Scale bar=200 microns.

To confirm this invasive phenotype, we stained for 2 basement membrane proteins, collagen IV and laminin. These studies also revealed that there was decreased invasiveness in the CCR2 KD DCIS.com tumors compared to control (Figure 10A&B).

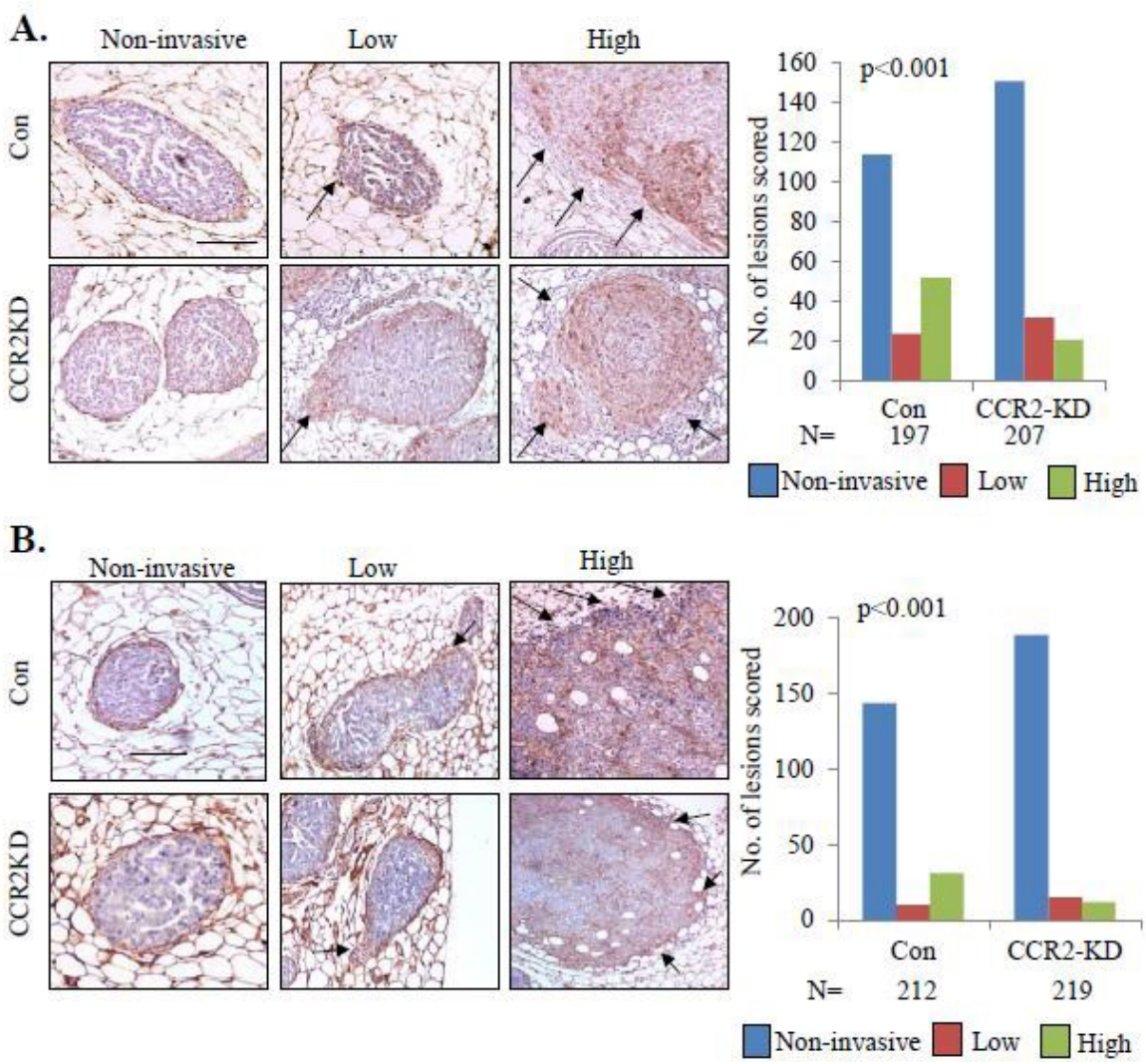


Figure 10 - Collagen and laminin expression in DCIS.com MIND lesions. CCR2 or control shRNA expressing DCIS.com MIND lesions were immunostained for A. collagen IV or B. laminin expression. Total sample size per group (N) are shown below graphs. Arrows point to areas of invasiveness. Scale bar= 200 microns. Statistical analysis was performed using Chi Square test. Statistical significance was determined by p<0.05.

To validate the effects of CCR2-KD on DCIS.com progression, the CCR2 gene was knocked out by CRISPR. Two wild-type clones and one homozygous knockout clone (CCR2-KO) were identified from 70 clones. By flow cytometry, wild-type clones showed similar CCR2 expression levels to parental cells, while CCR2-KO cells showed a significant reduction in CCR2 expression (Figure 11A). MIND injection of CCR2-KO cells resulted in a significant reduction in mammary tissue mass and fewer invasive lesions (Figure 11B&C), compared to WT xenografts. These data show that CCR2 KD or KO inhibits the progression from DCIS to IDC in DCIS.com breast cancer xenografts.

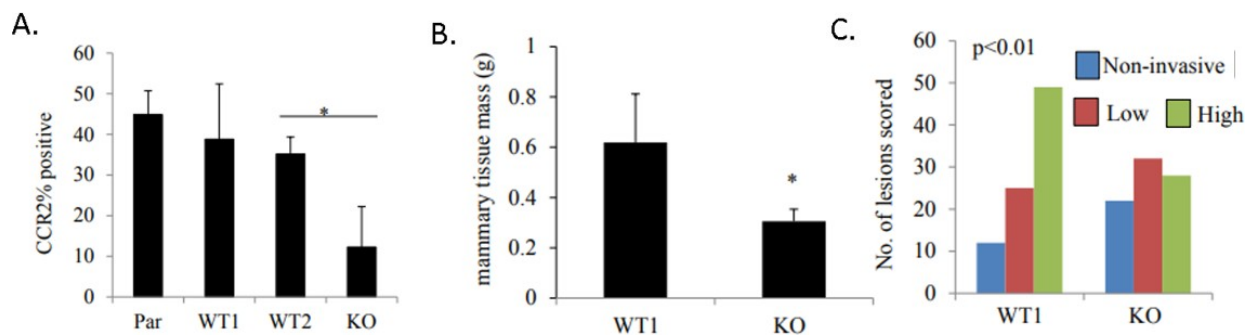


Figure 11 - Knockout of CCR2 in DCIS.com cells significantly decreases tumor growth and invasion in the MIND model. A. Flow cytometry analysis of WT and KO cells in comparison with parental (Par) cells. B&C. MIND model injection of WT1 or KO cells were examined for changes in mammary gland weight (B) or invasion (C). Statistical analysis was performed using One-way ANOVA with Bonferonni post-hoc comparison (A), Two-Tailed-test (B), or Chi square test (C). Statistical significance was determined by  $p < 0.05$ . \* $p < 0.05$ . Mean+SEM values are shown.

Increased angiogenesis, fibrosis and macrophage recruitment are associated with invasive breast cancer [147]. To determine how epithelial CCR2 expression affected the surrounding mammary stroma, immunostaining was performed to analyze expression of biomarkers for macrophages (F4/80) and endothelial cells (VWF8). To account for fibroblast heterogeneity, we immunostained for 2 different markers: Fsp1 and PDGFR-A [154, 155]. DAB expression of stromal biomarkers was quantified by pixel density analysis and normalized to total stromal area, using an Image J protocol described previously [127]. There were no significant changes in VWF8 or F4/80 expression with CCR2 overexpression or knockdown (Figure 12A&B). Fsp1 and PDGFR- $\alpha$  were expressed in fibroblastic stroma and in epithelial cells, consistent with studies showing mesenchymal marker expression in breast cancer cells [127, 156].

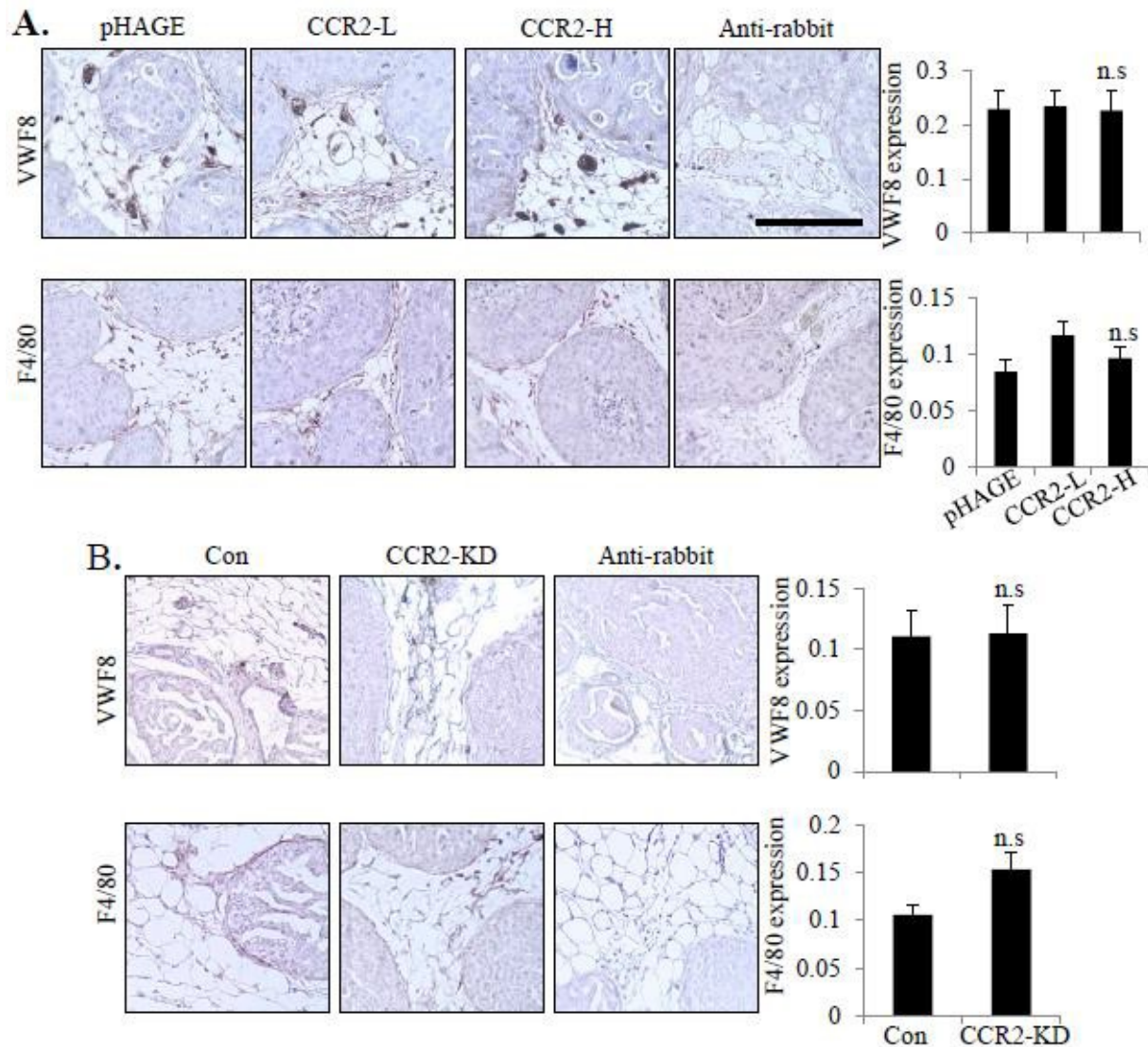


Figure 12 - Effect of CCR2 overexpression and knockdown on stromal reactivity. Immunostaining for VWF8 or F4/80 expression was performed in **A.** SUM225 MIND lesions or **B.** DCIS.com MIND lesions. Secondary rabbit biotinylated antibody staining shown as a control. Scale bar=200 microns. Statistical analysis was determined using One Way ANOVA with Bonferonni post-hoc comparisons to all groups. Statistical significance was determined by  $p < 0.05$ . n.s.=not significant. Values shown as mean+SEM.

CCR2 overexpressing SUM225 xenografts showed increased stromal expression of Fsp1 and PDGFR-A (Figure 13A-B), associated with stromal CCL2 expression (Figure 13C). Conversely, CCR2 deficient DCIS.com MIND xenografts showed a significant decrease in fibroblastic cells and decreased CCL2 expression in the stroma (Figure 14). These data indicate that CCR2 overexpression or knockdown is associated with changes in CCL2 expressing fibroblasts in the DCIS stroma.

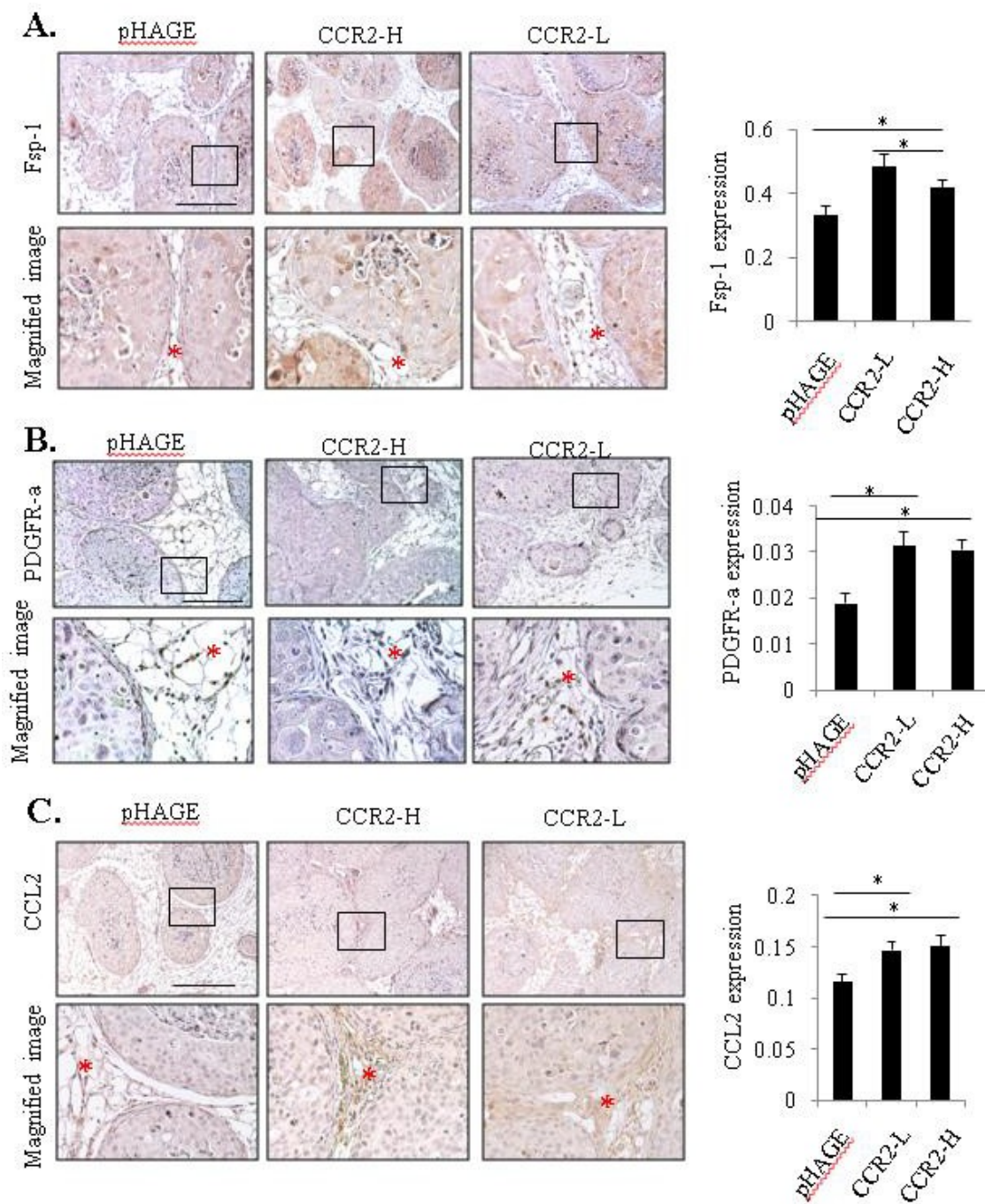


Figure 13 - CCR2 overexpression in SUM225 MIND xenografts increases the levels of CCL2 expressing fibroblasts. Sum 225 MIND lesions were immunostained for A. Fibroblast Specific Protein 1 (Fsp1), B. Progesterone Growth Factor Receptor- $\alpha$  (PDGFR- $\alpha$ ), or C. CCL2 expression. Representative images are shown with magnified image underneath. The stroma is marked with an asterisk in the magnified image. Expression in the stroma was quantified by Image J, in arbitrary units. Statistical analysis was performed using one-way ANOVA with Bonferonni post-hoc comparison. Statistical significance was determined by  $p < 0.05$ . \* $p < 0.05$ , \*\*\* $p < 0.001$ . Mean  $\pm$  SEM values are shown. Scale bar=400 microns.

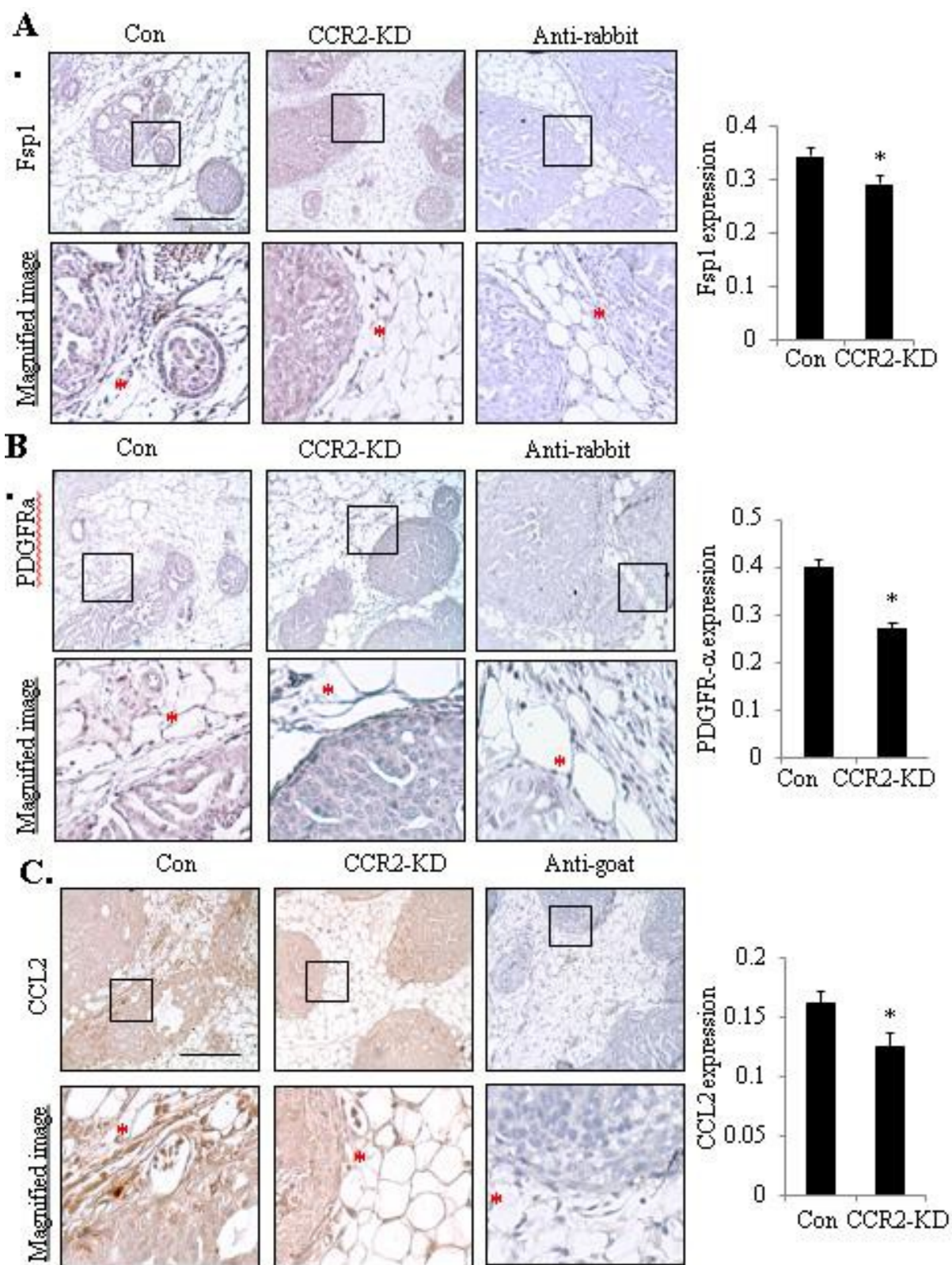


Figure 14 - CCR2 shRNA knockdown in DCIS.com MIND xenografts reduces the levels of CCL2 expressing fibroblasts DCIS.com MIND lesions were immunostained for A. Fibroblast Specific Protein 1 (Fsp1), B. Progesterone Growth Factor Receptor- $\alpha$  (PDGFR- $\alpha$ ) or C. CCL2 expression. Representative images are shown with magnified image underneath. Asterisk denotes stroma. Statistical analysis was performed using Two-Tailed T-test (B). Statistical significance was determined by  $p < 0.05$ . \* $p < 0.05$ . Mean $\pm$ SEM values are shown. Scale bar= 400 microns.

## **CCL2 from DCIS fibroblasts is important for CCR2 mediated breast cancer survival and invasion**

While previous studies have established an important role for carcinoma-associated fibroblasts from invasive breast cancers [157, 158], the role of fibroblasts derived from DCIS tissues remain poorly understood. To figure out the functional role of CCL2 derived from DCIS fibroblasts in CCR2 mediated breast cancer progression, we utilized the subrenal capsule model. Mammary carcinoma cells grafted in the subrenal capsule form tumors similarly to orthotopic injection [7, 8]. Unlike injecting into the stroma-rich mammary gland, the subrenal capsule space is devoid of fibroblasts and is immunologically privileged, enabling us to determine the relative contribution of co-grafted fibroblasts without interference from host stroma. To establish whether tumoral CCR2 affects tumor formation and progression in the absence of stroma, DCIS.com cells with CCR2-KD or control shRNA were grafted without fibroblasts. CCL2 levels were significantly lower in the CCR2 KD tumor cells (Figure 15A), but DCIS.com cells grafted alone did not show significant differences in tumor growth or invasion compared to control shRNA cells grafted alone (Figure 15B-C).

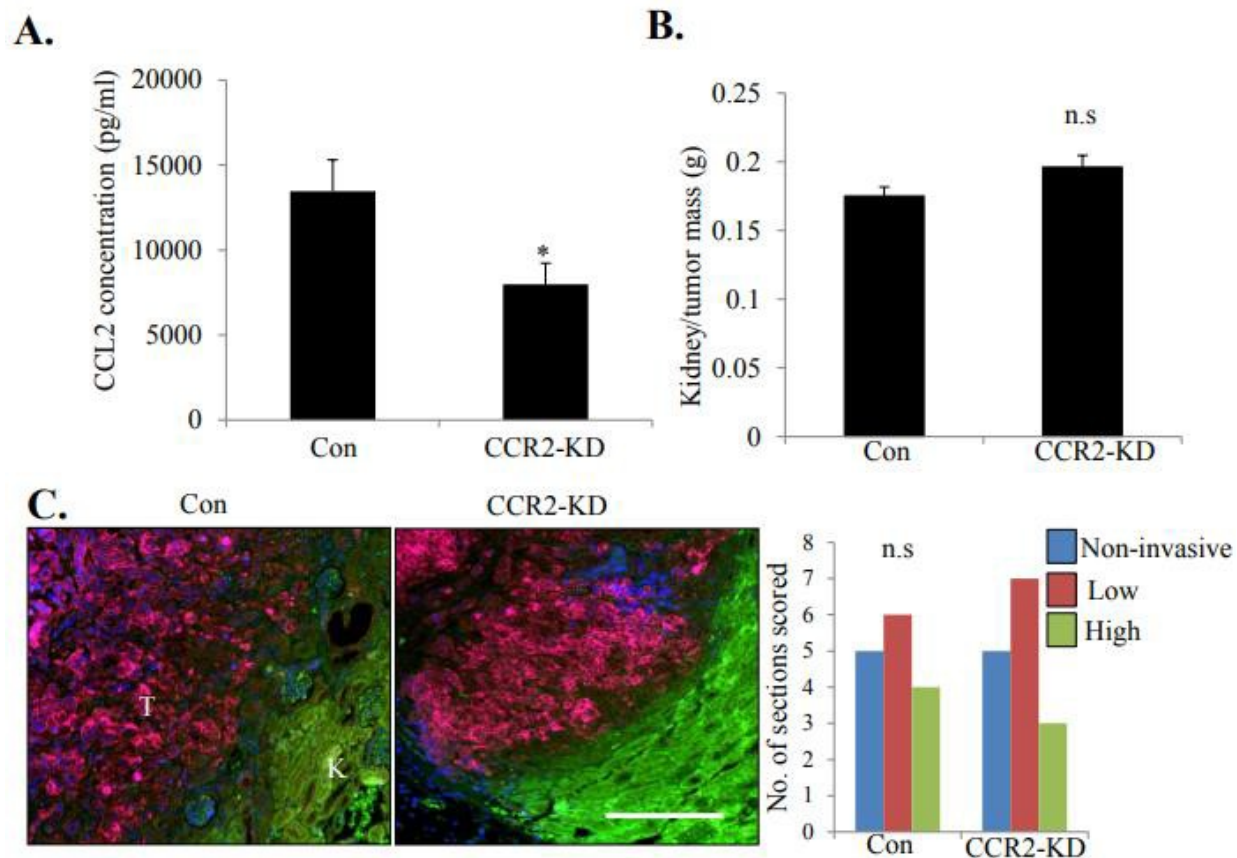


Figure 15 - CCR2 knockdown alone does not significantly affect progression of DCIS.com breast cancer cells. A. CCL2 ELISA of conditioned medium from Control shRNA (Con) or CCR2 shRNA expressing (CCR2-KD) DCIS.com breast cancer cells B. Tumor mass of DCIS.com cells grafted alone in the kidney capsule of NOD-SCID mice. C. Scoring of tumor sections immunostained with antibodies to pan-cytokeratin (red) and phalloidin (green). 3 sections/tumor, n=5 samples/group. T=tumor, K=Kidney. Scale bars = 200 microns. Statistical analysis was performed using Two-Tailed T-test. Statistical significance was determined by  $p < 0.05$ .

To further characterize the expression of CCL2 in DCIS stroma, fibroblasts were isolated from patient samples of normal breast (named hNAF2525, hNAF8727) or DCIS tissues (named 1213-249, 80H, HPO70213) and analyzed for CCL2 expression. By ELISA, the 80H and 1213-249 DCIS-derived fibroblast lines expressed higher levels of CCL2 compared to normal fibroblasts and DCIS.com cells ( Figure 16A). To determine the role of fibroblast-derived CCL2 on tumor growth and invasion, DCIS.com cells were co-grafted into the renal capsule of NOD-SCID mice with 1213-249. Fibroblasts co-grafted with parental DCIS.com cells had increased tumor mass compared to DCIS.com cells grafted alone ( Figure 16B). CCR2 deficient DCIS.com cells co-grafted with 1213-249 fibroblasts showed a 20% decrease in tumor mass compared to fibroblasts co-grafted with control DCIS.com cells

To examine for changes in tumor invasion into normal kidney tissue, we performed CO-IF staining for pan-cytokeratin (pan-CK) and phalloidin to distinguish tumor cells from kidney tissues. In the subrenal capsule model, pan-CK antibodies stained DCIS.com tumors more clearly than CK5 antibodies used in the MIND model. Pan-CK antibodies recognized CK:4,5,6,8,10,13 and 18, and preferentially stained breast cancer cells over kidney tissues, which expressed fewer of the cytokeratins [159]. Using this approach, tumor invasion was characterized by a poorly-defined border between tumor and kidney tissues. CCR2 deficient cells co-grafted with fibroblasts showed a reduction in tumor invasion, characterized by more cohesive tumors and a clearer delineation between tumor and kidney tissues than control tumors (Figure 16 C). CCR2 KD also inhibited proliferation and increased apoptosis by PCNA and CC3 staining (Figure 16D-E). CCR2-KD DCIS.com cells grafted alone did not show significant differences in tumor growth or invasion compared to control shRNA cells grafted alone (Figure 17). These

studies indicate that CCR2 knockdown in DCIS.com breast cancer cells inhibit fibroblast-mediated tumor growth and invasion.

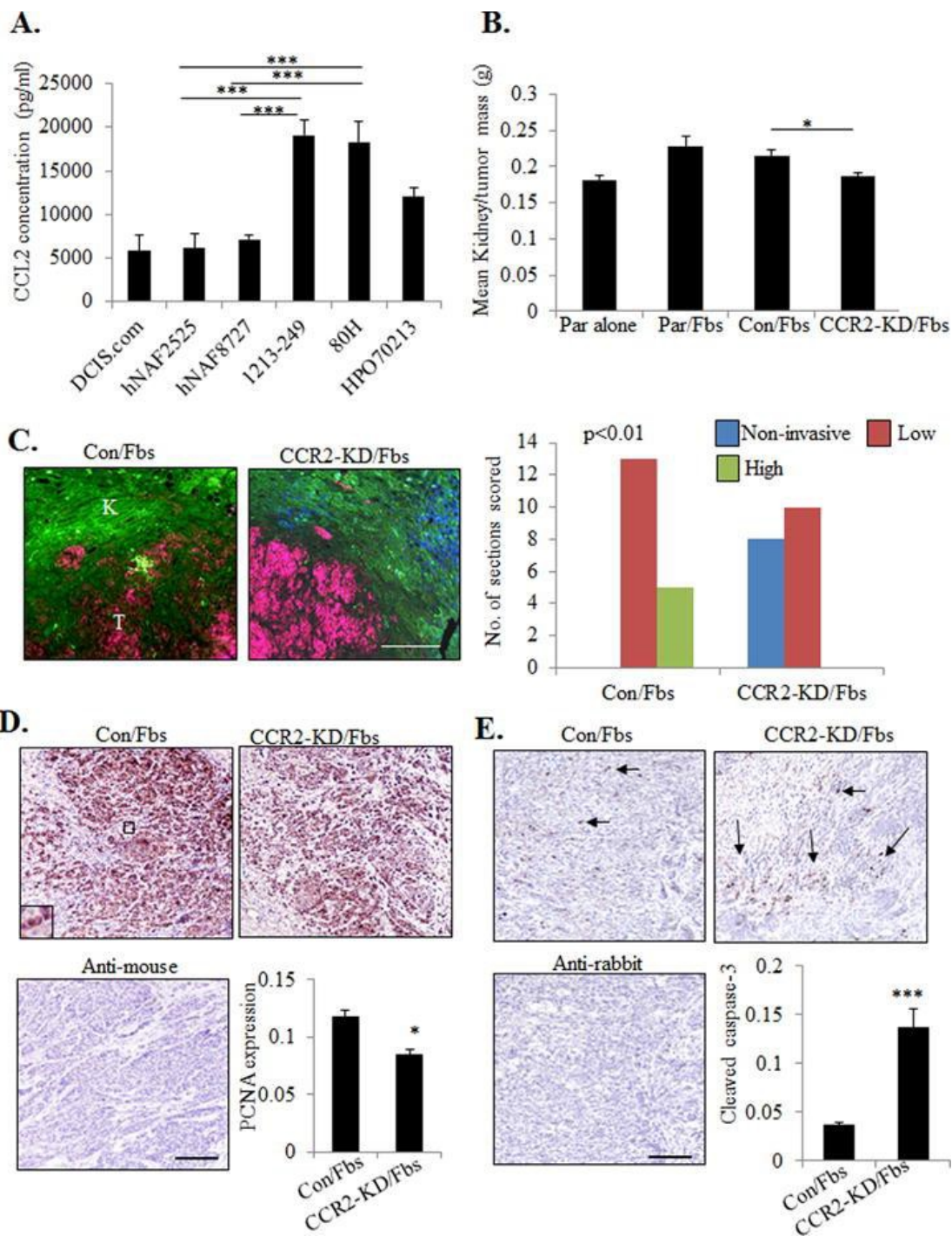


Figure 16 - CCR2 knockdown in DCIS.com cells inhibits fibroblast-mediated cancer progression. A. CCL2 ELISA of conditioned medium from fibroblasts derived from normal breast (hNAF2525, hNAF8727) or DCIS tissues (1213-249, 80H, HPO70213), in comparison with DCIS.com breast cancer cells. B-E. 1213-249 fibroblasts (Fbs) were co-grafted with parental (Par) DCIS.com cells or DCIS.com cells expressing control (Con) or CCR2 shRNAs (CCR2-KD) in the subrenal capsule of NOD-SCID mice for 21 days. Kidney tissues were measured for tumor mass (B), scored for tumor invasion into normal kidney by pan-cytokeratin (red) and phalloidin (green) staining (C), tumor-cell proliferation by PCNA immunostaining (D), tumor-cell apoptosis by cleaved caspase-3 immunostaining (E). Scale bar=400 microns. Arrows point to examples of positive staining. Expression in tissues was quantified by Image J. n=7 mice per group. Statistical analysis was performed using One-way ANOVA with Bonferonni post-hoc comparison (B) or Two-Tailed T-test (D, E). Statistical significance was determined by  $p < 0.05$ . \* $p < 0.05$ , \*\*\* $p < 0.001$ . Mean $\pm$ SEM are shown.

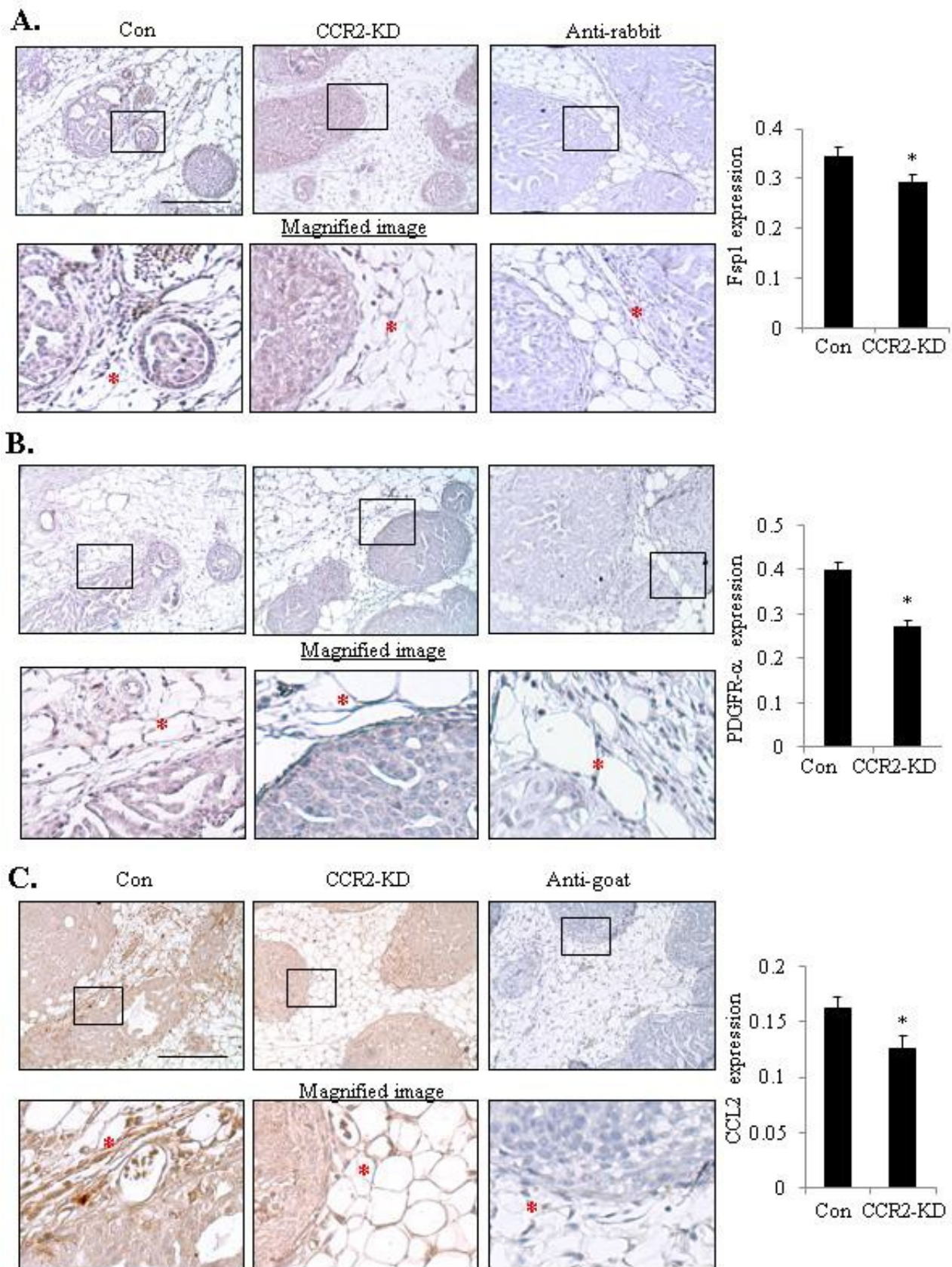


Figure 17 - CCR2 shRNA knockdown in DCIS.com MIND xenografts reduces the levels of CCL2 expressing fibroblasts. DCIS.com MIND lesions were immunostained for A. Fibroblast Specific Protein 1 (Fsp1), B. Progesterone Growth Factor Receptor- $\alpha$  (PDGFR- $\alpha$ ) or C. CCL2 expression. Representative images are shown with magnified image underneath. The stroma is marked with an asterisk in the magnified image. Expression in the stroma was quantified by Image J, in arbitrary units. Statistical analysis was performed using Two-Tailed T-test (B).

To determine the relevance of CCL2 expression in DCIS fibroblasts, fibroblasts were immortalized by hTERT expression to enable stable shRNA expression. Two CCL2 deficient fibroblast lines were generated from 2 different shRNA systems. A 47% decrease in CCL2 expression was observed using the GFP-c-shLenti Origene system (CCL2-pLenti). A 30% decrease in CCL2 expression using the GIPZ Dharmacon system (CCL2/GIPZ) (Figure 18A). CCL2 deficient or control fibroblasts were co-grafted with DCIS.com breast cancer cells in the subrenal capsule and analyzed for changes in tumor progression. CCL2 deficient fibroblasts co-grafted with DCIS.com cells resulted in smaller tumors and reduced tumor invasion, associated with decreased tumor-cell proliferation and increased apoptosis ( Figure 18B-C). These studies indicate that CCL2 derived from DCIS fibroblasts enhances progression of DCIS.com breast cancer tumors.

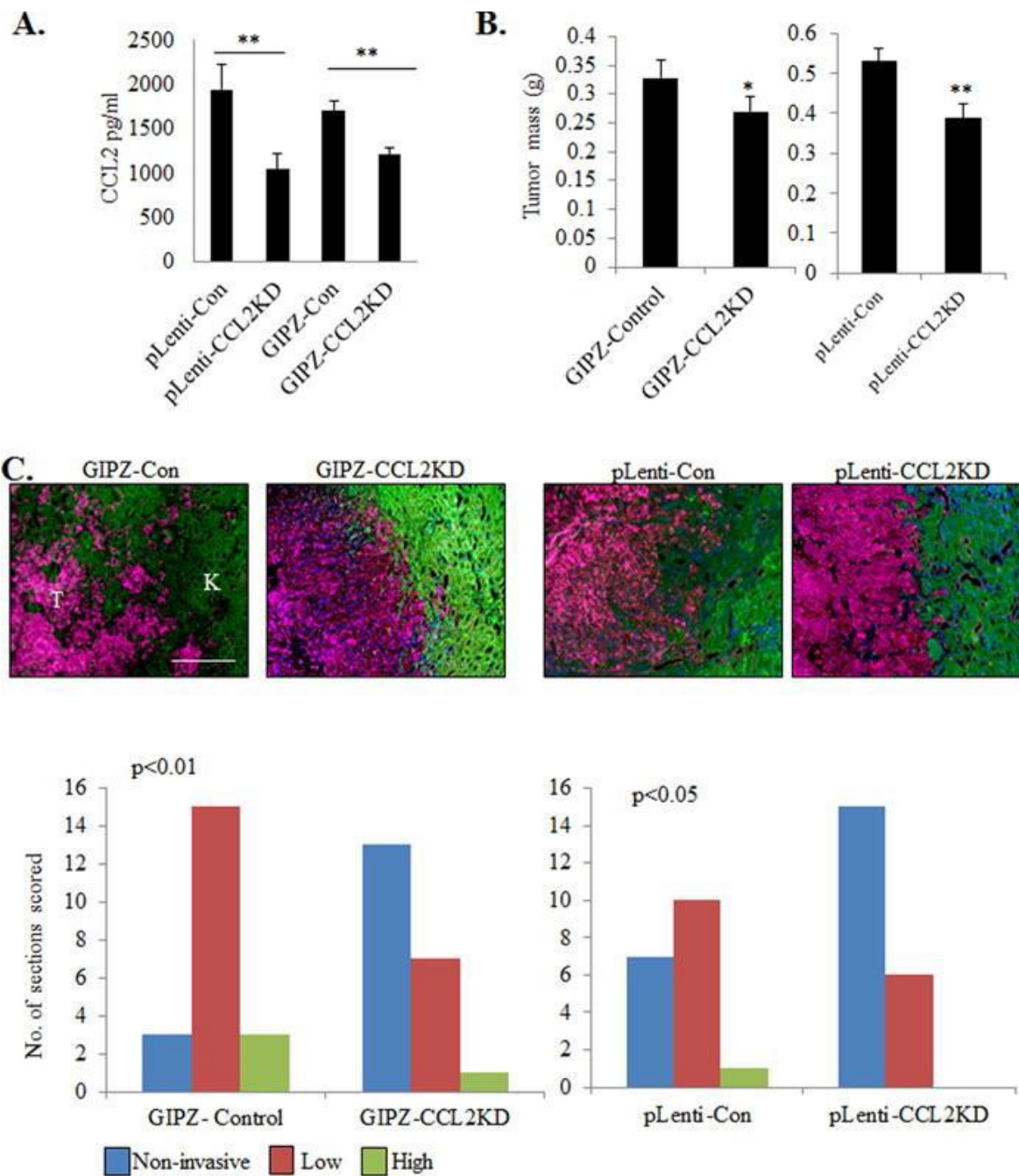


Figure 18 - CCL2 derived from DCIS fibroblasts is important for progression of DCIS.com breast cancer cells. A. CCL2 ELISA of 1213-249 fibroblasts expressing control shRNA (Con) or CCL2 shRNAs from pLenti or GIPZ lentivirus systems. B-C. Control or CCL2 deficient 1213-249 fibroblasts were co-grafted with DCIS.com breast cancer cells in the subrenal capsule and analyzed for changes in tumor growth (B), and scored for tumor invasion into normal kidney tissue by pan-cytokeratin (red) and phalloidin (green) staining (C). N=7 mice/group. Scale bar=400 microns. K=kidney, T=tumor. Statistical analysis was performed using one-way ANOVA with Bonferonni post-hoc comparison. Statistical significance was determined by  $p < 0.05$ . \*\* $p < 0.01$ . Mean  $\pm$  SEM are shown.

## CCL2/CCR2 mediated invasion is associated with increased ALDH1A1 and decreased HTRA2 expression

Lastly, we analyzed the relationship between expression of downstream CCL2/CCR2 signaling proteins and increased breast cancer survival and invasion. Through candidate screening of factors related to breast cancer survival and invasion, we found that CCL2 treatment of DCIS.com breast cancer cells over time increased expression of ALDH1A1, a stem cell marker and pro-invasive factor, and reduced expression of HTRA2, a pro-apoptotic mitochondrial serine protease (Figure 19A & B) [160] [161].

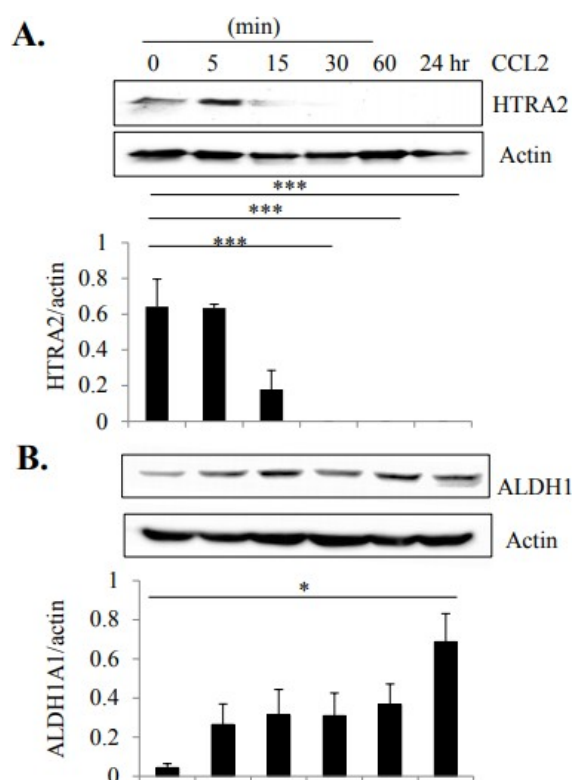


Figure 19 - CCL2 treatment of DCIS.com breast cancer cells increase ALDH1 and decreases HTRA2 expression. Immunoblot for A. HTRA2 and B. ALDH1A1 expression in DCIS.com breast cancer cells treated with 60 ng/ml CCL2 for up to 24 hours. Expression levels were determined by densitometry analysis. Experiments were performed in triplicate. Statistical analysis was performed using One Way ANOVA with Bonferonni post-hoc comparison. Statistical significance was determined by  $p < 0.05$ . \* $p < 0.05$ , \*\* $p < 0.01$ . Mean  $\pm$  SEM are shown.

CCR2 knockdown in DCIS.com breast cancer cells decreased expression of ALDH1A1 and increased HTRA2 in MIND xenografts by immunohistochemistry staining (Figure 20A-B).

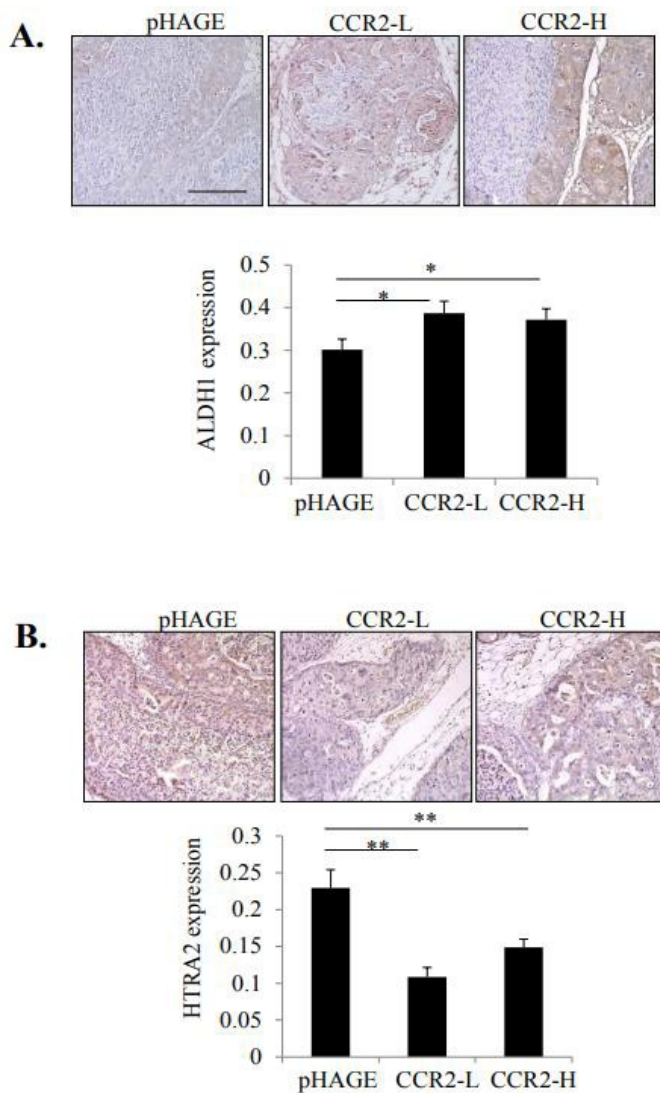


Figure 20 - Effect of CCR2 overexpression on ALDH1 and HTRA2 expression in SUM225 MIND xenografts. Sum225 MIND xenografts were immunostained for A. ALDH1 or B. HTRA2 expression. Expression was measured by Image J (arbitrary units). Statistical analysis was performed using One Way ANOVA with Bonferroni post-hoc comparison. Statistical significance was determined by  $p < 0.05$ . \* $p < 0.05$ , \*\* $p < 0.01$ . Mean+SEM values are shown. n=8 mice per group.

Conversely, CCR2 overexpression in Sum255 MIND xenografts enhanced ALDH1A1 expression and decreased HTRA2 expression (Figure 21A-B), indicating that epithelial CCR2 can regulate ALDH1A1 and HTRA2 expression. Furthermore, CCL2 knockdown in fibroblasts increased HTRA2 expression and decreased ALDH1 expression in DCIS.com cells in the subrenal capsule model ( Figure 21C-D), indicating that paracrine CCL2 signaling from the fibroblastic stroma was important for regulating ALDH1A1 and HTRA2 expression. Through KM Plotter analysis [162], increased CCR2 and ALDH1A1 and decreased HTRA2 expression were significantly associated with decreased metastasis free survival of breast cancer patients (Figure 21E). These data demonstrate a clinical relevance for CCL2/CCR2 signaling proteins in breast cancer.

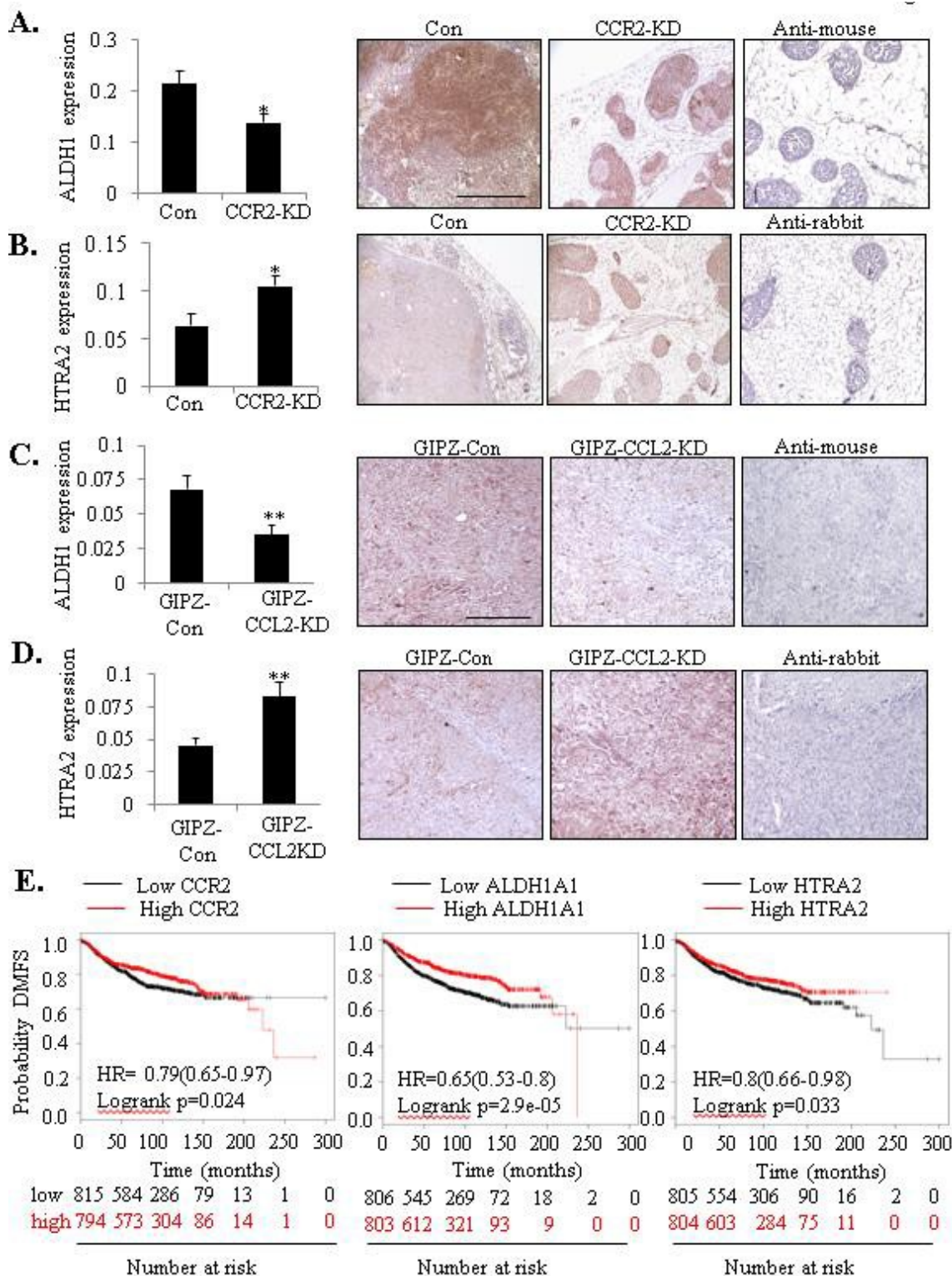


Figure 21- CCL2/CCR2 mediated DCIS progression is associated with increased ALDH1 and decreased HTRA2 expression. **A-D**. ALDH1 and HTRA2 expression was examined by immunostaining of tumor tissues in the DCIS.com MIND Model (A-B) and subrenal capsule model (C-D). Expression in tissues was quantified by Image J. K=kidney tissue. T= tumor. Scale bar= 400 microns. **E**. RNA Expression of CCR2 (Affyid 207794\_at), ALDH1A1 (Affyid 212224\_at) and HTRA2 (Affyid 2030809\_s\_at) were analyzed for associations with Distance Metastasis Free Survival (DMFS) through KM Plotter. Statistical analysis was performed using Two-Tailed-T-test (A-B) or Log-rank Test (C). HR= Hazard Ratio. Statistical significance was determined by  $p < 0.05$ . \* $p < 0.05$ , \*\* $p < 0.01$ . Mean  $\pm$  SEM are shown.

## Discussion

The role of fibroblasts in DCIS progression is poorly understood. Fibroblasts derived from invasive breast ductal carcinomas promote tumor growth, invasion, metastasis and chemoresistance (32,33). One study showed that fibroblasts from normal, IDC or arthritic tissues enhanced progression of MCF10A cell lines in a subcutaneous injection model through Transforming Growth Factor- $\beta$  and Hedgehog dependent mechanisms (38). For the first time, we show that fibroblasts derived from DCIS patient samples accelerate progression from DCIS to IDC through CCR2 dependent mechanisms. Moreover, CCL2/CCR2 mediated breast cancer progression is associated with increased expression of clinical relevant pro-invasive factors (ALDH1A1) and decreased expression of pro-apoptotic factors (HTRA2).

Here, we noted some complementary and conflicting phenotypes through CCR2 overexpression and knockdown. CCR2 overexpression in SUM225 cells enhanced formation of invasive lesions and increased the presence of CCL2+ fibroblasts, associated with increased ALDH1 and decreased HTRA2. CCR2 knockdown and knockout in DCIS.com cells inhibited invasive progression and decreased the presence of CCL2+ fibroblasts, associated with decreased ALDH1 and increased HTRA2 expression. However, whereas CCR2 knockdown significantly affected mammary tumor mass, CCR2 overexpression did not. While CCR2 overexpression increased tumor-cell proliferation and survival of SUM225 lesions, these levels were still lower than the cell proliferation and survival detected in DCIS.com MIND xenografts. CCR2 expression levels in overexpressing cells did not reach the levels detected in DCIS.com breast cancer cells. Therefore, it is possible that the increase in cell proliferation and survival in CCR2 overexpressing cells was not sufficient to affect overall mammary tissue mass. The levels of CCR2 expression in DCIS.com cells are consistent with previous studies showing that CCR2

expression levels are higher in basal-like breast cancer cells compared to luminal breast cancer cells (13). Because SUM225 cells are luminal/Her2+, additional oncogenic pathways may be important to DCIS progression of this subtype. Regardless of subtype, by analyzing the effects of CCR2 overexpression in SUM225 cells with CCR2 knockdown in DCIS.com cells, we demonstrate a critical role for epithelial CCR2 receptor expression in DCIS progression.

Despite a two-fold increase in the number of CCR2+ cells in the CCR2-H SUM225 cell line, CCR2-H cells did not show increased invasion, proliferation or survival compared to CCR2-L cells. It is possible a threshold of receptor expression modulates cellular activity. Such a threshold has been detected in T cells whereby 8000 T cell receptors/cell are needed for a commitment to proliferate (39,40). A threshold also exists for EGFR levels in regulating Cbl and Grb2 dependent signaling in epithelial cells (41). In our studies, CCR2-L cells may have reached a threshold for CCR2 expression in determining cellular invasion. While more cells expressed CCR2 in the CCR2-H cell line, the level of expression may not have been sufficient to commit these cells to invade. Histogram analysis revealed that while more cells overexpressed CCR2 in the CCR2-H cell line, expression levels did not vary highly between CCR2-L and CCR2-H cells. In addition to a receptor threshold, heterogeneity in expression of intracellular signaling components in breast cancer (42) may also explain why CCR2-H cells did not result in further DCIS progression. As we are unable to control which SUM225 cells express CCR2, it is possible some CCR2 overexpressing cells did not exhibit the necessary downstream signaling components to induce invasion. As CCR2 overexpression in SUM225 cells did not reach the levels of invasion detected in DCIS.com cells, it is likely that other oncogenic factors would be required to further enhance carcinoma invasion. Several oncogenic signaling pathways including Notch, EGF, and HGF signaling are associated with DCIS progression (43,44). It would be of

interest to further understand how CCL2/CCR2 coordinates DCIS progression with other oncogenic factors.

We also observed that CCR2 overexpression and knockdown affected the levels of fibroblasts in DCIS stroma. We expected that CCR2 signaling in breast cancers modulated fibroblast growth through expression of soluble growth factors such as PDGF and WNT5A, positive regulators of fibroblast proliferation (45,46). However, cultured DCIS fibroblasts treated with conditioned medium from CCR2 deficient or control DCIS.com control cells showed no significant changes in cell growth (Figure 22).

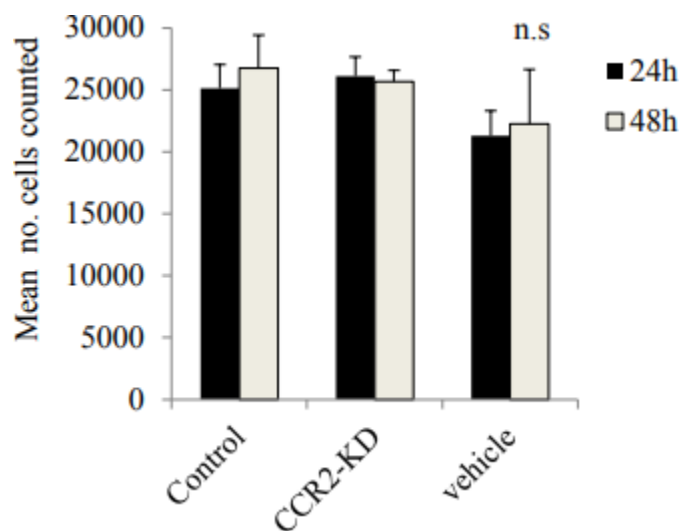


Figure 22 - CCR2 deficiency in DCIS.com breast cancer cells does not affect fibroblast growth. Conditioned medium from control shRNA or CCR2-KD DCIS.com cells were used to treat 1213-249 DCIS fibroblasts. Fibroblasts were counted after 24 and 48 hours of treatment by hemocytometer. Serum free medium was used as a vehicle control. Statistical significance was determined by One Way ANOVA with Bonferonni post-hoc comparison. Statistical significance was determined by  $p < 0.05$ . \* $p < 0.05$ , \*\* $p < 0.01$ . Mean  $\pm$  SEM are shown.

Furthermore, there were no changes in blood vessel density or macrophage recruitment, indicating that epithelial CCR2 would not regulate fibroblast accumulation indirectly through these stromal cell types. It is possible that epithelial CCR2 acts on other stromal components to indirectly modulate fibroblast growth, including adipocytes or granulocytes. Another possibility may involve the extracellular matrix. Hyaluronan and fibronectin increase fibroblast cell growth, while collagen suppresses fibroblast growth through mechano-signal transduction mechanisms (47,48). These factors would be present in mammary tissues, but not in conditioned medium. Studies are currently underway to understand how CCL2/CCR2 signaling breast cancer cells modulate the surrounding breast tumor microenvironment.

We show that increased ALDH1 and decreased HTRA2 expression are associated with CCL2/CCR2 mediated DCIS progression. Previous studies have implicated ALDH1 expression in cancer stem cell renewal, invasion and drug resistance (49). Emerging studies indicate an important role for HTRA2 in positively regulating mitochondrial dependent apoptosis (50). The increased expression of HTRA2 in CCR2 deficient lesions is consistent with the increased expression of cleaved caspase-3, as an indicator of apoptosis. CCL2/CCR2 signaling in breast cancer cells may promote DCIS progression by enhancing ALDH1+ tumor initiating cells, or activating invasive pathways through ALDH1 activity in breast cancer cells. CCL2/CCR2 signaling may facilitate survival of DCIS lesions through suppression of HTRA2 mediated apoptosis pathways.

In summary, these studies identify a novel role for CCL2/CCR2 signaling in cancer progression, identify potentially new prognostic factors for DCIS, and potentially new molecular targets for the prevention of invasive breast cancer.

Chapter 4: CCR2 signaling in breast carcinoma cells enhances tumor growth and invasion by coordinating cytokine-dependent crosstalk with tumor microenvironment

## Introduction

Invasive breast cancers are characterized by inflammation, including increased angiogenesis, tissue remodeling, and immunosuppression. Elevated M2 macrophages[163, 164], and decreased CD8<sup>+</sup> cytotoxic T cells are associated with poor prognosis of luminal and basal-like breast cancers. [165, 166] [167] M2 macrophages support tumor growth and progression through secretion of growth factors, angiogenic factors and extracellular matrix proteins. M2 macrophages also suppress T cell proliferation and inhibit the ability of CD8<sup>+</sup> T cell to interact with, and eliminate tumor cells[168-171]. Macrophage recruitment and activity are regulated in part by chemokines, small soluble molecules (8kda) that form molecular gradients to induce cellular chemotaxis[172, 173]. The chemokine C-C ligand 2 (CCL2) regulates macrophage recruitment by signaling to CCR2, a seven-transmembrane G-protein-coupled receptors[172, 174]. CCL2 overexpression by tumor cells correlates with macrophage recruitment, tumor vascularity, and poor patient prognosis[102, 138, 175]. Targeting CCL2 through siRNA or antibody neutralization inhibits macrophage recruitment associated with decreased breast tumor growth, invasion and metastasis[102-104]. These studies indicate that the CCL2 signaling pathway is a critical regulator of macrophage-mediated tumor progression. Though most studies characterize CCR2 as the chemotactic-receptor on macrophages for tumor-derived CCL2, CCR2 is also overexpressed in breast carcinoma of multiple subtypes[93]. Targeting CCR2 in breast carcinoma cell lines by siRNA knockdown inhibits CCL2-induced survival and motility[93], suggesting that CCL2/CCR2 signaling to breast cancer cells regulate breast cancer progression.

While CCL2 remains a therapeutic target of interest, its translation to the bedside remains controversial. CCL2 neutralizing antibodies effectively block cancer progression in some animal

models[102-104], and several clinical studies were initiated for its treatment of late stage solid tumors[105]. However, the use of CCL2 antibody neutralization in murine breast cancer models and in human trials reveal a paradoxical increase in systemic CCL2, leading to enhanced tumor angiogenesis and subsequent metastasis[106]. Recent studies from our lab suggested that targeting chemokine expression at the level of transcription may be more effective at inhibiting chemokine signaling activity[105, 107].

Targeting critical oncogenes through delivery of small interfering RNAs (siRNAs) could overcome present barriers at targeting CCL2/CCR2 and holds significant therapeutic potential [176-178] One peptide carrier that penetrates tissues efficiently and is currently being tested in clinical trials is the HIV-1 derived trans-activating transcriptor peptide (TAT<sub>49-57</sub>: RKKRRQRRR). TAT peptides exhibit unique properties by efficiently penetrating cell membranes independent of temperature and cell-surface receptor expression, but do not form stable complexes with nucleic acids[179-181]. Studies recently demonstrated that calcium ions induce the formation of non-covalent interactions TAT peptides and siRNAs, and become condensed into nanoparticles (Ca-TAT/siRNAs). These Ca-TAT/siRNA complexes efficiently transfect cells and penetrate tissues to induce gene knockdown more efficiently than and with lower toxicity than TAT peptides alone or conventional polyethyleneimine particles[182-184]. Furthermore, Ca-TAT/siRNA complexes could be formulated to selectively transfect mammary carcinoma cells over stromal cells including macrophages and fibroblasts based on calcium chloride concentration[185]. Given that the stromal component of breast tumors varies with cell type and cell number[186-188], Ca-TAT peptides are a useful tool to induce gene knockdown in breast tumor tissues.

Here, we sought to understand how epithelial CCR2 signaling contributes to breast cancer progression. Delivery of CA-TAT/CCR2 siRNA complexes to PyVmT mammary tumor-bearing mice specifically inhibited CCR2 expression in carcinoma cells and inhibited tumor growth and invasion associated with decreased angiogenesis, M2 macrophage recruitment and elevated CD8<sup>+</sup> T cell recruitment and activity. These anti-tumor phenotypes were associated with decreased tumoral expression of CCL2 and increased expression of CD154, an immunostimulatory soluble ligand. CCR2 deficient mammary carcinoma cells showed decreased wound closure and proliferation, which was rescued with CD154 antibody neutralization or CCL2 treatment. Recruitment of endothelial cells and macrophages is inhibited when epithelial CCR2 is targeted, and rescued with CD154 antibody neutralization or CCL2 treatment. Using live imaging and a novel 3D macrophage infiltration assay, we show that CCR2 signaling in mammary carcinoma cells regulates the recruitment of macrophages and proliferation of carcinoma cells. Immunostaining of breast tumor tissues show an inverse correlation between CCR2 and CD154 expression. Datamining analysis demonstrate that CD154 expression correlates with relapse free survival for breast cancer patients. In summary, these data show that CCR2 signaling in breast cancer cells facilitates breast cancer growth and spread through stroma-dependent and stroma-independent mechanisms. Furthermore, this report indicates that M2 macrophage recruitment could be suppressed and CD8<sup>+</sup> T cell activity could be enhanced through modulation of CCL2/CCR2 and CD154 signaling mechanisms, with important implications on targeted and immuno-therapies.

## Materials and Methods:

### **Animal care and surgery**

Female FVB mice at 8 weeks age were purchased from Charles River. Mammary intraductal injections were performed as described[9, 149]. Briefly, 20,000 PyVmT cells were directly injected in 5 uL of sterile PBS into mammary ducts of the 4<sup>th</sup> and 9<sup>th</sup> mammary glands; successful injections were visualized with dextran blue. When the tumors reached 0.4 cm in diameter, 10 µg (100 µl) of Ca-TAT/control or Ca-TAT/CCR2 siRNA nanoparticles were injected into the primary tumor in four different areas of the tumor, using a 27-gauge needle. Each mouse received a total of three injections of Ca-TAT/siRNA complexes at one-week intervals. Animals were monitored twice weekly for tumor formation by palpation and measurement by caliper. Animals were euthanized 28 days after first injection, when control tumors reached maximum allowable tumor size, approximately 1.5 cm<sup>3</sup>. Animals were maintained at the University of Kansas Medical Center, in accordance with the AALAC. All animal experiments were performed at the University of Kansas Medical Center under an approved IACUC.

### **Cell culture**

Raw264.7 and MCF10A cell lines[189] were purchased from ATCC. DCIS.com expressing wild-type CCR2 (WT) or CRISP/R ablated for CCR2 expression were generated and characterized as described in previous studies[190]. MCF10-DCIS.com (DCIS.com) breast cancer cells[189] were kindly provided by Fariba Behbod (University of Kansas Medical Center). Raw 264.7 mcherry cells were generated by lentiviral transduction using pSico-Ef1a-mCherry plasmid (Addgene, Cambridge, MA). PyVmT carcinoma cells were isolated and

characterized as described[191]. Unless indicated, cells were cultured in DMEM/10% FBS/1% penicillin-streptomycin (Cellgro cat no.30-004-CI).

### **siRNA and gRNA**

Sense and anti-sense oligonucleotides were synthesized and annealed by Dharmacon Fisher (cat no L-041015). The following siRNA targeting sequences were designed: enhanced green fluorescent protein (eGFP) as a negative control: 5'-GCUGACCCUGAAGUUCAUC-3'. DCIS.com cells with wild-type, heterozygous deletion, and knockout of CCR2 were generated as previously described[190]. CCR2 targeting sequence was 50-TTCACAGGGCTGTATCACATCGG-30, targeting genomic region encoding extracellular domain between second and third transmembrane regions, and clones screened by DdeI restriction digest of PCR products generated with primers 5'-ACATGCTGGTCGTCCTCATC & 3'-AAACCAGCCGAGACTTCCTG.

### **Preparation of Ca-TAT complexes**

TAT peptides [sequence N to C: (+)H-RKKRRQRRR-NH<sub>2</sub>(+)] were synthesized to purity >95% by Biomatik (Cambridge, Ontario). The following formula was used to determine the amount of TAT peptide needed for a specific *N/P* ratio per  $\mu\text{g}$  of DNA or siRNA:  $\mu\text{g}$  of TAT =  $0.446 \times (N/P \text{ ratio}) + 0.116$  as previously described[107]. TAT peptides were mixed with siRNA or plasmid DNA in 45  $\mu\text{l}$  sterile deionized water containing 75 mM CaCl<sub>2</sub>. The solution was pipetted 20 times and incubated on ice for 20 minutes. For in vivo studies, 25  $\mu\text{l}$  of 10 % glucose was added to the complexes, and diluted with PBS to a total volume of 100  $\mu\text{l}$  before use. For in vitro studies, these complexes were added directly to cells.

### **Generation of conditioned media**

500,000 cells were seeded in 10 cm plates for 24 hours, transfected with siRNA complexes as needed for 24 hours, and incubated in 7 ml DMEM/1% FBS for 24 hours. Medium was collected, centrifuged to eliminate debris and filtered through 0.45-micron PES membranes.

### **Wound closure assay**

200,000 cells/well were seeded in 24 well plates, transfected with siRNA complexes in growth media for 24 hours. Cells were serum starved for 24 hours and scratched in DMEM/1% FBS with or without 3 ug/ml CD154, 1 ug/ml anti-CD154 (cat no.552559, BD Biosciences) or control mouse IgG (Millipore cat no.12-371). Images were captured at 10x magnification at 0 and 24 hours. Wound closure was measured using Image J, with MRI\_Wound\_Healing\_Tool.ijm.

### **Flow cytometry**

Adherent cells were detached from plastic using Accutase (Innovative Cell Technologies, cat no. AT104). Cells were rinsed three times with PBS, and blocked in PBS/10% FBS for 10 minutes. Cells were then incubated for 3 minutes PBS/1% BSA/1 g/L dextrose with or without human specific anti-CD40-FITC (R&D Systems, cat no. MAB6321) or murine specific anti-CD40-FITC (BD Biosciences cat no. 12040181) at 1:100 dilution. Cells were washed with PBS/1% BSA 3 times, and analyzed using a BD LSR II flow cytometer. Tumor tissues were processed for flow cytometry using methods described [107]. Briefly, 3-4 mm<sup>3</sup> in size were minced with fine scissors, enzymatically digested to single-cell suspensions overnight on ice, incubated in 5 ml red blood cell lysis buffer for 7 minutes at room

temperature and centrifuged to eliminate debris. Approximately 200,000 cells were stained at 1:100 dilution antibodies to: CD24-FITC (BD Pharmingen cat no. 560992), F4/80-PE (Serotec cat no.MCA497PE), CD69-FITC (Biolegend Cat no.104505), CD4-PE-Cy5 (BD Pharmingen cat no.553654). CD8-APC (Biolegend cat no.100711), CD11b-APC-Cy7 (BD Pharmingen cat. no 557657). Samples were analyzed using a BD LSRII flow cytometer. Compensation controls were performed to minimize spectral overlap artifacts. Isotype control antibodies were utilized for background correction.

### **Histology/Immunohistochemistry**

Tumor tissues were fixed in 10 % neutral formalin buffer, embedded in wax and stained by H&E as described[107]. For immunostaining, five-micron sections were dewaxed and subject to antigen retrieval through pressure cooking at low pressure for 2 minutes in 10 mM Sodium Citrate pH 6.0. Endogenous peroxidases were quenched with PBS/10% methanol/10% H<sub>2</sub>O<sub>2</sub>. Sections were blocked with PBS/3% FBS and incubated with primary antibodies (1:100) to: cleaved caspase-3 (Cell Signaling Technology catalog no. 9579), PCNA (Biolegend, cat no. 307902), Von Willebrand Factor 8 (VWF8; Millipore, catalog no.Ab7356), CCR2 (Santa Cruz Biotechnology, cat no.sc-6228), CD154 (BD Biosciences cat no.552559), and CCL2 (Santa Cruz Biotechnology, cat no. 1304). Cleaved caspase-3, PCNA, VWF8, CCR2 and CD154 were detected with rabbit biotinylated antibodies (1:1000). CCL2 was detected with goat biotinylated antibodies (1:1000). Secondary antibodies were bound to streptavidin-peroxidase (Vector Laboratories, cat no. PK-6100), and incubated with DAB substrate (Vector Laboratories, cat no.SK4100,). Slides were counterstained in Mayer's hematoxylin and mounted with Cytoseal. 5 images per field at 20x magnification were captured using the EVOS FL Auto-Imaging System. Protein expression was quantified using Image J as described

previously[175]. CCR2, CCL2, CD154 and VWF8 expression were analyzed as positive staining pixel density normalized to total area. Ki67 and cleaved caspase-3 were quantified by determining the relative area of positive stained cells to total number of cells.

### **Immunofluorescence**

3D cultures were fixed in 10 % NBF, embedded in 4% agarose and paraffin as described[192]. 5-micron tumor or 3D culture sections were dewaxed and subject to antigen retrieval by heating under low pressure for 2 minutes in 10 mM Sodium Citrate, pH 6.0. Sections were blocked with PBS/3% FBS for 1 hour and incubated with antibodies (1:100) to: CD8 (Biolegend cat no.100715), CD69-FITC (Biolegend cat no.104505), CD11b-APC-Cy7 (BD Pharmingen cat. no. 557657), Arginase-1 (Santa Cruz Biotechnology cat no.sc20150) or PCNA (Biolegend cat no.307902) 4°C overnight. CD8 was detected with anti-rat-AlexaFluor 568 (Invitrogen cat no.A-11077). Arginase I was detected with anti-rabbit-AlexaFluor 488 (Invitrogen cat no.A-11034). PCNA was detected with anti-mouse-Alexa-Fluor488 (Invitrogen cat no. A-A11001). Sections were counterstained with DAPI and mounted using 1:1 PBS: glycerol. Images were captured at 10x magnification using the EVOS FL Auto-Imaging System. Expression was quantified using Image J as described[105]. Expression was normalized to DAPI staining.

### **CD154 ELISA**

High-protein binding plates were coated with 1  $\mu$ g/ml capture CD154 antibody (BD Bioscience, San Jose, CA, cat no.552559) overnight. Plates were blocked in PBS/10% BSA for 2 hours at room temperature. Samples were diluted 1:1 in PBS/1% BSA/Tween-20, and plated at 100  $\mu$ l/well for 24 hours at 4°C. Wells were washed with PBS three times, and incubated with 100  $\mu$ l/well 0.5  $\mu$ g/ml biotinylated anti-CD154 (BD Biosciences, cat no.

552560) for 2 hours, followed by streptavidin-peroxidase (Vector Laboratories, cat no. PK-6100) for 30 minutes. Reactions were catalyzed using tetramethylbenzidine substrate (cat no. 34028, Pierce). Absorbance was read at OD 450nm using a BioTek Microplate Reader. Concentrations were determined from standard curve ranging from ten pg/ml to 10 ng/ml recombinant CD154 (Peprotech, Rocky Hill, NJ, cat no. 310-02).

### **Macrophage infiltration assay**

TheraKan devices<sup>TM</sup> were manufactured by Fennik Life Sciences (Kansas City, KS). Macrophage infiltration was determined using methods previously described [107]. Briefly, 100,000 breast cancer cells were embedded in 250 ul rat tail collagen (BD Pharmingen) for each device. Devices were placed in six well dishes and incubated in DMEM/10% FBS overnight. 500,000 Raw264.7 or THP1 mCherry labeled cells were counted and resuspended into 2.5 ml of DMEM/10% FBS for each device. Devices were opened and cells were pipetted into each well, outside of the device. Devices were imaged daily at 10x magnification using an EVOS FL Auto-Imaging System (Invitrogen) for up to 48 hours. The number of macrophages were measured by quantification of fluorescence as described[193].

### **Live imaging co-culture assays**

Control shRNA and CCL2\_3 knockdown PyVmT cells at 50% confluency were treated with TAT-siRNA particles for 48 hours, then trypsinized, counted, and resuspended in a 1:1 mixture of growth-factor-reduced basement membrane extract to rat tail collagen at  $1 \times 10^7$  cells/ml on ice. 40 ul of this solution was pipetted into the center of a 24 well plate and incubated at 37C for 30 min. 200,000 Raw macrophages (a 5:1 macrophage: tumor-cell ratio) in 1 mL of DMEM with 1% FBS were then placed into the well, and allowed to adhere for 12 hours. Media was replaced by serum-free DMEM containing no additives, 100 ng/ml of CCL2 or 1 ug/ml of CD154.

Plates were imaged for 24 hours at 15-minute intervals. T-stacked images were analyzed with TrackMate plugin of Fiji to obtain track and spot data. n=4 experiments per group, with >100 cells tracked per group.

### **Biospecimens**

The BR802b tissue microarray was obtained from US Biomax, INC (Rockville, MD). Additional patient samples were obtained from the University of Kansas Tissue Repository. Patient samples were collected under approval by IRB at KUMC. All samples were de-identified by US Biomax or the Biospecimen Core, an IRB-approved facility, prior to distribution.

### **Ethics statements**

The tissues collected for these studies were de-identified and classified as “Exempted” according to regulations set forth by the Human Research Protection Program (ethics committee) at the University of Kansas Medical Center (#080193). Written informed consent for tissue collection was obtained by the Biospecimen Core Repository. Tissue samples were de-identified by the National Cancer Institute Diagnostics Program and the Biospecimen Core Repository prior to distribution to the investigators. Existing medical records were used in compliance with the regulations of the University of Kansas Medical Center and National Cancer Institute. These regulations are aligned with the World Medical Association Declaration of Helsinki.

### **Datamining**

mRNA breast cancer datasets were accessed on [www.kmplot.com](http://www.kmplot.com) on October 12, 2018 to assess the significance of CD154 (207892\_at) with the following parameters: relapse free survival, basal=879, luminal A (n=1933), Luminal B (n=1149), HER2+ (n=251).

### Statistical analysis

Statistical analysis was performed using Graphpad Prism software. Student's Two-Tailed T-test was used for two groups. One Way ANOVA with Bonferroni's post-hoc comparison was used for more than two groups. *In vitro* experiments were conducted with triplicate samples, and performed a minimum of three times. \* $p < 0.05$ , \*\* $p < 0.01$ , \*\*\* $p < 0.001$ , ns= not significant. Data are presented as mean $\pm$ SEM.

## Results

### Delivery of CCR2 siRNAs complexed to Ca-TAT peptides decreases mammary tumor growth and invasion

Previous studies showed Ca-TAT complexed to plasmid or siRNA preferentially transfected mammary carcinoma cells with minimal uptake in stromal cells including macrophages and fibroblasts[185]. Using a luciferase promoter plasmid complexed to Ca-TAT peptides, we compared uptake of these complexes to normal mammary tissues and PyVmT tumor tissues. PyVmT mammary tumor tissues showed a significant uptake in luciferase complexes over normal tissues (Figure 23).

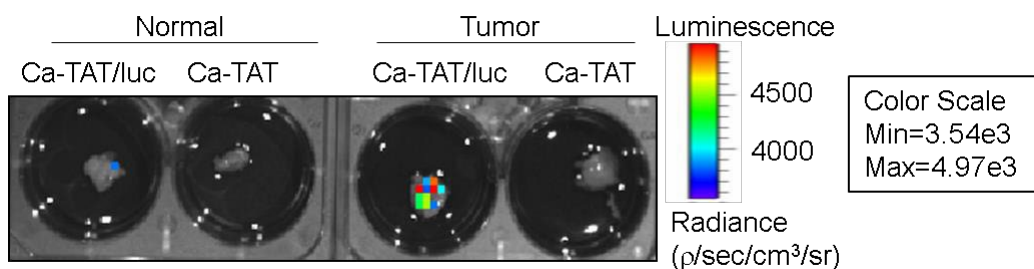


Figure 23 Ca-TAT complexes are preferentially taken up in PyVmT mammary tumor tissues. Ex vivo cultures injected with Ca-TAT alone or Ca-TAT/luc complexes were analyzed for luciferase activity by IVIS imaging. N=3/group. Representative results are shown. Statistical analysis was performed by One Way ANOVA followed by Bonferonni post hoc comparisons. Statistical significance was determined by p value less than 0.05 through comparison with Control siRNA group within Tumor or Normal group,

MMTV-PyVmT transgenic mice progress to invasion and metastasis in a stage dependent manner. [194-197]. However, tumor initiation and progression vary among progeny making it difficult to assess the effects of molecular targeting in transgenic mice. To increase consistency in tumor initiation and progression over time, mammary tumors were established in FVB mice via Mammary Intraductal injection of PyVmT mammary carcinoma cells, which closely mimics the development and progression of IDC in patients ([9, 198]). When mammary tumors reached 0.4 cm<sup>3</sup> in volume (~49 days), mice were intratumorally injected with either PBS vehicle, or Ca-TAT peptides complexed to control siRNAs (si\_CTRL) or CCR2 siRNAs (si\_CCR2), once a week for 3 weeks (Figure 24A).

Mice were sacrificed one week after their last injection, or when tumors reached approximately 1.5 cm in diameter, the maximum allowable size set by IACUC guidelines. To assess carcinoma-specific CCR2 knockdown, mammary tumor-cell suspensions co-stained for CCR2+/CD24+ cells (mammary carcinoma cells) or CCR2+/Cd11b+ cells (myeloid cells). CCR2 expression was unchanged in Cd11b+ cells, but was reduced by 40% in mammary carcinoma cells by flow cytometry (Figure 24B). Si\_CCR2 complexes inhibited tumor growth visibly (Figure 24C), reduced tumor mass by 54% and tumor volume by 56% compared to si\_CTRL or PBS treatment (Figure 24D-E). Compared to si\_CTRL treatment, si-CCR2 treated tumors showed significantly decreased tumor-cell proliferation, as indicated by PCNA immunostaining (Figure 24F-G), but no change in apoptosis, as indicated by cleaved caspase-3 immunostaining (Figure 24H-I). These data indicate that delivery of si\_CCR2 complexes inhibits mammary tumor progression associated with decreased CCR2 expression in mammary carcinoma cells.

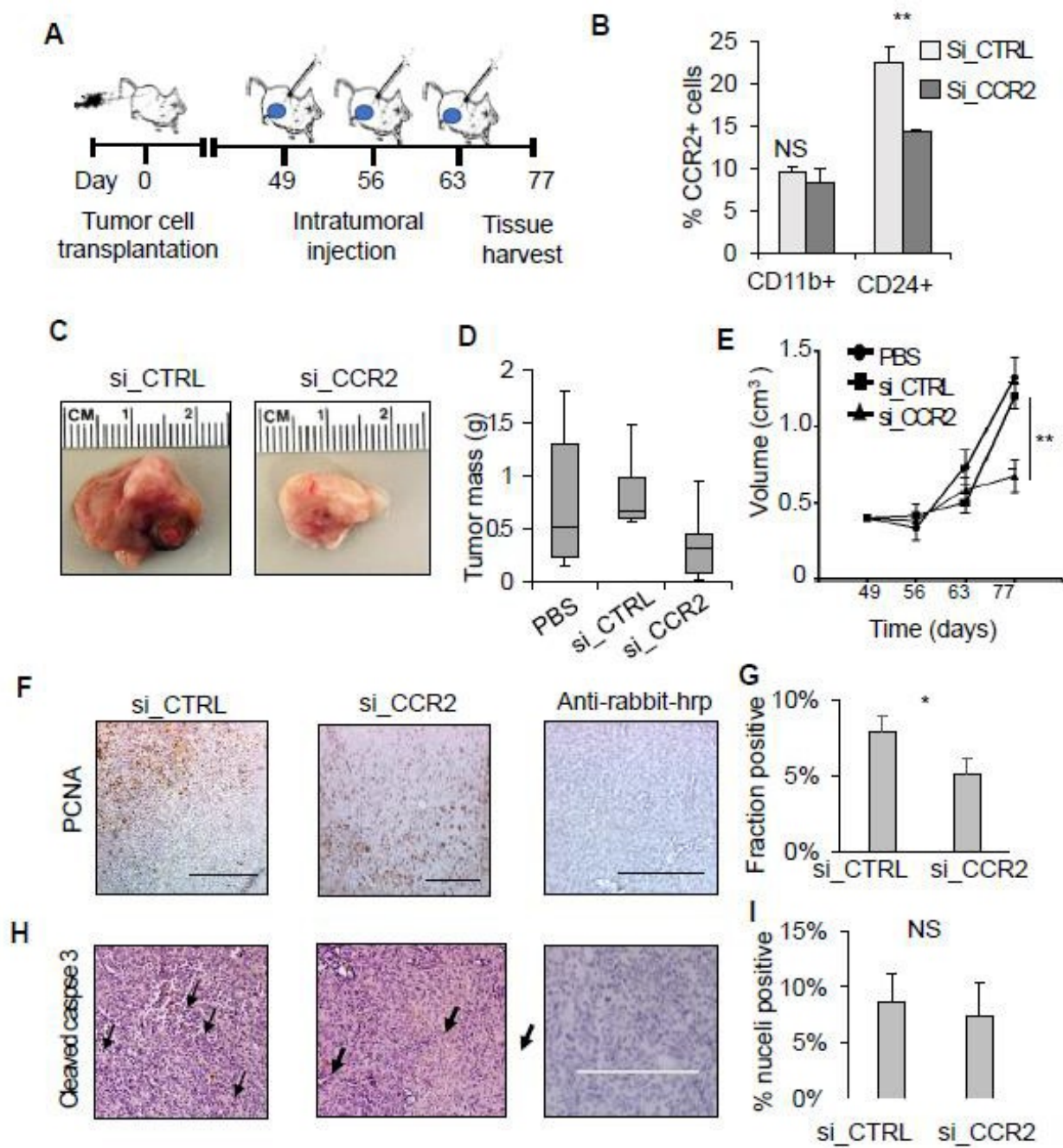


Figure 24 Effect of intratumoral injections of TAT-Ca<sup>2+</sup> nanoparticles complexed with CCR2 siRNA on tumor growth, cellular proliferation, and apoptosis. A) In vivo experimental design: Mice injected intraductally at day 0 with 20,000 polyoma middle T cells. Once tumors reached 0.4 cm<sup>2</sup> in size, 3 doses of \_\_\_\_\_ug siRNA complexed to Ca-TAT nanoparticles were injected intratumorally. Mice were sacrificed one week after the last dose. B) Efficiency of targeted knockdown of CCR2 in epithelial cells versus stromal cells (CD11b<sup>+</sup>) as detected by flow cytometry. C) Representative images of tumors from siCTRL and siCCR2 treated mice. N=6 mice per group. D) Box and whisker plots depicting tumor mass at endpoint by treatment group. E) Growth curve of tumor volume measured weekly prior to injection for each group. F-I) Representative images of IHC staining of formalin fixed tumors from siCTRL-treated and siCCR2-treated mice with quantification for PCNA (F&G) and CC3 (H&I). For (H) arrowheads depict positive CC3 staining. Images taken at 10x. Scale bar = 200 um. N=7 per group. Analyzed by two-sided univariate t-test for significance. \*p<0.05 PCNA = proliferating cell nuclear antigen; CC3 = cleaved caspase 3.

### **CCR2 targeting of carcinoma cells reduces M2 macrophage recruitment, associated with decreased angiogenesis and increased cytotoxic T cell infiltration**

Given that M2-polarized macrophages are known to drive early invasion and tumor growth, we stained tumors for CD11b<sup>+</sup>/F4-80<sup>+</sup> macrophages by flow cytometry. SiCCR2-therapy decreased CD11b<sup>+</sup>/F480<sup>+</sup> macrophage populations by 68% (Figure 25A). To localize the macrophage populations to the tumor and assess their M2 phenotype, we stained serial sections of paraffin-embedded tumors for CD11b<sup>+</sup>/arginase<sup>+</sup> cells. Co-immunofluorescence revealed 78% fewer arginase<sup>+</sup>/CD11b<sup>+</sup> cells in the siCCR2 tumors compared to siCTRL (Figure 25B). Associated with this decreased inflammatory infiltrate, mammary tumors treated with si\_CCR2 complexes showed decreased tumor invasion compared to si\_CTRL treatment (Figure 25C). Tumors were examined for changes in tumor vascularity and lymphocytic infiltrate to see if decreased M2 macrophage content of siCCR2 tumors affected anti-tumor immunity or angiogenesis. Si\_CCR2 treatment decreased intratumoral vascularity by 82%, as indicated by VWF8 immunostaining of capillary structures (Figure 25D). To quantify lymphocytic populations, we stained tumor digests for CD4, CD8, and CD69, a marker of T cell activation and tissue residency. Compared to si\_CTRL treated tumors, si\_CCR2 treated tumors showed significantly increased CD8<sup>+</sup>/CD69<sup>+</sup> T cells indicating increased numbers of resident activated CD8<sup>+</sup> cytotoxic T cells; there were no significant differences in the numbers of CD4<sup>+</sup> helper cells between groups (Figure 25E). Co-immunofluorescent (CO-IF) staining of CCR2 deficient mammary tumors revealed that CD8<sup>+</sup>/CD69<sup>+</sup> T cells were distributed throughout the tumor including necrotic areas (Figure 25F). These data indicate that si\_CCR2 treatment reduces tumor promoting M2 macrophages, decreases angiogenesis, and increases tumoricidal activated T cell responses.

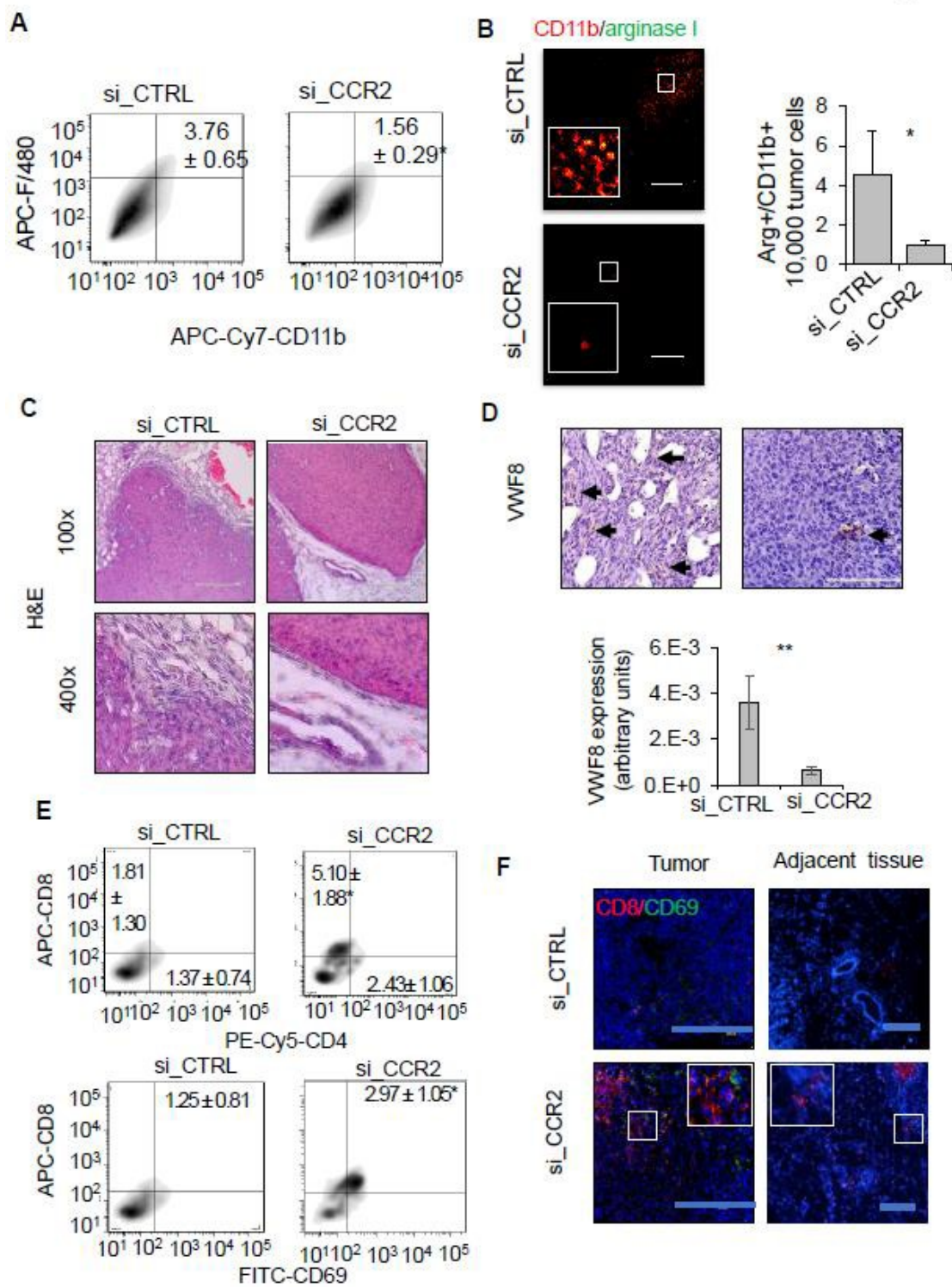


Figure 25 - Delivery of CCR2 siRNA complexes inhibit tumor angiogenesis and enhances CD8+ T cell levels. Whole tumors were digested and analyzed for macrophage content by gating for an F4/80+/CD11b+ population via flow cytometry. Mean $\pm$ SEM for percentage of gated viable cells that were F4\_80+/CD11b+, and (C) representative scatter plots and selected population. n=6 per treatment group. Tumor sections were immunostained for CD11b and arginase 1 (Arg1), an M2 macrophage marker. Whole tumor samples were imaged at 10x by automated fluorescent microscopy, and cell number was quantified by ImageJ. Bar **A.** PyVmT mammary tumor tissues digested and analyzed for macrophage content by gating for an F4/80+/CD11b+ population via flow cytometry. Mean $\pm$ SEM for percentage of gated viable cells shown. **B.** Co-immunofluorescence staining for CD11b (red) /arginase I (green) expression. **C.** Invasive fronts of tumors imaged by H&E. **D.** Von Willebrand factor 8 (VWF8) immunostaining; positive staining indicated by black arrows, **E.** flow cytometry analysis for CD4+/CD8+ cells, CD8+/CD69+ cells (C) or F/480+/ CD11b+ cells, **F.** Co-immunofluorescence staining for CD8 (red)/CD69 (green) expression; or E. co-immunofluorescence staining for CD11b (red) /arginase I (green) expression. Scale bar= 200 microns. N=6 tumors per group, with >15 images per tumor section. Immunostaining was quantified by Image J, and normalized to hematoxylin (B) or DAPI (D). Statistical analysis was performed using 2-tailed T test. Statistical significance was determined by p<0.05. \*p<0.05. Mean $\pm$ SEM are shown.

### **Intratumoral depletion of CCR2 increases expression of CD154**

To determine the effect of Ca-TAT/siRNA complexes on regional CCR2 expression within the tumor, mammary tumor sections were immunostained for CCR2. In si\_CTRL treated tumors, CCR2 expression was detected in carcinoma cells, blood vessels and inflammatory infiltrating cells (Figure 26A). si\_CCR2 treated tumors showed a reduction in overall CCR2 expression by 80%, corresponding to lower expression levels in the tumor epithelium, decreased vasculature and fewer inflammatory infiltrating cells (Figure 26A). Given that M2 macrophages are a significant source of CCL2 in breast cancer, and the observed decrease in CCL2 of siCCR2-treated epithelium, vasculature, and inflammatory infiltrate than in siCTRL tumors (Figure 26B), these data indicate that epithelial CCR2 may enhance CCL2 levels in tumors by recruiting CCL2-secreting stromal cells.

Given the significant changes in angiogenic and immune responses in mammary tumors with CCR2 knockdown, we hypothesized that CCL2/CCR2 signaling regulates other pro-inflammatory molecules. Though CCL2-deficient MDA-MB-231 breast tumor xenografts develop fewer tumor metastasis associated with a reduction in macrophage recruitment[107], cytokine array profiling of these CCL2-deficient cells revealed that IL6 and VEGF were minimally changed in CCL2 deficient tumor cells, but that expression of CD154 was significantly elevated in CCL2-deficient cells *in vitro* and *in vivo*. Similarly, immunostaining revealed significantly elevated CD154 in the tumor epithelium of CCR2-deficient PyVmT mammary tumors (Figure 26C). We then treated PyVmT *cells in vitro* with siCCR2, and found that while CCR2 decreased and CD154 increased after siCCR2-treatment, there was no change in CCL2 expression (Figure 26D-E). Similarly, we found that CCR2 knockout increased CD154,

but did not change CCL2, in DCIS.com cells (Figure 26F). Furthermore, these data indicate an inverse association between CCR2 expression and CD154 expression in mammary tumor tissues.

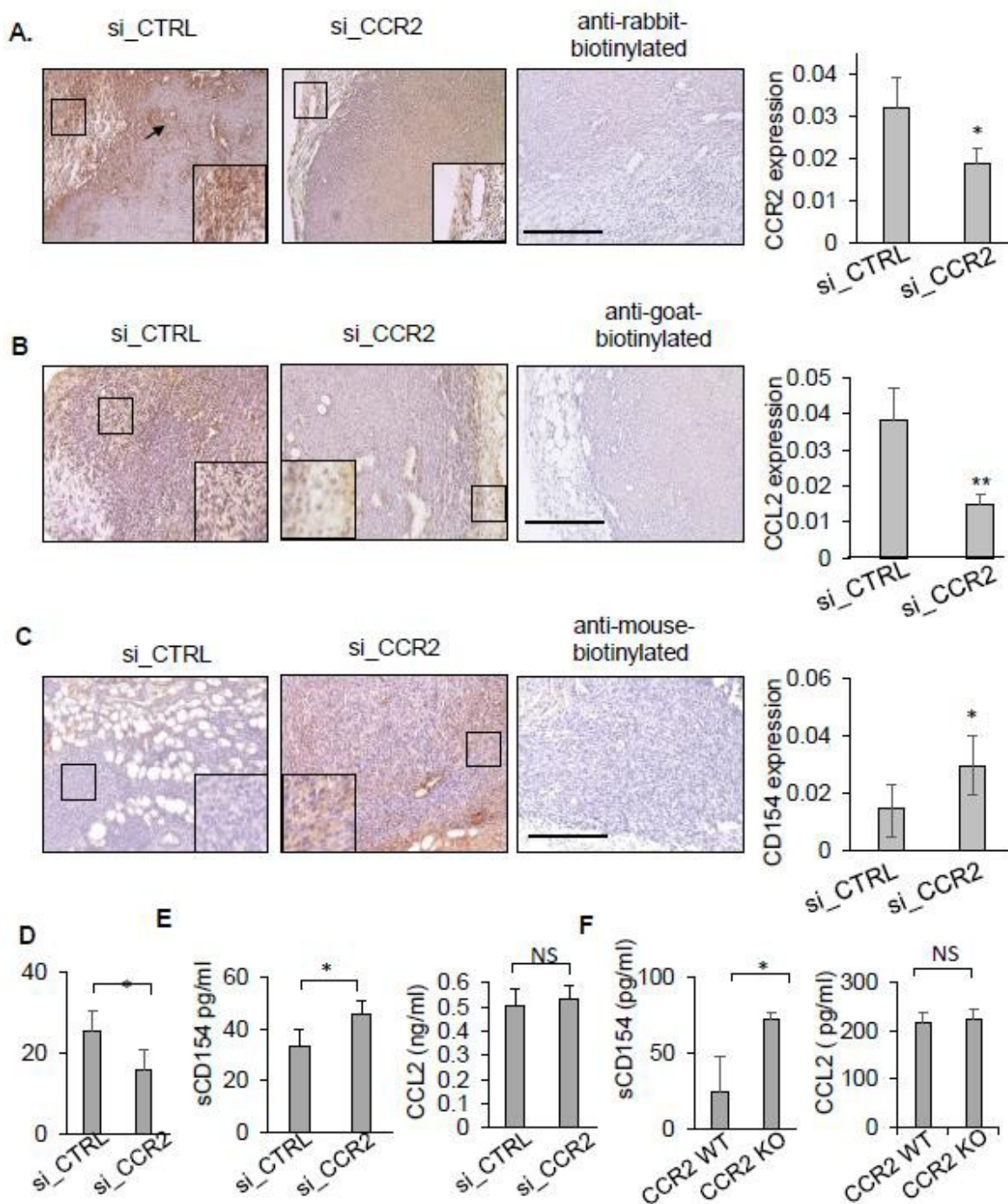


Figure 26 - CCR2 siRNA upregulates CD154, but not CCL2, in human and mouse tumor-cell lines. Immunohistochemical staining of PyVmT tumors for A) CCR2, B) CCL2, and C) CD154. Representative images of si\_CTRL (left panel), si\_CCR2 (middle panel), and isotype control (right panel). Positive staining quantified in ImageJ and represented in bar graphs on far right as a ratio of positive staining area to total tumor area. Insets shown for detail. N=6 mice per group, with 4 10x bright field images per tumor sample. Scalebar = 100 microns. D) CCR2 expression analyzed by flow cytometry, calculated by Overton subtraction method of positivity relative to isotype-stained control. E) Enzyme-linked immunosorbent assay results for CD154 and CCL2 levels in supernatants collected after 24 hrs from E) PyVmT cells treated with siCTRL or siCCR2 and F) DCIS.com cells with wild-type CCR2 (WT) or homozygous knockout of CCR2 (KO). N=4 experiments per group. Positive controls included a murine macrophage line (Raw) and a human megakaryoblast line (Meg-01). Statistical significance calculated with 2-tailed, univariate student's T test with an alpha of 0.05. Significant differences = \* ( $p < 0.05$ ).

### **CD154 antagonizes CCR2 synergism to mediate tumor-cell proliferation and migration**

CD154 is a member of the Tumor necrosis family of ligands that is expressed as a type II transmembrane protein (35kda) or proteolytic cleaved soluble biologically active protein (18 kda). CD154 stimulates a cytotoxic T cell response, promote M2 to M1 macrophage conversion, and inhibits breast tumor growth, indicating that CD154 functions as a tumor suppressor[59, 199-201]. To better understand the role of upregulated CD154 in CCR2-deficient tumors, we used cell culture models of the *in vivo* phenotypes we observed to be affected by siCCR2 knock. PyVmT mammary carcinoma cells were transfected with si\_CTRL or si\_CCR2, treated with neutralizing antibodies to CD154 or recombinant CCL2 protein, and analyzed for cell proliferation by PCNA staining and migration by wound closure assay.

For these assays, we generated stable PyVmT cells lines expressing control shRNA (control KD) or CCL2 shRNA (CCL2 KD) to mitigate the possibility of residual CCR2 signaling or signaling through an alternate chemokine receptor. CCL2 or CD154 neutralization significantly increased proliferation, in both siCTRL and siCCR2-treated, but this effect was significantly reduced by siCCR2 (Figure 27A). SiCCR2 treatment also inhibited wound closure, which was rescued with both CD154 antibody neutralization and CCL2 treatment (Figure 27B), but not by CCL2 in CCL2 KD lines. These results indicate CCR2 regulates proliferation and migration thru CD154 suppression, and low levels of CCR2 are sufficient for CCL2-induced signaling to suppress CD154.

To see if complete ablation of CCR2 more severely affected proliferation or migration, these studies were repeated in CCR2-KO DCIS.com cells. CCR2 KO decreased proliferation compared to WT in a CD154-dependent manner (Figure 27C). In DCIS.com cells, both CCR2 KO and CCL2 KD decreased migration (Figure 27D). CCL2 rescued migration in WT cells with

CCL2 KD, but it had no effect on CCR2 KO cells in either group. CD154 neutralization rescued migration in CCR2 KO cells, but not had no effect on WT cells. These data show that CCR2 enhances migration in breast cancer cells in a CD154-dependent manner, and that in absence of CCR2, CCL2 has no effect on proliferation or migration.

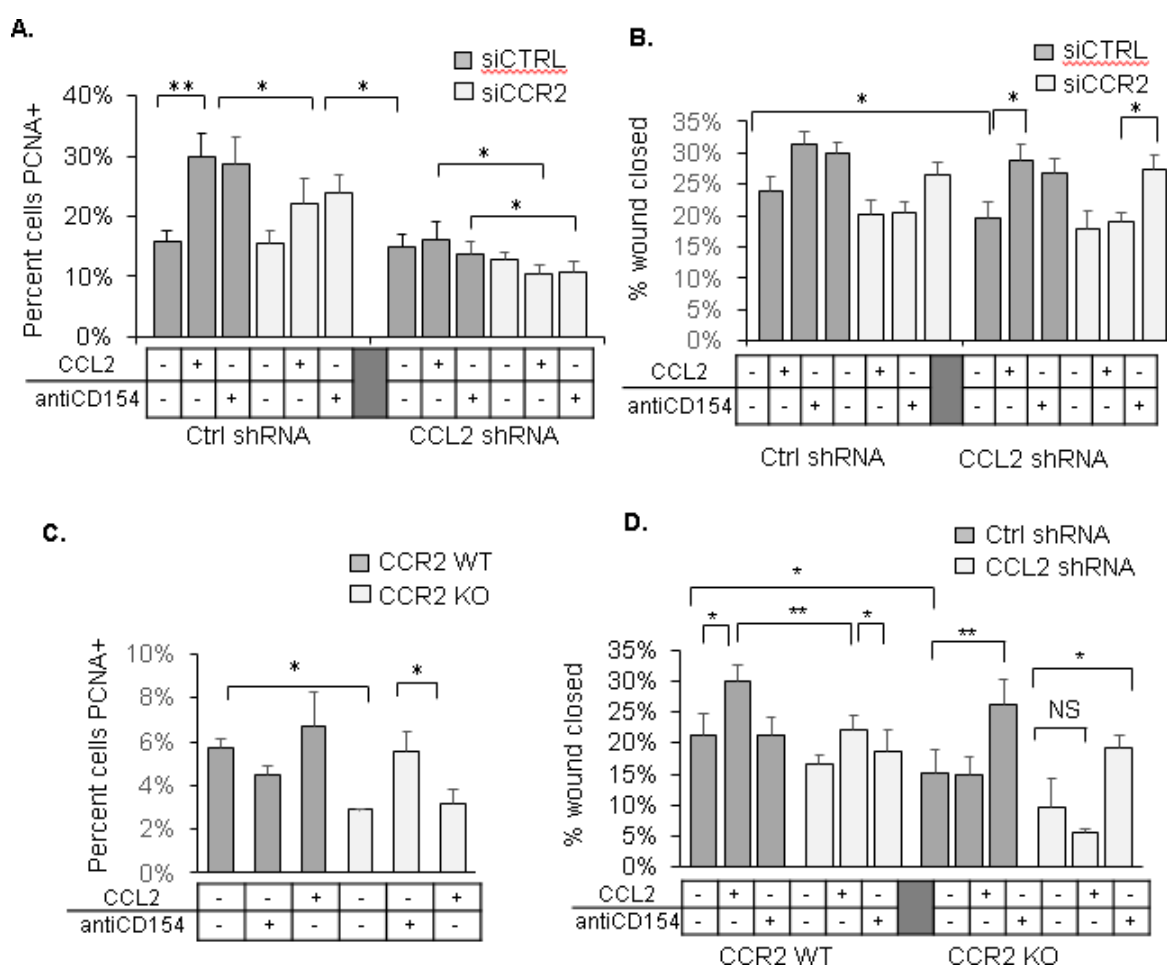


Figure 27 - CCR2 has expression-level effects on proliferation and migration in murine and human breast cancer cells. A) PyVmT cells with alterations described were treated with Serum-free (SF) DMEM, 100 ng/ml of recombinant exogenous CCL2, or one ug/ml of CD154 neutralizing antibodies. Proliferation measured as the ratio of PCNA positive nuclei: DAPI positive nuclei as measured by fluorescence microscopy with 200x images. B) PyVmT cells were grown to a confluent monolayer, serum starved for 24 hours, and a wound was made with a p200 ul pipette tip. Four 4x images were taken of the scratch at identical locations per well, and the area of the wound was measured by ImageJ. Percent wound closed =  $(1 - (\text{area 24 hours} / \text{area 0 hours})) * 100$ . C) DCIS.com with CRISPR-Cas9-directed knockout of CCR2 (CCR2 KO) or wild-type CCR2 (CCR2 WT) were assessed for proliferation in the presence of CCL2 or CD154 neutralizing antibodies as in (A). D) Wound closure assay results with experimental conditions identical to (B) without TAT-siRNA treatment. N=4 experiments with duplicates per experiment for each group. Statistical significance calculated with 2-tailed, univariate student's T test with an alpha of 0.05. Significant differences = \* ( $p < 0.05$ ) and \*\* ( $p < 0.005$ ).

## **CCR2 promotes endothelial recruitment and budding thru a CD154-independent mechanism**

Studies conflict over the role of CD154 in angiogenesis, as in one study CD154 inhibits endothelial cell migration[202], and others show a pro-angiogenic function[203, 204]. To determine the relevance of CCR2 mediated suppression of CD154 to tumor angiogenesis, tumor-cell recruitment of endothelial cells was analyzed by trans well assay. Endothelial cells were seeded on the topside of Matrigel coated trans wells, and conditioned media from PyVmT cells was placed in the lower well (Figure 28A). CCR2 knockdown in mammary carcinoma cells decreased invasion of endothelial cells, and rescued by CD154 antibody neutralization or CCL2 treatment (Figure 28B). Conditioned media from siCCR2-treated or CCL2 KD cells decreased the branching morphology of endothelial cells, but anti-CD154 had no effect on branching (Figure 28C-E). These data indicate that CCR2 promotes endothelial cell recruitment to tumor cells through suppression of CD154 and increased CCL2 expression, and CCL2/CCR2 appear to promote endothelial budding in a CD154-independent manner.

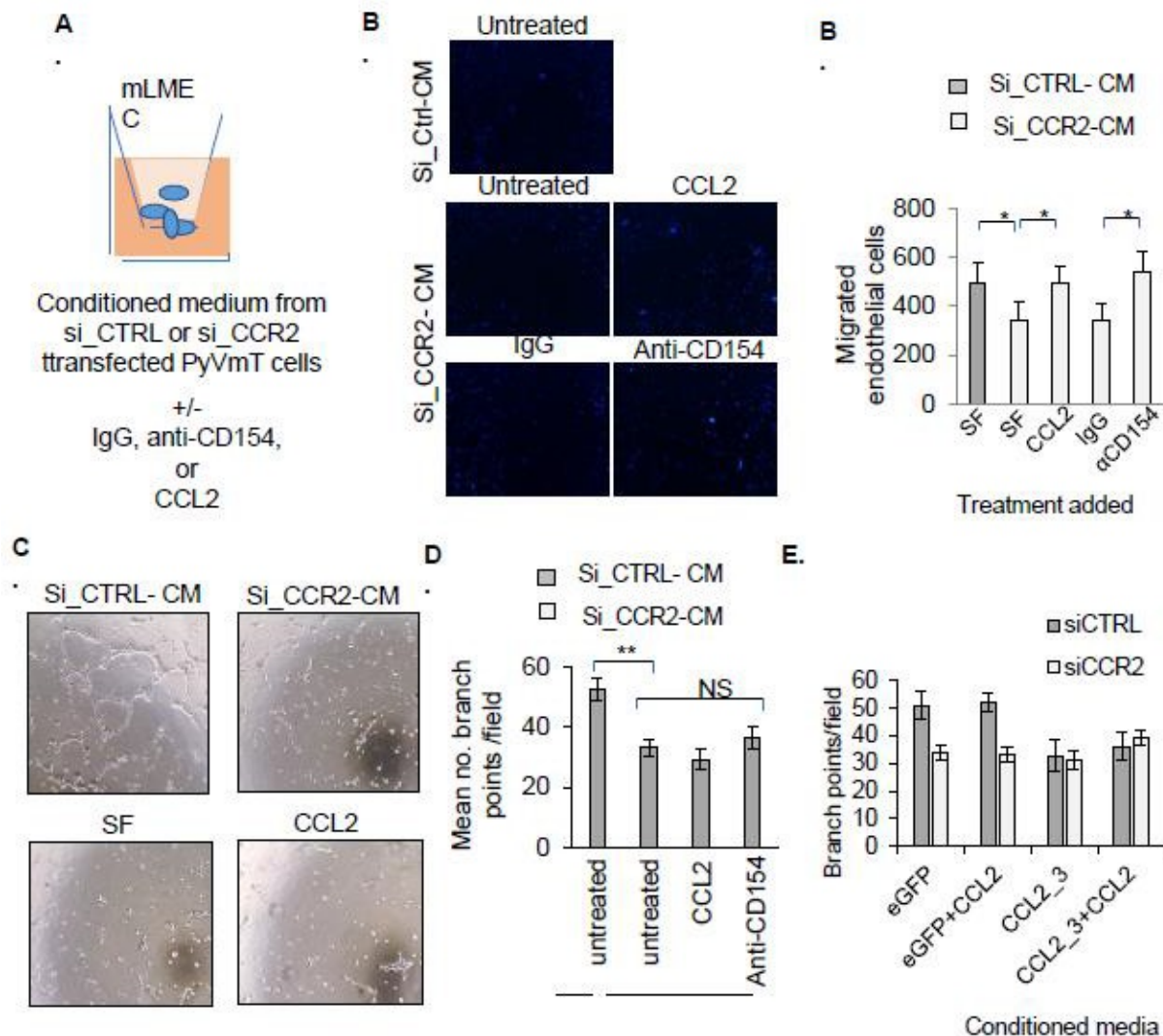


Figure 28 - CD154 neutralization and CCL2 rescues endothelial cell recruitment inhibited by CCR2 deficiency, but not endothelial sprouting, in mammary carcinoma cells. A) Diagram of endothelial cell recruitment assay. B) Endothelial cells at the underside of transwells were identified by DAPI staining, imaged by EVOS FL Auto-Imaging and counted. Lung microvascular endothelial cells were plated on Matrigel coated 96 well plates, treated with 40 ng/ml VEGF (positive control) or CCL2 (B), or conditioned medium from PyVmT cells transfected with si\_CTRL or si\_CCR2 complexes, with or without 1 mg/ml IgG control or anti-CD154 or 100 ng/ml CCL2 for 24 hours, and analyzed for branching (C). Mean number of branch points were counted. Statistical analysis was performed using One Way ANOVA with Bonferroni post-hoc comparison. Statistical significance was determined by  $p < 0.05$ . \* $p < 0.05$ , \*\* $p < 0.01$ . Mean+SEM are shown.

## **Tumoral CCR2 enhances macrophage recruitment, M2 polarization associated with increased invasiveness and proliferation in co-culture assays**

In previous studies, we quantified macrophage recruitment using a three-dimensional model that mimics chemotactic gradients from tumor cells, in which infiltration in TheraKan<sup>TM</sup> was dependent on the presence of tumor cells[107]. PyVmT mammary carcinoma cells treated with siCCR2 or siCTRL were embedded in collagen and placed into the inner chamber of the TheraKan device. mCherry labeled Raw264.7 macrophages were plated outside the devices, and measured for infiltration into the 3D cultures. Si\_CTRL PyVmT cells showed robust macrophage recruitment, which was significantly decreased with CCR2 knockdown (Figure 29A-B). Treatment of 3D cultures with CD154 neutralizing antibodies increased macrophage recruitment in CCR2 deficient 3D cultures, whereas CCL2 knockdown further decreased macrophage recruitment by siCCR2-treated cells (Figure 29B). These data indicate that CCR2 promotes macrophage recruitment by suppressing CD154, and that tumoral CCL2 is necessary for this mechanism.

Based on our findings that siCCR2 treated had fewer M2 macrophages, we analyzed how epithelial CCR2 affects M2 polarity in the context of CD154 and CCL2. Raw264.7 cells were treated with CCL2, CD154, or conditioned medium from PyVmT carcinoma cells transfected with si\_CTRL or si\_CCR2 complexes and immunostained for arginase I expression. In the absence of cells, CCL2 increased arginase expression 3-fold compared to CD154-supplemented DMEM (Right columns of Figure 29C). Conditioned medium from siCCR2-treated cells decreased arginase I expression, and both CCL2 and CD154 neutralization rescued this phenotype (Figure 29C). These data indicate that CCR2 signaling in mammary carcinoma cells

enhances macrophage recruitment and polarization through both CD154 and CCL2-dependent mechanisms.

### **Epithelial CCR2 expression affects macrophage-mediated proliferation and migration of cancer cells**

Based on the *in vivo* increases in proliferation and invasion, we assessed the effects of macrophage recruitment on tumor cells in the 3D recruitment assays. The collagen plugs from the macrophage recruitment assays were fixed, sectioned, and stained for PCNA. SiCCR2-treated cells showed decreased PCNA expression compared to si\_CTRL-treated cells (Figure 29D). CCL2 treatment or CD154 antibody neutralization rescued PCNA expression in CCR2 deficient cultures. CD154 treatment of control cultures did not affect PCNA expression (Figure 29D).

Finally, we utilized a live imaging assay of macrophage-mediated invasion to assess how epithelial CCR2 promotes invasion in the presence or absence of macrophages. We found that macrophages greatly enhanced invasion in PyVmT cells *in vitro* (Supp videos 3-4), and that recombinant CD154 was as potent as CCL2 KD or siCCR2 in decreasing tumor-cell invasion. The effect of CD154 on siCCR2-treated cells was additive, whereas knockdown of CCL2 had no effect on the invasiveness of siCCR2 treated cells (Figure 29E-F). These results suggest that epithelial CCR2 promotes invasion thru CD154-dependent mechanisms, and that CD154 suppresses invasion in a CCR2-independent manner.

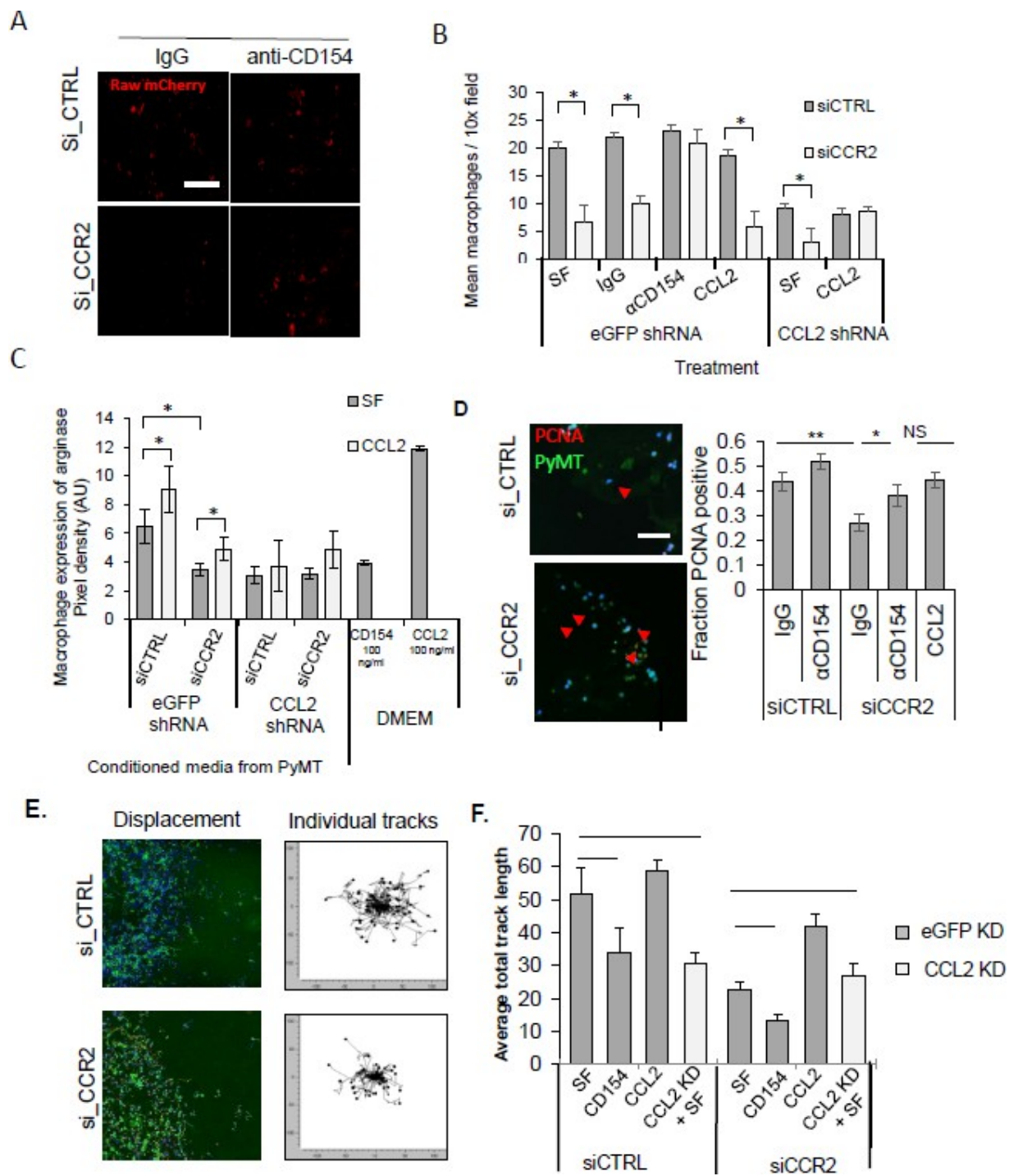


Figure 29 - CD154 rescues macrophage recruitment in CCR2 deficient mammary carcinoma cells. **A.** TrackMate plugin for Fiji used to generate models and graphs; scale bar in microns. **B.** Raw macrophages were incubated with conditioned media from Polyoma -middle-T antigen (PyMT) cells with stable CCL2 knockdown and/or siCCR2 TAT; n=3 replicate experiments. **C.** 3D cultures of PyVmT mammary carcinoma cells transfected with si\_CTRL or si\_CCR2 complexes were established in the devices. Cultures were incubated with Raw 264.7 mCherry cells with/without IgG or one ug/ml anti-CD154 and analyzed for macrophage recruitment into 3D cultures. **E.** 24 hour captures of PyMT cells migrating out of Matrigel plug onto 2D culture of Raw macrophages (left); Euclidian displacement tracks for all cells tracked (right). **F.** Average track length was calculated with TrackMate plugin of Fiji and subsequent track analysis by the Chemotaxis plugin. Cells were treated with CCL2 at 100 ng/ml or CD154 at one ug/ml, or expressed stable knockdown to CCL2 and treated with SF media. Statistical analysis was performed using One Way ANOVA with Bonferroni post-hoc comparison (A, D, E) or 2-tailed T test (B, C). Statistical significance was determined by  $p < 0.05$ . \* $p < 0.05$ , Mean $\pm$ SEM are shown.

**CD154 expression is a marker for favorable prognosis in breast cancers and correlates inversely with CCR2 expression in human breast tissue**

CD154 protein expression is downregulated in breast carcinoma tissues [68]; however, its relationship to CCL2/CCR2 signaling has not been determined. To determine whether epithelial CCR2 expression correlates with CD154 expression in humans, we immunostained tumor and adjacent-normal-matched sections for CCR2 and CD154 (Figure 30A). Images of each tumors were processed identically by color deconvolution, thresholding, and calculated as a ratio of DAB+ area over the total area of the tumor. Quantification showed a strong negative correlation between CCR2 and CD154 within individual tissues (Spearman's  $\rho = -0.68$ ; Figure 30B), with tumor tissues having high CCR2 and low CD154 relative to normal adjacent tissue (Figure 30 C&D). Survival analysis of gene expression in 1101 unique primary breast carcinomas showed that elevated tumoral expression of CD154 correlated positively with overall survival in breast cancer patients (Figure 30E). These data indicate that tumor tissues express high levels of CCR2 and low levels of CD154, and that normal adjacent tissue express high CD154 and low CCR2, suggesting that high CCR2 expression and/or low CD154 expression. RNAseq data from breast cancer patients also show that CD40 is correlated with patient prognosis (Figure 31), and that high CD154 expression correlates with decreased tumor stage and metastasis in patients (Figure 32). These data suggest a marker for favorable prognosis, providing further evidence for its role in tumor suppression.

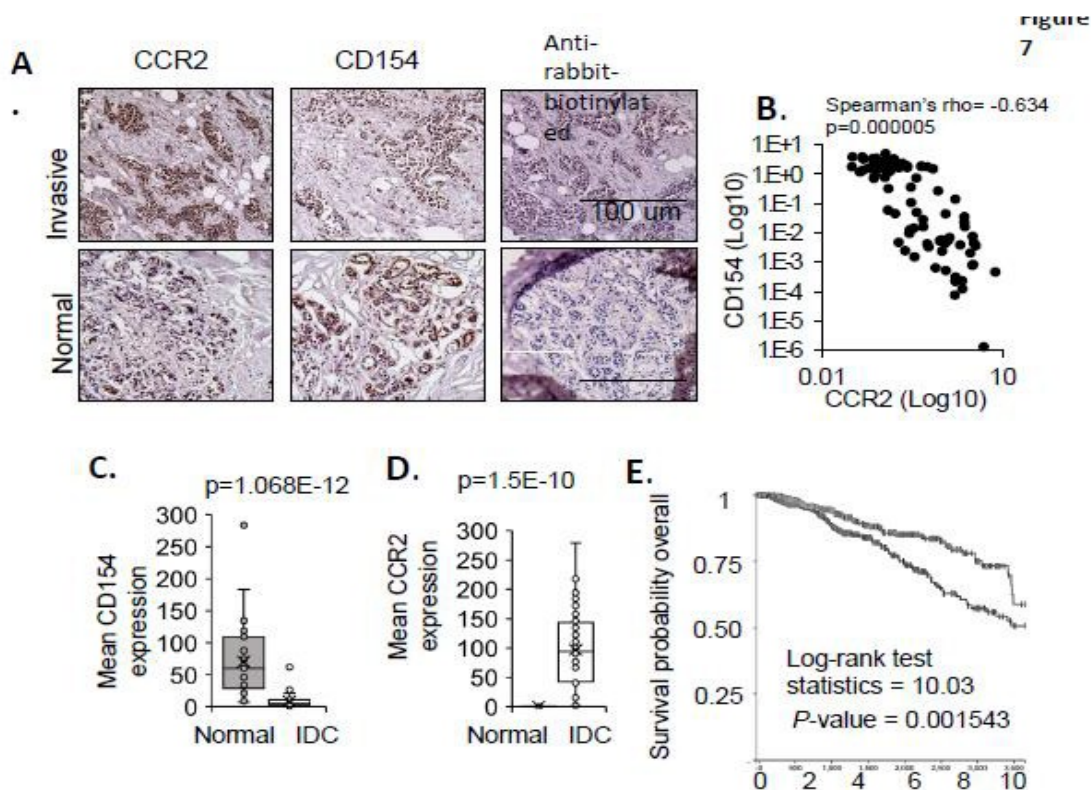


Figure 30 - CCR2 expression in breast tissues inversely correlates with CD154, a marker associated with favorable survival in breast cancer patients. A-D. Normal breast (n=35) or IDC tissues (n=48) were immunostained for CCR2 or CD154 (A). Expression of CCR2 (B) and CD154 (C) was quantified by Image J. Statistical analysis was performed using Mann Whitney test. Associations were analyzed by Spearman correlation analysis (D). E. mRNA luminal A/B, HER2+ and basal-like breast cancer datasets were analyzed for associations between CD154 expression and relapse free survival. Statistical analysis was performed using Log-rank test with Hazard ratios (HR) shown. Statistical significance was determined by  $p < 0.05$ .

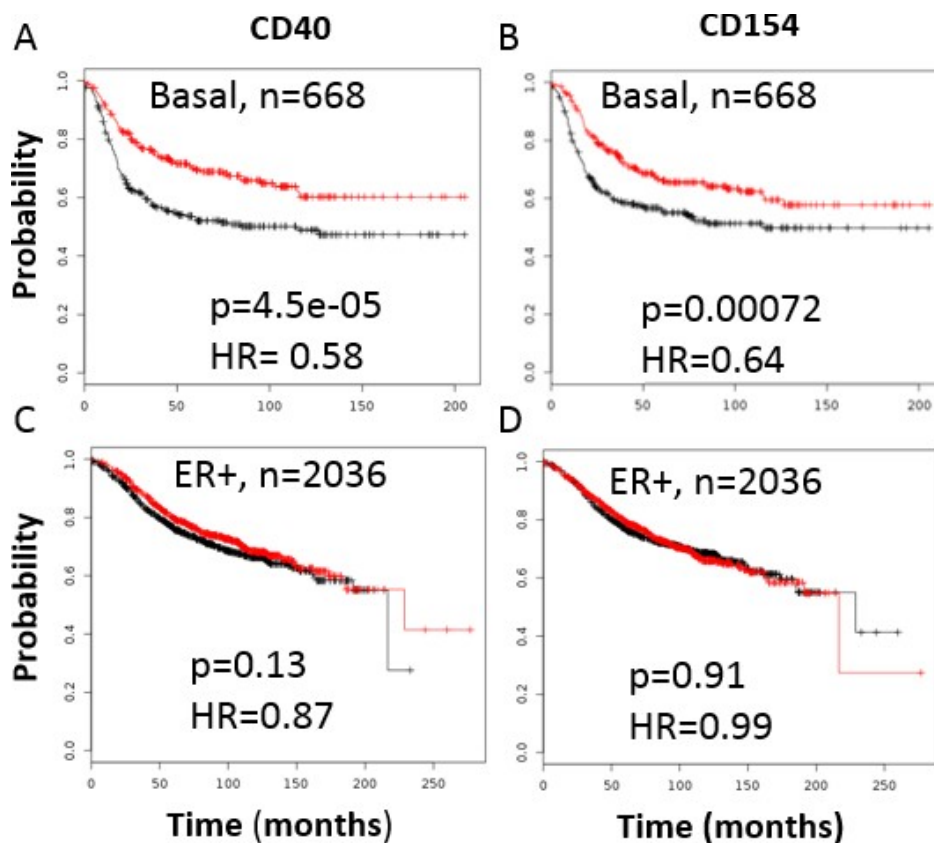
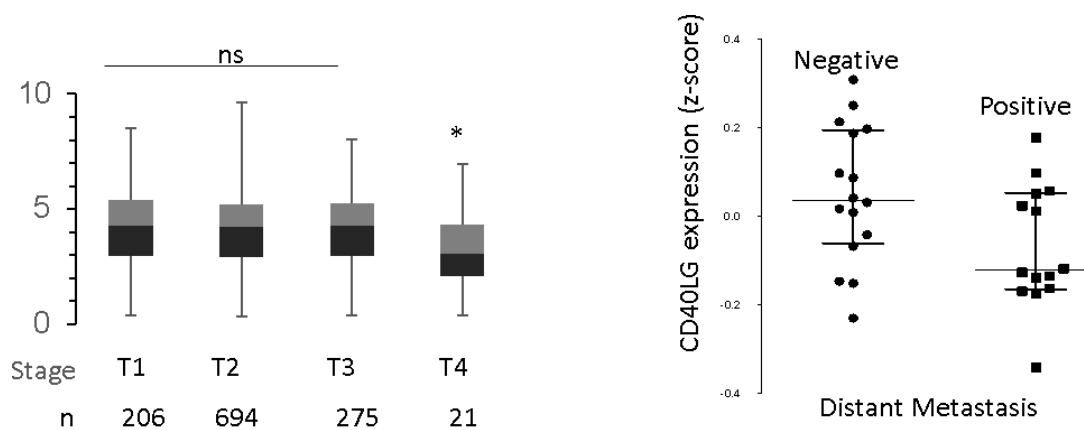


Figure 31 Regression-free survival of patients based on CD154, CD40 expression by subtype. Kaplan Meier recurrence free survival curves were generated for CD154 and CD40 expression using a median cutoff expression value, with breast tumor tissue samples stratified by PAM50 subtype. Red lines indicate high expression and black lines indicate low expression, as determined by median cutoffs. PAM50 subtyping and mRNA expression were accessed from GDC-TCGA RNA SEQ data and curves were generated with KMPlotter web-based application. HR indicating risk of recurrence by high expression group are shown, as well as log-rank p value. P values determined by log-rank test of survival.



T1 = non-invasive  
 T2 = direct nodal spread  
 T3 = indirect nodal spread  
 T4 = chest wall or pleural spread

N=14 per group, taken from  
 Caldas et al. with ESTIMATE scores  
 and path confirmation of tumor  
 cell percentage, cutoff @ 80%

Figure 32 - Expression of CD40LG mRNA in human tissue samples correlates inversely with invasive stage and metastatic spread. Left panel shows invasive stage from breast cancer TCGA RNA seq data for patients with pathological T-scoring. On right, accessed with XenaBrowser web plugin for dataset described.

## Discussion

The ability of breast cancer cells to recruit tumor-promoting macrophages is well-documented but poorly understood. Though many studies have described how tumor-derived CCL2 recruits tumor-promoting CCR2-expressing macrophages, little is known of how tumoral CCR2 affects the composition of the tumor microenvironment [128, 174]. It is possible that tumor cells continue to shape the microenvironment after stromal cells and macrophages are recruited. Based on the data presented here, we suggest CCR2 expression by tumor cells is a major contributor to these continued interactions, by maintaining tumor-promoting microenvironment both in composition and in tumor-promoting capacity.

Recent studies have shown that increased CCR2 signaling in breast cancers enhances cell survival and motility[93] and enhances development of invasive breast cancers in animal models[190]. Here we demonstrate that CCR2 signaling to carcinoma cells facilitates tumor-cell growth and migration by suppressing CD154 and increasing CCL2 bioavailability. CCR2 deficient PyVmT and DCIS.com cells showed elevated CD154 levels, which suggests that CCR2 negatively regulates CD154 expression. CCR2 deficiency in breast cancer cells had no effect on CCL2 expression in cultured cells, however, CCR2 deficient tumors showed decreased overall levels of CCL2, indicating that tumoral CCL2 expression is regulated by other mechanisms.

CCR2 expression may affect CCL2 levels *in vivo* due to the recruitment and accumulation of CCL2-secreting M2 macrophages[205], as targeting CCR2 expression in tumor cells decreased intratumoral M2 macrophages. Alternatively, CCL2 expression is regulated by other cytokines such as IL1beta and TNFa[206, 207] that are secreted by immune cells and endothelial cells[208, 209]. A reduction in tumoral CCR2 could inhibit these stromal responses

and corresponding regulatory factors, thus inhibiting CCL2 expression. The evidence suggests that CD154 expression is likely a regulatory mechanism intrinsic to tumor cells, as CD154 expression levels increased when CCL2 or CCR2 expression was decreased both *in vivo* and *in vitro* across multiple mouse models and cancer cell lines.

We show that CCR2 mediates tumor-cell migration through suppression of autocrine CD154 signaling. The tumor-suppressive effects of CD154 in PyVmT and DCIS.com cells are consistent with previous studies showing that CD154/CD40 signaling inhibits proliferation and induces apoptosis in ovarian, and cervical carcinoma and decreases migration of colon cancer cells[76, 210]. A few studies characterizing the role of CD154 in breast cancer cells show that CD154 inhibits proliferation in breast cancers through CD40 dependent mechanisms [68, 211]. Interestingly, CD154 neutralization did not affect cell proliferation of PyVmT or DCIS.com cells, but did rescue cell migration. The biological effects of CD154 were not associated with CD40 expression, which was detected in DCIS.com but not PyVmT cells, suggesting CD154 suppresses migration through another receptor. CD154 is capable of binding integrin receptors to facilitate immune cell activity[59]. It is possible that integrin receptors expression on PyVmT cells mediate CD154 signaling, as we have observed that most breast cancer cell lines express high levels of integrins known to associate with CD154.

Most studies on CD154 focus on its function as a co-stimulatory molecule during immune activation. CD154 is downregulated in breast tumors, and its expression is associated with increased relapse free survival. The immune-stimulatory effects of CD154 combined with its ability to inhibit growth and migration of cancer cells make it an ideal immunotherapeutic agent. Further studies on this pathway in carcinoma cells are necessary to fully understand the role of CD154 signaling in cancer progression.

We show that CCR2 mediates tumor-cell proliferation through paracrine mechanisms. Si\_CCR2 treated PyVmT cells and DCIS.com CCR2-KO breast cancer cells showed no differences in cell proliferation compared to si\_CTRL transfected cells or cells expressing wild-type CCR2. Furthermore, CD154 treatment did not affect proliferation of these cell lines. However, M2 macrophages recruited to breast cancer cultures were associated with increased tumor-cell proliferation. These data are consistent with previous studies showing that M2 macrophages are associated with increased tumor growth, and secrete growth factors that favor tumor progression[212]. CD154 levels in tumors also correlated with activation of T cells, consistent with the ability of CD154 to promote T cell activation and proliferation. In addition, M2 macrophages inhibit CD8<sup>+</sup> cell activity and secrete angiogenic factors, facilitating tumor growth in an indirect manner[212, 213].

Our data show that CCR2 alters macrophage recruitment and polarization by increasing intratumoral CCL2 levels and decreasing expression of CD154 by tumor cells. The presence of M2 macrophages are associated with breast tumor growth and invasion, as mice with impaired macrophage recruitment and differentiation show inhibited mammary tumor and metastasis[214]. In addition, targeting M2 macrophages that express pattern recognition receptors inhibits breast tumor growth in animal models[215]. CCL2 treatment in cell culture models rescued mammary carcinoma cell migration inhibited by CCR2 deficiency, and recruits M2 macrophages that are associated with tumor-cell proliferation. In addition, we showed that suppression of CD154 in tumor cells mediated macrophage recruitment and polarization in the presence of breast cancer cells. These data are consistent with previous studies demonstrating tumoricidal activities from macrophages activated by CD154[77, 216].

In addition to inducing M2 macrophage recruitment, our studies show that tumoral CCR2 may also be directly involved in tumor angiogenesis. Coopting of blood vessels is a well-known hallmark of cancer, supported by findings that angiogenesis inhibitors block tumor growth [2, 217]. In addition, the leaky vasculature in tumors are associated with T cell anergy, contributing to limited cytotoxic T cell activity in tumors [218]. Previous studies have shown that CCL2 stimulates angiogenesis [219, 220]. CD154 also functions as an angiogenic factor [204, 221]. Here, we show that mammary tumor cells recruitment of endothelial cells is dependent on CCR2 expression, and that CCR2 mediates endothelial recruitment in part through suppression of CD154.

Here, we show that targeting CCR2 promotes an environment to enhance T cell expansion and activation by elevating expression of immune reactive cytokines such as CD154 and inhibiting expression of immunosuppressive cytokines such as CCL2. Thus, targeting CCR2 could enhance effectiveness of therapeutic vaccines or CD25 blocking antibodies that target T regulatory cells. Further studies are necessary to discern these possibilities.

Chemotherapeutic failure and disease recurrence remains significant in treatment of invasive breast cancer[222, 223]. Recent studies show that the immune landscape is a major factor influencing therapeutic responsiveness. The presence of tumor infiltrating lymphocytes are associated with clinical responsiveness to neoadjuvant chemotherapy in HER2+ and triple-negative breast cancers[224-227]. Depletion of M2 macrophages through targeting CSFR1 enhanced responsiveness to paclitaxel in animal models of breast cancer [122]. Studies suggest that M2 macrophage secrete soluble factors such as TGF- $\beta$  and arginase I that facilitate tumor-cell survival, limited chemotherapy induced cell death[228]. Our studies show that targeting CCR2 could both reduce tumor-promoting M2 macrophages and increase the resident

lymphocyte population. As the efficacy of many immunotherapeutics hinges on the ability of lymphocytes to access a tumor, any mechanism or therapy that could increase lymphocytic infiltrates warrants further investigation.

In summary, our studies demonstrate the importance of CD154 suppression by CCR2 signaling in breast cancer progression, and suggest that epithelial CCR2 plays as important a role in macrophage-mediated breast cancer progression as macrophage CCR2. At a time when the clinical utility of combined immune checkpoint therapies is increasing, these studies prompt future studies testing combination therapy that specifically targets CCR2 and potentiates the anti-tumor effects of CD154. These results implicate CD154 suppression as a mechanism by which CCR2/CCL2 axis promotes breast cancer progression, and warrants further studies targeting this CD154-suppressing mechanism to enhance immunotherapy in CCR2-driven breast cancers.

Chapter 5: Discussion

## Summary of Results

The tumor-promoting CCL2/CCR2 axis in breast cancer is complex. Many studies show that tumor cells express CCL2 to recruit CCR2-expressing monocytes to the tumor microenvironment. These macrophages polarize to an M2 phenotype, then facilitate angiogenesis, which facilitates vascular spread of the carcinoma cells and ultimately metastatic seeding. This model fits with much of the evidence, but it is a unilateral model of interaction between tumor macrophage and do not account for a reciprocal mechanism. CCR2 is overexpressed in many IDCs, and though macrophages are plentiful in the microenvironment and known to secrete high levels of CCL2, the role of epithelial CCR2 signaling in breast cancers is poorly understood. The studies presented here support a role for CCR2 in recruiting, shaping, and maintaining a tumor-promoting microenvironment, in addition to its role in directly promoting the proliferation and invasion of tumor cells through CCL2 ligation.

These results of these suggest a novel mechanism of crosstalk between tumor and macrophages, wherein epithelial CCR2 signaling suppresses CD154 expression in carcinoma cells to recruit a CCL2-rich stroma. This CCL2 rich stroma is composed primarily of macrophages and fibroblasts, as tumoral CCR2 expression was shown to recruit these cell types in chapters 3 and 4. Chapter 2 describes how CCL2 levels in tumor cells correlate with CD154 expression levels. By knocking down CCL2 in the presence or absence of CD154, I provide evidence that tumor-derived CCL2 directly promotes cancer cell migration, survival, and stem cell renewal in a CD154 dependent manner. In the absence of CCL2 or CCR2, whether due to pharmacologic inhibition, genetic manipulation, or basal expression patterns, suppression of CD154 is lost. In these CCL2/CCR2 deplete tumor cells, CD154 inhibits the functions that CCL2/CCR2 signaling would normally promote. These studies illustrate how CCL2 and CD154

expression can directly affect the tumor-intrinsic functions of carcinoma cells, but only tangentially implicate CCR2 in this mechanism. To rule out the possibility that CCL2 suppresses CD154 by signaling through one of its alternate receptors, we knocked down and knocked out CCR2 in multiple breast cancer cell lines.

By transplanting these cells into murine compartments of variable stromal exposure, the role of tumoral CCR2 was investigated in the context of stromally-dependent and stromally-independent mechanisms. These studies show that in the presence of fibroblasts, tumoral CCR2 expression can promote invasive progression. CCR2 expression directly correlated with the level of CCL2-expressing fibroblasts in the tumor microenvironment, suggesting that CCR2 signaling in carcinoma cells regulates fibroblast populations in the microenvironment. In the absence of fibroblasts, CCR2 expression does not correlate with invasion or growth, suggesting that *in vivo*, stromal interactions are necessary for CCR2-driven tumor progression. The level of macrophages recruited to these tumors was unaffected by tumoral CCR2 expression, which could be due to the fact that these studies were conducted in immune-compromised mice where lymphoid populations are severely decreased and myeloid populations display decreased function.

To determine how tumoral CCR2 might affect the tumor microenvironment in the presence of a fully intact immune system, we utilized a syngeneic mouse model and selectively targeted tumor-cell CCR2. In this immune-competent mouse model, however, we observed multiple stromal responses not before characterized in the context of tumoral CCR2. We found that where tumoral CCR2 was selectively targeted, CD154 was overexpressed, which correlated with decreased M2 macrophages, decreased angiogenesis, and an increase in the number of activated cytotoxic T cells.

Previous studies show that CD154 overexpression in cancer cells leads to M1 polarization, can activate T cells, and that it has growth-inhibitory effects on breast carcinoma cells[71, 76, 79, 81]. Functional studies revealed that tumoral CCR2 promotes both recruitment of macrophages and M2 polarization, and this recruitment is dependent on CD154 suppression. The inhibitory effect of CCR2 block on proliferation and invasion was magnified in the presence of macrophages, further illustrating that epithelial CCR2 promotes tumor growth through stromal interactions. Taken together, a model emerges where epithelial CCR2 promotes tumor progression thru negatively regulating CD154 expression and promoting recruitment of a CCL2-rich stroma (Figure 33).

This model links the broad range of tumor promoting functions of CCL2/CCR2 signaling with the equally broad tumor-suppressing properties of CD154, which have been studied extensively and even taken to clinical trial separately. These findings reveal the importance of CD154 suppression in CCL2/CCR2-driven tumors. Additionally, these studies show that epithelial CCR2 signaling recruits CCL2-secreting stroma, providing a feed forward mechanism for inflammatory progression. This novel mechanism is supported by the data presented in this document and the countless studies characterizing the effects of CCL2 and CD154 on the tumor microenvironment. There are both CCR2 inhibitors and CD154-based agonistic therapies going that are already at the clinical trial stage now. These results suggest those two therapies could be rationally combined in treating CCR2+ breast cancers.

## Critical Review and Proposed Solutions

The role of the CCL2/CCR2 chemokine axis in breast cancer is complex. Traditional models theorized that CCL2 secretion by the tumor recruited monocytes expressing CCR2, and once resident tumor macrophages, they polarize to an M2 phenotype. From the studies provided here, a new crosstalk model emerges, wherein CCL2 expression by both tumor and macrophage facilitates monocyte recruitment, immune suppression, and direct effects on the tumor cells that synergistically promotes tumor progression.

Through controlled *in vitro* experiments, I have mapped how CD154 suppression plays a major role some in CCL2/CCR2 tumor-promoting functions. However, cytokine expression levels in the tumor microenvironment are plastic, where increased signaling by one cytokine upregulates or downregulates a network of others [229]. It is likely that the many functions of CCR2/CCL2 in the tumor microenvironment are due to its impact on the expression of other cytokines as well. Indeed, though these results provide clear evidence that CD154 suppression is required for CCL2/CCR2-signaling to drive tumor progression, there are some findings that were surprising or will require further investigation.

The mechanism by which CCR2 promotes angiogenesis and invasion are not investigated in these studies, but previous work in our lab and others provide insight. CCL2 directly induces cellular invasion by signaling thru MAPK and RhoA in 4T1, PyVmT, and MDA-231 cells, and thru facilitating epithelial-mesenchymal transition via activation of Hedgehog signaling in hepatocellular carcinoma[93] [230]. It is likely that the increased M2 macrophage population contribute to early invasion, as macrophages are known to facilitate invasion by secreting MMPs[231], or dissolving cell-cell junctions [32]. The increase in angiogenesis is also likely

due to the increase in M2 macrophage content of the tumors, which are known to produce IL-6 and VEGF [190]. However, we found that CCL2 blockade did not affect VEGF or IL-6 *in vivo* or *in vitro*. These findings are from human cells transplanted into immune-compromised mice, so it could be due to a dysfunctional myeloid compartment, or it could be due to failure of human chemokines to trigger chemotaxis of macrophages in murine systems.

Another surprising finding was the variable effect of CCR2 blockade on CCL2 levels in DCIS.com cells. CCR2 knockout has no effect on CCL2 expression, but knockdown of CCR2 decreases CCL2 levels. Residual CCR2 expression may allow for regulatory signaling to decrease CCL2 levels in the CCR2 KD cells but not in the CCR2-null knockout cells, as CCR2 levels have been shown to directly correlate with CCL2 expression in some cell types [232]. Results from other labs on the effect of CCR2 expression on tumoral CCL2 expression are similarly confounding. One study compared CCL2 secretion by cell lines derived wild-type-CCR2 and CCR2-knockout MMTV-*neu* mice and compared CCL2 secretion levels, and found that CCL2 secretion by CCR2 knockout lines ranged from 50% to 750% of the levels of wild-type CCR2 cells [233]. It appears that the regulation of CCL2 by CCR2 is context dependent and cell-type specific. Future studies should investigate how CCR2 levels regulate CCL2 expression in breast cancer cell lines of varying genetic background and molecular subtype to better understand how these factors affect CCL2 regulation.

The impact of the increased T cell populations in siCCR2 treated tumors is unclear, as there was no change in apoptosis in the siCCR2 treated tumors, despite higher levels of activated T cells which normally induce apoptosis[234]. There are 2 possibilities to explain this – that T cells are inducing cell death or suppressing tumor growth independent of apoptosis, or the actual effect is being masked by another process that is elevating apoptosis in the siCTRL group.

Although the most common mechanism of tumor-cell-killing by T cells is apoptosis, there are several apoptosis-independent mechanisms of cell death as well, including necrosis and autophagy [235, 236]. In chapter 3 I demonstrate that these mechanisms of death are active when tumoral CCR2 is blocked in NOD-SCID mice, but the lack of lymphocytes in these mice make a correlation tenuous. Further studies investigating the mechanism of CD154-mediated T cell activation and its effects on tumor development are warranted.

A major weakness in these studies is that all *in vivo* characterizations of the function of CD154 in CCL2/CCR2-mediated breast cancer progression are correlational in nature. None of the experiments directly implicate CD154 in antagonizing the functions of CCL2/CCR2 signaling through the use of an *in vivo* model. The correlational data is backed by literature and the data are relatively strong, as CD154 appears to be upregulated in all mouse models that disrupt CCL2 or CCR2 expression via shRNA, siRNA, or CRISPR knockout. A more direct method investigating the role of CD154 in CCR2-driven tumors would be to monitor tumor progression in murine transplants of cells expressing both high levels of CCR2 and CD154 (or conversely, knockout of CCR2 and CD154).

It is difficult to judge the role of tumoral CCL2 and CCR2 on macrophage recruitment and angiogenesis from chapters 2 and 3 due to the use of immune-compromised mice and human xenografts. Although immune-compromised mice are required to prevent rejection of human tumor cells, these studies would have been strengthened by the use of humanized mice, or if the *in vivo* models made use of murine mammary carcinoma cells in syngeneic immune-competent hosts. The lack of homology between murine and human CCL2/CCR2 and CD154/CD40 could explain why in chapter 4, despite altered levels of CCL2 in CCR2 overexpressing SUM225 cells and CCR2 KD DCIS.com cells, there was no change in macrophage recruitment or angiogenesis.

It is possible that the alterations in epithelial CCR2 did not regulate overall tumor CCL2 levels in SUM-225 or DCIS.com xenografts because murine CCR2 doesn't recognize human CCL2. This theory is supported by the similar findings that there is no change in angiogenesis in the DCIS.com or SUM-225 tumors; whereas when the syngeneic immune-competent model was used, macrophage content, angiogenesis, and CCL2 levels were all correlated with tumoral CCR2 expression.

The regulatory mechanism by which CCL2/CCR2 signaling suppresses CD154 signaling is unclear. These results suggest that CD154 expression is enhanced in both membrane-bound and soluble form, meaning that it is not simply being cleaved from its membrane-bound form at a higher rate after CCR2 blockade. It is likely that the upregulation occurs at the transcriptional level. Studies on the regulation of CD154 expression in carcinoma cells are few, but data from other cell types suggest that nuclear factor of activated T cells (NFAT) can induce CD154 expression in megakaryocytes, however, it is not clear whether this would be relevant to cancer cells [237]. Future studies investigating this regulatory mechanism should focus on downstream effectors of CCR2, including PI3k, Akt, and MAPK signaling pathways. Better understanding this pathway may allow therapeutic design of molecules that upregulate CD154 independent of CCR2 blockade, which could prove useful in non-CCR2 driven tumors.

Finally, though useful in understanding its tumor-promoting mechanisms in a laboratory setting, targeting CCR2/CCL2 for cancer therapy has proven difficult. Although CCL2/CCR2-signaling promotes the progression of breast cancers, it is also essential for proper immune function. T cells express CCR2, and CCR2 knockout promotes T cells to mature into immune suppressive T regulatory cells and Th17 subtypes [238]. Absence of CCL2/CCR2-signaling in mice has been shown to accelerate metastatic spread in mice [239]. Several mouse trials and

human trials show that systemic depletion of CCL2 can actually hasten disease progression [106] [135, 240]. Attempts are now being made to develop a safer method of targeting CCL2/CCR2 signaling. A small molecule CCR2 inhibitor, CCX872-B, has shown fewer side effects and may be more effective than FOLFIRANOX based on preliminary results of a phase 1b trial for advanced pancreatic cancer, suggesting CCR2 inhibition might be safer than earlier CCL2-neutralizing strategies. Based on the findings of my studies, specifically targeting CCR2 in the tumor microenvironment may also be an effective strategy.

### **Perspective**

The ability of tumor cells to avoid immune detection while actively recruiting the very cells responsible for eliciting such a response illustrates the difficulty of mounting an effective immune response against well-established tumors. The most promising immunotherapies in cancer therapy today rely on a large population of intratumoral lymphocytes that are ready to respond. In the case of breast cancer though, over 50% of infiltrating cells are macrophages, which not only promote tumor growth and angiogenesis, but actively block the recruitment and maintenance of cytotoxic T lymphocytes. The mechanism by which cancer cells coordinate this sophisticated immunologic smokescreen may allow for sensitization to immune checkpoint blockade therapies, or illuminate novel therapeutic techniques that make use of the macrophages which already reside within the tumor.

By better understanding how tumoral CCR2 blockade and increased levels of CD154 contribute to T cell activation, these mechanisms might be used to increase the efficacy of current immunotherapies. PDL1 and CTLA4 are currently targeted molecules in

immunotherapy, as they both are checkpoint inhibitors that serve to suppress an immune response. The efficacy of these therapies, however, is dependent on a Th1-type tumor microenvironment, which is characterized by the presence of M1 macrophages, CD8<sup>+</sup> T cells, CD4<sup>+</sup> T cells, as well as IL-2, IFN-gamma, IL12, and TNF [241]. These lymphocyte-rich, cytotoxic microenvironments are termed “hot tumors”, as they are primed for immune activation.

The problem for breast cancer immunotherapy is that breast tumors are Th2-dominated “cold” microenvironments, characterized by Treg and Breg lymphocytes, M2 macrophages, TAFs, and IL4, IL6, IL10, and TGFbeta [242]. Therefore, the tumor microenvironment must be converted back to a Th1 environment in order for checkpoint blockade to work. The studies presented in this dissertation suggest that CCR2 inhibition or CD154-based therapies shift from a Th2 to a Th1 immune background CD154 can decrease the M2 phenotype of macrophages, and CCR2 blockade decreases the M2 macrophages and increases both total numbers of infiltrating T lymphocytes and their activation state. Furthermore, studies utilizing CD40-agonizing antibodies have shown tumor responses in the absence of T cells due to cytotoxic myeloid-derived cells, including M1 macrophages [75, 243-245]. The net effect of CCR2 blockade is to flip the microenvironment from a tumor-friendly to a tumor-hostile environment.

As breast tumors are often macrophage-rich, a combined CCR2-blocking and CD154/CD40-agonizing therapy could provide the necessary switch to turn a cold tumor hot, susceptible to checkpoint blockade immunotherapy. As we begin to understand how breast cancer cells suppress the immune response and generate a tumor-promoting microenvironment, we are finding redundant and overlapping mechanisms that protect tumors from immune detection and promote their growth. Therefore, therapies should target multiple overlapping mechanisms to overcome tumor defenses, in a similar way that virologists combined anti-viral

therapies to finally turn HIV into a survivable infection. By combining the stimulatory effects of CCR2-blockade or CD154-upregulation with current immune checkpoint blockade therapy, a durable anti-tumor response could be generated that persists in immune memory. Although we are just beginning to understand the complexity of this disease, so too are we quickly developing more and more complex therapies to treat it. Hopefully someday the complexity of our therapies will eclipse the complexity of this deadly disease.

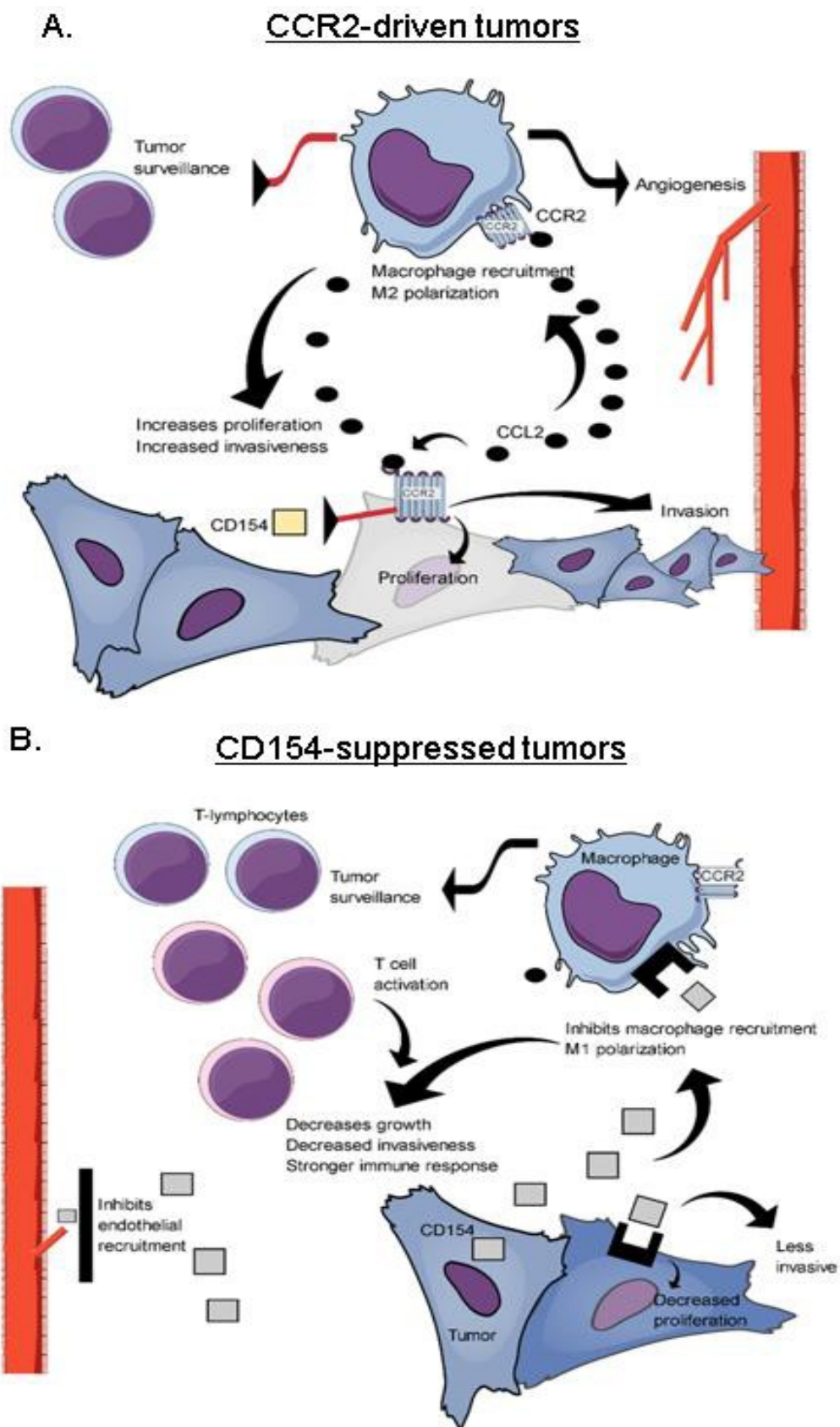


Figure 33 - Mechanism for CCR2 to promote breast cancer progression through suppressing tumoral expression of CD154.

A) In CCR2-driven tumors, CD154 is repressed. Tumor cells secrete CCL2, which recruits and polarizes M2 macrophage to the tumor microenvironment. M2 macrophages secrete high levels of CCL2, promoting further CD154 suppression. CCL2 directly promotes cancer cell invasion and proliferation, and decreases apoptosis. M2 macrophage inhibit immune surveillance by cytotoxic T cells, and facilitate angiogenesis through secretion of angiogenic factors. B) In the absence of CCR2, CD154 (grey boxes) is expressed by tumor cells. CD154 directly inhibits the migration and proliferation of tumor cells. CD154 favors M1 macrophage activation which secrete less CCL2 than M2 macrophages, thereby decreasing overall CCL2 levels in the tumor. M1 macrophages and soluble CD154 activate T cells to proliferate and recognize tumor cells. The M1 macrophages phagocytose tumor and cytotoxic T cells are then capable of recognizing and killing tumor cells, decreasing tumor growth and invasion. Increased CD154, along with a decrease in the M2-derived angiogenic factors leads to decreased endothelial recruitment and angiogenesis

## References

1. Breasted, J.H. and New-York Historical Society. Library., *The Edwin Smith surgical papyrus*. 1930, Chicago, Ill.,: The University of Chicago Press.
2. Hanahan, D. and R.A. Weinberg, *Hallmarks of cancer: the next generation*. Cell, 2011. **144**(5): p. 646-74.
3. Brien, C.A., A. Kreso, and C.H.M. Jamieson, *Cancer Stem Cells and Self-renewal*. Clinical Cancer Research, 2010. **16**(12): p. 3113.
4. Al-Hajj, M., et al., *Prospective identification of tumorigenic breast cancer cells*. Proc Natl Acad Sci U S A, 2003. **100**(7): p. 3983-8.
5. Sheridan, C., et al., *CD44+/CD24-breast cancer cells exhibit enhanced invasive properties: an early step necessary for metastasis*. Breast Cancer Research, 2006. **8**(5): p. R59.
6. Ginestier, C., et al., *ALDH1 Is a Marker of Normal and Malignant Human Mammary Stem Cells and a Predictor of Poor Clinical Outcome*. Cell Stem Cell, 2007. **1**(5): p. 555-567.
7. Zhang, C., et al., *Advancing bioluminescence imaging technology for the evaluation of anticancer agents in the MDA-MB-435-HAL-Luc mammary fat pad and subrenal capsule tumor models*. Clin Cancer Res, 2009. **15**(1): p. 238-46.
8. Cheng, N., et al., *Enhanced hepatocyte growth factor signaling by type II transforming growth factor-beta receptor knockout fibroblasts promotes mammary tumorigenesis*. Cancer Res, 2007. **67**(10): p. 4869-77.
9. Behbod, F., et al., *An intraductal human-in-mouse transplantation model mimics the subtypes of ductal carcinoma in situ*. Breast Cancer Res, 2009. **11**(5): p. R66.
10. Sflomos, G., et al., *A Preclinical Model for ERalpha-Positive Breast Cancer Points to the Epithelial Microenvironment as Determinant of Luminal Phenotype and Hormone Response*. Cancer Cell, 2016. **29**(3): p. 407-422.
11. Perou, C.M., et al., *Molecular portraits of human breast tumours*. Nature, 2000. **406**(6797): p. 747-752.
12. Sørlie, T., et al., *Gene expression patterns of breast carcinomas distinguish tumor subclasses with clinical implications*. Proceedings of the National Academy of Sciences, 2001. **98**(19): p. 10869-10874.
13. Sørlie, T., et al., *Repeated observation of breast tumor subtypes in independent gene expression data sets*. Proceedings of the National Academy of Sciences, 2003. **100**(14): p. 8418-8423.
14. Olshen, A.B., M. Ladanyi, and R. Shen, *Integrative clustering of multiple genomic data types using a joint latent variable model with application to breast and lung cancer subtype analysis*. Bioinformatics, 2009. **25**(22): p. 2906-2912.
15. Parker, J.S., et al., *Supervised Risk Predictor of Breast Cancer Based on Intrinsic Subtypes*. Journal of Clinical Oncology, 2009. **27**(8): p. 1160-1167.
16. Russnes, H.G., et al., *Breast Cancer Molecular Stratification: From Intrinsic Subtypes to Integrative Clusters*. The American Journal of Pathology, 2017. **187**(10): p. 2152-2162.
17. McGale, P., et al., *Effect of radiotherapy after mastectomy and axillary surgery on 10-year recurrence and 20-year breast cancer mortality: meta-analysis of individual patient data for 8135 women in 22 randomised trials*. Lancet, 2014. **383**(9935): p. 2127-35.

18. Martinez, F.O. and S. Gordon, *The M1 and M2 paradigm of macrophage activation: time for reassessment*. F1000Prime Rep, 2014. **6**: p. 13.
19. Zhang, M., et al., *A high M1/M2 ratio of tumor-associated macrophages is associated with extended survival in ovarian cancer patients*. J Ovarian Res, 2014. **7**: p. 19.
20. Mosmann, T.R., et al., *Two types of murine helper T cell clone. I. Definition according to profiles of lymphokine activities and secreted proteins*. The Journal of Immunology, 1986. **136**(7): p. 2348-2357.
21. West, E.E., et al., *PD-L1 blockade synergizes with IL-2 therapy in reinvigorating exhausted T cells*. The Journal of clinical investigation, 2013. **123**(6): p. 2604-2615.
22. Bachmann, M.F., et al., *Maintenance of memory CTL responses by T helper cells and CD40-CD40 ligand: antibodies provide the key*. Eur J Immunol, 2004. **34**(2): p. 317-26.
23. Bowdish, D.M.E. and S. Gordon.
24. Bilyk, N. and P.G. Holt, *Cytokine modulation of the immunosuppressive phenotype of pulmonary alveolar macrophage populations*. Immunology, 1995. **86**(2): p. 231-237.
25. Lambert, C., et al., *Dendritic cell differentiation signals induce anti-inflammatory properties in human adult microglia*. J Immunol, 2008. **181**(12): p. 8288-97.
26. Rath, M., et al., *Metabolism via Arginase or Nitric Oxide Synthase: Two Competing Arginine Pathways in Macrophages*. Frontiers in immunology, 2014. **5**: p. 532-532.
27. Rodell, C.B., et al., *TLR7/8-agonist-loaded nanoparticles promote the polarization of tumour-associated macrophages to enhance cancer immunotherapy*. Nature Biomedical Engineering, 2018. **2**(8): p. 578-588.
28. Chuang, Y., et al., *Regulation of the IL-10-driven macrophage phenotype under incoherent stimuli*. Innate immunity, 2016. **22**(8): p. 647-657.
29. de Waal Malefyt, R., et al., *Interleukin 10 (IL-10) and viral IL-10 strongly reduce antigen-specific human T cell proliferation by diminishing the antigen-presenting capacity of monocytes via downregulation of class II major histocompatibility complex expression*. The Journal of experimental medicine, 1991. **174**(4): p. 915-924.
30. Lin, E.Y. and J.W. Pollard, *Tumor-associated macrophages press the angiogenic switch in breast cancer*. Cancer Res, 2007. **67**(11): p. 5064-6.
31. Lee, S., et al., *Tumor-associated macrophages secrete CCL2 and induce the invasive phenotype of human breast epithelial cells through upregulation of ERO1-alpha and MMP-9*. Cancer Lett, 2018. **437**: p. 25-34.
32. Linde, N., et al., *Macrophages orchestrate breast cancer early dissemination and metastasis*. Nature Communications, 2018. **9**(1): p. 21.
33. Roca, H., et al., *CCL2 and Interleukin-6 Promote Survival of Human CD11b+ Peripheral Blood Mononuclear Cells and Induce M2-type Macrophage Polarization*. Journal of Biological Chemistry, 2009. **284**(49): p. 34342-34354.
34. DeNardo, D.G. and B. Ruffell, *Macrophages as regulators of tumour immunity and immunotherapy*. Nature Reviews Immunology, 2019.
35. El Kasmí, K.C., et al., *Toll-like receptor-induced arginase 1 in macrophages thwarts effective immunity against intracellular pathogens*. Nature Immunology, 2008. **9**: p. 1399.
36. Biswas, S.K. and A. Mantovani, *Macrophage plasticity and interaction with lymphocyte subsets: cancer as a paradigm*. Nature Immunology, 2010. **11**: p. 889.
37. Murray, Peter J., et al., *Macrophage Activation and Polarization: Nomenclature and Experimental Guidelines*. Immunity, 2014. **41**(1): p. 14-20.

38. Sappino, A.P., et al., *Smooth-muscle differentiation in stromal cells of malignant and non-malignant breast tissues*. Int J Cancer, 1988. **41**(5): p. 707-12.
39. Olumi, A.F., et al., *Carcinoma-associated fibroblasts direct tumor progression of initiated human prostatic epithelium*. Cancer Res, 1999. **59**(19): p. 5002-11.
40. Balkwill, F., et al., *Human lymphoblastoid interferon can inhibit the growth of human breast cancer xenografts in athymic (nude) mice*. Eur J Cancer, 1980. **16**(4): p. 569-73.
41. Palmieri, C., et al., *Fibroblast growth factor 7, secreted by breast fibroblasts, is an interleukin-1beta-induced paracrine growth factor for human breast cells*. J Endocrinol, 2003. **177**(1): p. 65-81.
42. Clark-Lewis, I., et al., *Structure-activity relationships of chemokines*. Journal of Leukocyte Biology, 1995. **57**(5): p. 703-711.
43. Bachelier, F., et al., *International Union of Basic and Clinical Pharmacology. [corrected]. LXXXIX. Update on the extended family of chemokine receptors and introducing a new nomenclature for atypical chemokine receptors*. Pharmacological reviews, 2014. **66**(1): p. 1-79.
44. Bachelier, F., et al., *An atypical addition to the chemokine receptor nomenclature: IUPHAR Review 15*. British journal of pharmacology, 2015. **172**(16): p. 3945-3949.
45. Rajagopal, S., et al., *Biased agonism as a mechanism for differential signaling by chemokine receptors*. The Journal of biological chemistry, 2013. **288**(49): p. 35039-35048.
46. Kufareva, I., C.L. Salanga, and T.M. Handel, *Chemokine and chemokine receptor structure and interactions: implications for therapeutic strategies*. Immunology and cell biology, 2015. **93**(4): p. 372-383.
47. Tsitsikov, E.N., N. Ramesh, and R.S. Geha, *Structure of the murine CD40 ligand gene*. Molecular Immunology, 1994. **31**(12): p. 895-900.
48. Yellin, M.J., et al., *Functional interactions of T cells with endothelial cells: the role of CD40L-CD40-mediated signals*. J Exp Med, 1995. **182**(6): p. 1857-64.
49. Villa, A., et al., *Organization of the human CD40L gene: implications for molecular defects in X chromosome-linked hyper-IgM syndrome and prenatal diagnosis*. Proc Natl Acad Sci U S A, 1994. **91**(6): p. 2110-4.
50. Lobo, F.M., et al., *Calcium-dependent activation of TNF family gene expression by Ca<sup>2+</sup>/calmodulin kinase type IV/Gr and calcineurin*. J Immunol, 1999. **162**(4): p. 2057-63.
51. Schubert, L.A., et al., *The Human gp39 Promoter: TWO DISTINCT NUCLEAR FACTORS OF ACTIVATED T CELL PROTEIN-BINDING ELEMENTS CONTRIBUTE INDEPENDENTLY TO TRANSCRIPTIONAL ACTIVATION*. Journal of Biological Chemistry, 1995. **270**(50): p. 29624-29627.
52. Pietravalle, F., et al., *Human Native Soluble CD40L Is a Biologically Active Trimer, Processed Inside Microsomes*. Journal of Biological Chemistry, 1996. **271**(11): p. 5965-5967.
53. Jin, Y., et al., *Characterization of soluble CD40 ligand released from human activated platelets*. J Med Dent Sci, 2001. **48**(1): p. 23-7.
54. Graf, D., et al., *A soluble form of TRAP (CD40 ligand) is rapidly released after T cell activation*. Eur J Immunol, 1995. **25**(6): p. 1749-54.

55. Yacoub, D., et al., *CD154 is released from T-cells by a disintegrin and metalloproteinase domain-containing protein 10 (ADAM10) and ADAM17 in a CD40 protein-dependent manner*. The Journal of biological chemistry, 2013. **288**(50): p. 36083-36093.
56. Ludewig, B., et al., *Induction, regulation, and function of soluble TRAP (CD40 ligand) during interaction of primary CD4<sup>+</sup> CD45RA<sup>+</sup> T cells with dendritic cells*. European Journal of Immunology, 1996. **26**(12): p. 3137-3143.
57. Schönbeck\**Rid="\*"Id="\*" Corresponding author, U. and P. Libby, The CD40/CD154 receptor/ligand dyad**RID="&dagger;"ID="&dagger;" Review*. Cellular and Molecular Life Sciences CMLS, 2001. **58**(1): p. 4-43.
58. van Kooten, C. and J. Banchereau, *CD40-CD40 ligand*. J Leukoc Biol, 2000. **67**(1): p. 2-17.
59. Jin, R., et al., *Soluble CD40 ligand stimulates CD40-dependent activation of the beta2 integrin Mac-1 and protein kinase C zeta (PKCzeta) in neutrophils: implications for neutrophil-platelet interactions and neutrophil oxidative burst*. PLoS One, 2013. **8**(6): p. e64631.
60. Hostager, B.S., et al., *Different CD40-mediated signaling events require distinct CD40 structural features*. J Immunol, 1996. **157**(3): p. 1047-53.
61. An, H.-J., et al., *Crystallographic and mutational analysis of the CD40-CD154 complex and its implications for receptor activation*. The Journal of biological chemistry, 2011. **286**(13): p. 11226-11235.
62. Elgueta, R., et al., *Molecular mechanism and function of CD40/CD40L engagement in the immune system*. Immunol Rev, 2009. **229**(1): p. 152-72.
63. Aruffo, A., et al., *The CD40 ligand, gp39, is defective in activated T cells from patients with X-linked hyper-IgM syndrome*. Cell, 1993. **72**(2): p. 291-300.
64. Young, L.S., et al., *CD40 and epithelial cells: across the great divide*. Immunology Today, 1998. **19**(11): p. 502-506.
65. Zhou, Y., et al., *Expression of CD40 and growth-inhibitory activity of CD40 agonist in ovarian carcinoma cells*. Cancer Immunol Immunother, 2012. **61**(10): p. 1735-43.
66. Li, R., et al., *Influence of sCD40L on gastric cancer cell lines*. Mol Biol Rep, 2011. **38**(8): p. 5459-64.
67. Gyorffy, B., et al., *An online survival analysis tool to rapidly assess the effect of 22,277 genes on breast cancer prognosis using microarray data of 1,809 patients*. Breast Cancer Res Treat, 2010. **123**(3): p. 725-31.
68. Tong, A.W., et al., *Growth-inhibitory effects of CD40 ligand (CD154) and its endogenous expression in human breast cancer*. Clin Cancer Res, 2001. **7**(3): p. 691-703.
69. Eliopoulos, A.G., et al., *CD40 induces apoptosis in carcinoma cells through activation of cytotoxic ligands of the tumor necrosis factor superfamily*. Mol Cell Biol, 2000. **20**(15): p. 5503-15.
70. Beatty, G.L., et al., *A phase I study of an agonist CD40 monoclonal antibody (CP-870,893) in combination with gemcitabine in patients with advanced pancreatic ductal adenocarcinoma*. Clin Cancer Res, 2013. **19**(22): p. 6286-95.
71. Hill, S.C., et al., *Activation of CD40 in cervical carcinoma cells facilitates CTL responses and augments chemotherapy-induced apoptosis*. J Immunol, 2005. **174**(1): p. 41-50.

72. Georgopoulos, N.T., et al., *A novel mechanism of CD40-induced apoptosis of carcinoma cells involving TRAF3 and JNK/AP-1 activation*. Cell Death Differ, 2006. **13**(10): p. 1789-801.
73. Buhtoiarov, I.N., et al., *Anti-tumour synergy of cytotoxic chemotherapy and anti-CD40 plus CpG-ODN immunotherapy through repolarization of tumour-associated macrophages*. Immunology, 2011. **132**(2): p. 226-39.
74. Grangeon, C., et al., *In vivo induction of antitumor immunity and protection against tumor growth by injection of CD154-expressing tumor cells*. Cancer Gene Ther, 2002. **9**(3): p. 282-8.
75. Beatty, G.L., et al., *CD40 agonists alter tumor stroma and show efficacy against pancreatic carcinoma in mice and humans*. Science, 2011. **331**(6024): p. 1612-6.
76. Vardouli, L., et al., *Adenovirus delivery of human CD40 ligand gene confers direct therapeutic effects on carcinomas*. Cancer Gene Ther, 2009. **16**(11): p. 848-60.
77. Imaizumi, K., et al., *Enhancement of tumoricidal activity of alveolar macrophages via CD40-CD40 ligand interaction*. Am J Physiol, 1999. **277**(1 Pt 1): p. L49-57.
78. Weiss, J.M., et al., *Macrophage-dependent nitric oxide expression regulates tumor cell detachment and metastasis after IL-2/anti-CD40 immunotherapy*. J Exp Med, 2010. **207**(11): p. 2455-67.
79. Liljenfeldt, L., et al., *Enhanced therapeutic anti-tumor immunity induced by co-administration of 5-fluorouracil and adenovirus expressing CD40 ligand*. Cancer Immunol Immunother, 2014. **63**(3): p. 273-82.
80. Sun, Y., et al., *In vivo gene transfer of CD40 ligand into colon cancer cells induces local production of cytokines and chemokines, tumor eradication and protective antitumor immunity*. Gene Ther, 2000. **7**(17): p. 1467-76.
81. Hanyu, K., et al., *Immunogene therapy by adenovirus vector expressing CD40 ligand for metastatic liver cancer in rats*. Anticancer Res, 2008. **28**(5A): p. 2785-9.
82. Reiser, J. and A. Banerjee, *Effector, Memory, and Dysfunctional CD8(+) T Cell Fates in the Antitumor Immune Response*. J Immunol Res, 2016. **2016**: p. 8941260.
83. Kawai, M., A. Masuda, and M. Kuwana, *A CD40-CD154 interaction in tissue fibrosis*. Arthritis Rheum, 2008. **58**(11): p. 3562-73.
84. Nannizzi-Alaimo, L., et al., *Cardiopulmonary bypass induces release of soluble CD40 ligand*. Circulation, 2002. **105**(24): p. 2849-54.
85. Otterdal, K., T.M. Pedersen, and N.O. Solum, *Release of soluble CD40 ligand after platelet activation: studies on the solubilization phase*. Thromb Res, 2004. **114**(3): p. 167-77.
86. Amirkhosravi, A., et al., *Platelet-CD40 ligand interaction with melanoma cell and monocyte CD40 enhances cellular procoagulant activity*. Blood Coagul Fibrinolysis, 2002. **13**(6): p. 505-12.
87. Franco, A.T., A. Corken, and J. Ware, *Platelets at the interface of thrombosis, inflammation, and cancer*. Blood, 2015. **126**(5): p. 582-8.
88. Van Coillie, E., J. Van Damme, and G. Opdenakker, *The MCP/eotaxin subfamily of CC chemokines*. Cytokine & Growth Factor Reviews, 1999. **10**(1): p. 61-86.
89. Lu, B., et al., *Abnormalities in monocyte recruitment and cytokine expression in monocyte chemoattractant protein 1-deficient mice*. The Journal of experimental medicine, 1998. **187**(4): p. 601-608.

90. Noris, M., et al., *Monocyte chemoattractant protein-1 is excreted in excessive amounts in the urine of patients with lupus nephritis*. Laboratory investigation; a journal of technical methods and pathology, 1995. **73**(6): p. 804-809.
91. Kamei, N., et al., *Overexpression of monocyte chemoattractant protein-1 in adipose tissues causes macrophage recruitment and insulin resistance*. J Biol Chem, 2006. **281**(36): p. 26602-14.
92. Lu, Y., et al., *CCR2 expression correlates with prostate cancer progression*. J Cell Biochem, 2007. **101**(3): p. 676-85.
93. Fang, W.B., et al., *CCL2/CCR2 chemokine signaling coordinates survival and motility of breast cancer cells through Smad3 protein- and p42/44 mitogen-activated protein kinase (MAPK)-dependent mechanisms*. J Biol Chem, 2012. **287**(43): p. 36593-608.
94. Kitamura, T., et al., *CCL2-induced chemokine cascade promotes breast cancer metastasis by enhancing retention of metastasis-associated macrophages*. J Exp Med, 2015. **212**(7): p. 1043-59.
95. Bottazzi, B., et al., *Tumor-derived chemotactic factor(s) from human ovarian carcinoma: evidence for a role in the regulation of macrophage content of neoplastic tissues*. Int J Cancer, 1985. **36**(2): p. 167-73.
96. Yoshimura, T., et al., *Human monocyte chemoattractant protein-1 (MCP-1) Full-length cDNA cloning, expression in mitogen-stimulated blood mononuclear leukocytes, and sequence similarity to mouse competence gene JE*. FEBS Letters, 1989. **244**(2): p. 487-493.
97. Bottazzi, B., et al., *A chemoattractant expressed in human sarcoma cells (tumor-derived chemotactic factor, TDCF) is identical to monocyte chemoattractant protein-1/monocyte chemotactic and activating factor (MCP-1/MCAF)*. International Journal of Cancer, 1990. **45**(4): p. 795-797.
98. Ohta, M., et al., *Monocyte chemoattractant protein-1 expression correlates with macrophage infiltration and tumor vascularity in human gastric carcinomas*. Int J Oncol, 2003. **22**(4): p. 773-8.
99. Ueno, T., et al., *Significance of Macrophage Chemoattractant Protein-1 in Macrophage Recruitment, Angiogenesis, and Survival in Human Breast Cancer*. Clinical Cancer Research, 2000. **6**(8): p. 3282.
100. Valković, T., et al., *Correlation between vascular endothelial growth factor, angiogenesis, and tumor-associated macrophages in invasive ductal breast carcinoma*. Virchows Archiv, 2002. **440**(6): p. 583-588.
101. Zeisberger, S.M., et al., *Clodronate-liposome-mediated depletion of tumour-associated macrophages: a new and highly effective antiangiogenic therapy approach*. British Journal of Cancer, 2006. **95**(3): p. 272-281.
102. Fujimoto, H., et al., *Stromal MCP-1 in mammary tumors induces tumor-associated macrophage infiltration and contributes to tumor progression*. Int J Cancer, 2009. **125**(6): p. 1276-84.
103. Qian, B.Z., et al., *CCL2 recruits inflammatory monocytes to facilitate breast-tumour metastasis*. Nature, 2011. **475**(7355): p. 222-5.
104. Hembruff, S.L., et al., *Loss of transforming growth factor-beta signaling in mammary fibroblasts enhances CCL2 secretion to promote mammary tumor progression through macrophage-dependent and -independent mechanisms*. Neoplasia, 2010. **12**(5): p. 425-33.

105. Yao, M., et al., *Continuous Delivery of Neutralizing Antibodies Elevate CCL2 Levels in Mice Bearing MCF10CA1d Breast Tumor Xenografts*. *Transl Oncol*, 2017. **10**(5): p. 734-743.
106. Bonapace, L., et al., *Cessation of CCL2 inhibition accelerates breast cancer metastasis by promoting angiogenesis*. *Nature*, 2014. **515**(7525): p. 130-3.
107. Fang, W.B., et al., *Targeted gene silencing of CCL2 inhibits triple negative breast cancer progression by blocking cancer stem cell renewal and M2 macrophage recruitment*. *Oncotarget*, 2016.
108. Blum, S., F. Martins, and M. Lubbert, *Immunotherapy in adult acute leukemia*. *Leuk Res*, 2017. **60**: p. 63-73.
109. Arasanz, H., et al., *Immunotherapy in malignant melanoma: recent approaches and new perspectives*. *Melanoma Manag*, 2017. **4**(1): p. 39-48.
110. Du, L., R.S. Herbst, and D. Morgensztern, *Immunotherapy in Lung Cancer*. *Hematol Oncol Clin North Am*, 2017. **31**(1): p. 131-141.
111. Nanda, R., et al., *Pembrolizumab in Patients With Advanced Triple-Negative Breast Cancer: Phase Ib KEYNOTE-012 Study*. *J Clin Oncol*, 2016. **34**(21): p. 2460-7.
112. Dirix, L.Y., et al., *Avelumab, an anti-PD-L1 antibody, in patients with locally advanced or metastatic breast cancer: a phase Ib JAVELIN Solid Tumor study*. *Breast Cancer Res Treat*, 2018. **167**(3): p. 671-686.
113. Vonderheide, R.H., et al., *Tremelimumab in combination with exemestane in patients with advanced breast cancer and treatment-associated modulation of inducible costimulator expression on patient T cells*. *Clin Cancer Res*, 2010. **16**(13): p. 3485-94.
114. Stanton, S.E. and M.L. Disis, *Clinical significance of tumor-infiltrating lymphocytes in breast cancer*. *J Immunother Cancer*, 2016. **4**: p. 59.
115. Muenst, S., et al., *Expression of programmed death ligand 1 (PD-L1) is associated with poor prognosis in human breast cancer*. *Breast Cancer Res Treat*, 2014. **146**(1): p. 15-24.
116. Dill, E.A., et al., *PD-L1 Expression and Intratumoral Heterogeneity Across Breast Cancer Subtypes and Stages: An Assessment of 245 Primary and 40 Metastatic Tumors*. *Am J Surg Pathol*, 2017. **41**(3): p. 334-342.
117. Lan, G., et al., *Cytotoxic T lymphocyte associated antigen 4 expression predicts poor prognosis in luminal B HER2-negative breast cancer*. *Oncol Lett*, 2018. **15**(4): p. 5093-5097.
118. Kieber-Emmons, T., et al., *Harnessing benefit from targeting tumor associated carbohydrate antigens*. *Hum Vaccin Immunother*, 2017. **13**(2): p. 323-331.
119. Ladoire, S., et al., *[The anti-tumor immune response in breast cancer: Update and therapeutic perspectives]*. *Ann Pathol*, 2017. **37**(1): p. 133-141.
120. Costa, R.L.B., H. Soliman, and B.J. Czerniecki, *The clinical development of vaccines for HER2(+) breast cancer: Current landscape and future perspectives*. *Cancer Treat Rev*, 2017. **61**: p. 107-115.
121. Miles, D., et al., *Phase III multicenter clinical trial of the sialyl-TN (STn)-keyhole limpet hemocyanin (KLH) vaccine for metastatic breast cancer*. *Oncologist*, 2011. **16**(8): p. 1092-100.
122. DeNardo, D.G., et al., *Leukocyte complexity predicts breast cancer survival and functionally regulates response to chemotherapy*. *Cancer Discov*, 2011. **1**(1): p. 54-67.

123. Charo, I.F., et al., *Molecular cloning and functional expression of two monocyte chemoattractant protein 1 receptors reveals alternative splicing of the carboxyl-terminal tails*. Proceedings of the National Academy of Sciences, 1994. **91**(7): p. 2752-2756.
124. Wong, L.M., et al., *Organization and differential expression of the human monocyte chemoattractant protein 1 receptor gene. Evidence for the role of the carboxyl-terminal tail in receptor trafficking*. J Biol Chem, 1997. **272**(2): p. 1038-45.
125. Torres, S., et al., *Proteome profiling of cancer-associated fibroblasts identifies novel proinflammatory signatures and prognostic markers for colorectal cancer*. Clin Cancer Res, 2013. **19**(21): p. 6006-19.
126. Shi, C. and E.G. Pamer, *Monocyte recruitment during infection and inflammation*. Nature reviews. Immunology, 2011. **11**(11): p. 762-774.
127. Yao, M., et al., *Elevated expression of chemokine C-C ligand 2 in stroma is associated with recurrent basal-like breast cancers*. Mod Pathol, 2016.
128. Lim, S.Y., et al., *Targeting the CCL2-CCR2 signaling axis in cancer metastasis*. Oncotarget, 2016. **7**(19): p. 28697-710.
129. Ansari, A.W., A. Kamarulzaman, and R.E. Schmidt, *Multifaceted Impact of Host C-C Chemokine CCL2 in the Immuno-Pathogenesis of HIV-1/M. tuberculosis Co-Infection*. Front Immunol, 2013. **4**: p. 312.
130. Borsig, L., et al., *Inflammatory chemokines and metastasis--tracing the accessory*. Oncogene, 2014. **33**(25): p. 3217-24.
131. Dutta, P., et al., *MCP-1 is overexpressed in triple-negative breast cancers and drives cancer invasiveness and metastasis*. 2018.
132. Lu, Y., et al., *Monocyte chemotactic protein-1 (MCP-1) acts as a paracrine and autocrine factor for prostate cancer growth and invasion*. Prostate, 2006. **66**(12): p. 1311-8.
133. Yao, M., et al., *CCR2 Chemokine Receptors Enhance Growth and Cell-Cycle Progression of Breast Cancer Cells through SRC and PKC Activation*. 2019. **17**(2): p. 604-617.
134. Sierra-Filardi, E., et al., *CCL2 Shapes Macrophage Polarization by GM-CSF and M-CSF: Identification of CCL2/CCR2-Dependent Gene Expression Profile*. The Journal of Immunology, 2014.
135. Haringman, J.J., et al., *A randomized controlled trial with an anti-CCL2 (anti-monocyte chemotactic protein 1) monoclonal antibody in patients with rheumatoid arthritis*. Arthritis & Rheumatism, 2006. **54**(8): p. 2387-2392.
136. Li, M., et al., *A role for CCL2 in both tumor progression and immunosurveillance*. Oncoimmunology, 2013. **2**(7): p. e25474-e25474.
137. Fang, W.B., et al., *Targeted gene silencing of CCL2 inhibits triple negative breast cancer progression by blocking cancer stem cell renewal and M2 macrophage recruitment*. Oncotarget, 2016. **7**(31): p. 49349-49367.
138. Valkovic, T., et al., *Expression of monocyte chemotactic protein-1 in human invasive ductal breast cancer*. Pathol Res Pract, 1998. **194**(5): p. 335-40.
139. Pang, J.M., K.L. Gorringer, and S.B. Fox, *Ductal carcinoma in situ - update on risk assessment and management*. Histopathology, 2016. **68**(1): p. 96-109.
140. Park, T.S. and E.S. Hwang, *Current Trends in the Management of Ductal Carcinoma In Situ*. Oncology (Williston Park), 2016. **30**(9).

141. Virnig, B.A., et al., *Ductal carcinoma in situ of the breast: a systematic review of incidence, treatment, and outcomes*. J Natl Cancer Inst, 2010. **102**(3): p. 170-8.
142. Khan, S., et al., *Are We Overtreating Ductal Carcinoma in Situ (DCIS)?* Ann Surg Oncol, 2016.
143. Goldstein, S.N., *Controversies in pathology in early-stage breast cancer*. Semin Radiat Oncol, 2011. **21**(1): p. 20-5.
144. Kerlikowske, K., et al., *Biomarker expression and risk of subsequent tumors after initial ductal carcinoma in situ diagnosis*. J Natl Cancer Inst, 2010. **102**(9): p. 627-37.
145. Palomino, D.C. and L.C. Marti, *Chemokines and immunity*. Einstein (Sao Paulo), 2015. **13**(3): p. 469-73.
146. Balkwill, F.R., *The chemokine system and cancer*. J Pathol, 2012. **226**(2): p. 148-57.
147. Mardekian, S.K., A. Bombonati, and J.P. Palazzo, *Ductal carcinoma in situ of the breast: the importance of morphologic and molecular interactions*. Hum Pathol, 2016. **49**: p. 114-23.
148. Sambade, M.J., et al., *Lapatinib in combination with radiation diminishes tumor regrowth in HER2+ and basal-like/EGFR+ breast tumor xenografts*. Int J Radiat Oncol Biol Phys, 2010. **77**(2): p. 575-81.
149. Valdez, K.E., et al., *Human primary ductal carcinoma in situ (DCIS) subtype-specific pathology is preserved in a mouse intraductal (MIND) xenograft model*. J Pathol, 2011. **225**(4): p. 565-73.
150. Damiani, S., et al., *Myoepithelial cells and basal lamina in poorly differentiated in situ duct carcinoma of the breast. An immunocytochemical study*. Virchows Arch, 1999. **434**(3): p. 227-34.
151. Lazard, D., et al., *Expression of smooth muscle-specific proteins in myoepithelium and stromal myofibroblasts of normal and malignant human breast tissue*. Proc Natl Acad Sci U S A, 1993. **90**(3): p. 999-1003.
152. Patarroyo, M., K. Tryggvason, and I. Virtanen, *Laminin isoforms in tumor invasion, angiogenesis and metastasis*. Semin Cancer Biol, 2002. **12**(3): p. 197-207.
153. Ioachim, E., et al., *Immunohistochemical expression of extracellular matrix components tenascin, fibronectin, collagen type IV and laminin in breast cancer: their prognostic value and role in tumour invasion and progression*. Eur J Cancer, 2002. **38**(18): p. 2362-70.
154. Park, S.Y., H.M. Kim, and J.S. Koo, *Differential expression of cancer-associated fibroblast-related proteins according to molecular subtype and stromal histology in breast cancer*. Breast Cancer Res Treat, 2015. **149**(3): p. 727-41.
155. Sugimoto, H., et al., *Identification of fibroblast heterogeneity in the tumor microenvironment*. Cancer Biol Ther, 2006. **5**(12): p. 1640-6.
156. Carvalho, I., et al., *Overexpression of platelet-derived growth factor receptor alpha in breast cancer is associated with tumour progression*. Breast Cancer Res, 2005. **7**(5): p. R788-95.
157. Bussard, K.M., et al., *Tumor-associated stromal cells as key contributors to the tumor microenvironment*. Breast Cancer Res, 2016. **18**(1): p. 84.
158. Fang, W.B., M. Yao, and N. Cheng, *Priming cancer cells for drug resistance: role of the fibroblast niche*. Front Biol (Beijing), 2014. **9**(2): p. 114-126.
159. Livasy, C.A., et al., *Phenotypic evaluation of the basal-like subtype of invasive breast carcinoma*. Mod Pathol, 2006. **19**(2): p. 264-71.

160. Ginestier C, H.M., Charafe-Jauffet E, Monville F, Dutcher J, Brown M, Jacquemier J, Viens P, Kleer C, Liu S, Schott A, Hayes D, Birmbaum D, Wicha MS, Dontu G., *ALDH1 is a marker of normal and malignant human mammary stem cells and a predictor of poor clinical outcome*. Cell Stem Cell, 2007. **1**(5): p. 555-67.
161. Jeyaraju, D.V., et al., *Hax1 lacks BH modules and is peripherally associated to heavy membranes: implications for Omi/HtrA2 and PARL activity in the regulation of mitochondrial stress and apoptosis*. Cell Death Differ, 2009. **16**(12): p. 1622-9.
162. Szasz, A.M., et al., *Cross-validation of survival associated biomarkers in gastric cancer using transcriptomic data of 1,065 patients*. Oncotarget, 2016.
163. Medrek, C., et al., *The presence of tumor associated macrophages in tumor stroma as a prognostic marker for breast cancer patients*. BMC Cancer, 2012. **12**: p. 306.
164. Gwak, J.M., et al., *Prognostic value of tumor-associated macrophages according to histologic locations and hormone receptor status in breast cancer*. PLoS One, 2015. **10**(4): p. e0125728.
165. Al-Saleh, K., et al., *Predictive and prognostic significance of CD8(+) tumor-infiltrating lymphocytes in patients with luminal B/HER 2 negative breast cancer treated with neoadjuvant chemotherapy*. Oncol Lett, 2017. **14**(1): p. 337-344.
166. Liu, S., et al., *CD8+ lymphocyte infiltration is an independent favorable prognostic indicator in basal-like breast cancer*. Breast Cancer Res, 2012. **14**(2): p. R48.
167. Seo, A.N., et al., *Tumour-infiltrating CD8+ lymphocytes as an independent predictive factor for pathological complete response to primary systemic therapy in breast cancer*. Br J Cancer, 2013. **109**(10): p. 2705-13.
168. Huber, S., et al., *Alternatively activated macrophages inhibit T-cell proliferation by Stat6-dependent expression of PD-L2*. Blood, 2010. **116**(17): p. 3311-20.
169. Peranzoni, E., et al., *Macrophages impede CD8 T cells from reaching tumor cells and limit the efficacy of anti-PD-1 treatment*. Proc Natl Acad Sci U S A, 2018. **115**(17): p. E4041-E4050.
170. Owen, J.L. and M. Mohamadzadeh, *Macrophages and chemokines as mediators of angiogenesis*. Front Physiol, 2013. **4**: p. 159.
171. Caux, C., et al., *A Milestone Review on How Macrophages Affect Tumor Growth*. Cancer Res, 2016. **76**(22): p. 6439-6442.
172. Yao, M., et al., *Cytokine Regulation of Metastasis and Tumorigenicity*. Adv Cancer Res, 2016. **132**: p. 265-367.
173. Lacalle, R.A., et al., *Chemokine Receptor Signaling and the Hallmarks of Cancer*. Int Rev Cell Mol Biol, 2017. **331**: p. 181-244.
174. O'Connor, T., L. Borsig, and M. Heikenwalder, *CCL2-CCR2 Signaling in Disease Pathogenesis*. Endocr Metab Immune Disord Drug Targets, 2015. **15**(2): p. 105-18.
175. Yao, M., et al., *Elevated expression of chemokine C-C ligand 2 in stroma is associated with recurrent basal-like breast cancers*. Mod Pathol, 2016: p. 810-823.
176. Makley, L.N. and J.E. Gestwicki, *Expanding the number of 'druggable' targets: non-enzymes and protein-protein interactions*. Chem Biol Drug Des, 2013. **81**(1): p. 22-32.
177. Liu, T. and R.B. Altman, *Identifying druggable targets by protein microenvironments matching: application to transcription factors*. CPT Pharmacometrics Syst Pharmacol, 2014. **3**: p. e93.
178. Khurana, B., et al., *siRNA delivery using nanocarriers - an efficient tool for gene silencing*. Curr Gene Ther, 2010. **10**(2): p. 139-55.

179. Vives, E., P. Brodin, and B. Lebleu, *A truncated HIV-1 Tat protein basic domain rapidly translocates through the plasma membrane and accumulates in the cell nucleus*. J Biol Chem, 1997. **272**(25): p. 16010-7.
180. Tung, C.H., S. Mueller, and R. Weissleder, *Novel branching membrane translocational peptide as gene delivery vector*. Bioorg Med Chem, 2002. **10**(11): p. 3609-14.
181. Ignatovich, I.A., et al., *Complexes of plasmid DNA with basic domain 47-57 of the HIV-1 Tat protein are transferred to mammalian cells by endocytosis-mediated pathways*. J Biol Chem, 2003. **278**(43): p. 42625-36.
182. Baoum, A., et al., *"Soft" calcium crosslinks enable highly efficient gene transfection using TAT peptide*. Pharm Res, 2009. **26**(12): p. 2619-29.
183. Pickel, L., et al., *Overexpression of angiotensin II type 2 receptor gene induces cell death in lung adenocarcinoma cells*. Cancer Biol Ther, 2010. **9**(4).
184. Khondee, S., et al., *Calcium condensed LABL-TAT complexes effectively target gene delivery to ICAM-1 expressing cells*. Mol Pharm, 2011. **8**(3): p. 788-98.
185. Fang, W.B., et al., *The CCL2 chemokine is a negative regulator of autophagy and necrosis in luminal B breast cancer cells*. Breast Cancer Res Treat, 2015. **150**(2): p. 309-20.
186. Romagnoli, G., et al., *Morphological Evaluation of Tumor-Infiltrating Lymphocytes (TILs) to Investigate Invasive Breast Cancer Immunogenicity, Reveal Lymphocytic Networks and Help Relapse Prediction: A Retrospective Study*. Int J Mol Sci, 2017. **18**(9).
187. Ruffell, B., et al., *Leukocyte composition of human breast cancer*. Proc Natl Acad Sci U S A, 2012. **109**(8): p. 2796-801.
188. Catteau, X., et al., *Variable stromal periductular expression of CD34 and smooth muscle actin (SMA) in intraductal carcinoma of the breast*. PLoS One, 2013. **8**(3): p. e57773.
189. Miller, F.R., et al., *MCF10DCIS.com xenograft model of human comedo ductal carcinoma in situ*. J Natl Cancer Inst, 2000. **92**(14): p. 1185-6.
190. Brummer, G., et al., *Chemokine Signaling Facilitates Early-Stage Breast Cancer Survival and Invasion through Fibroblast-Dependent Mechanisms*. Mol Cancer Res, 2018. **16**(2): p. 296-308.
191. Fang, W.B., et al., *Loss of one Tgfr2 allele in fibroblasts promotes metastasis in MMTV: polyoma middle T transgenic and transplant mouse models of mammary tumor progression*. Clin Exp Metastasis, 2011. **28**(4): p. 351-66.
192. Artym, V.V. and K. Matsumoto, *Imaging cells in three-dimensional collagen matrix*. Curr Protoc Cell Biol, 2010. **Chapter 10**: p. Unit 10 18 1-20.
193. Cheng, N., et al., *Loss of TGF-beta type II receptor in fibroblasts promotes mammary carcinoma growth and invasion through upregulation of TGF-alpha-, MSP- and HGF-mediated signaling networks*. Oncogene, 2005. **24**(32): p. 5053-68.
194. Guy, C., R. Cardiff, and W. Muller, *Induction of mammary tumors by expression a polyomavirus middle T oncogene: a transgenic mouse model for metastatic disease*. Mol Cell Biol, 1992. **12**: p. 954-61.
195. Maglione, J.E., et al., *Transgenic Polyoma middle-T mice model premalignant mammary disease*. Cancer Res, 2001. **61**(22): p. 8298-305.
196. Schwab, L.P., et al., *Hypoxia-inducible factor 1alpha promotes primary tumor growth and tumor-initiating cell activity in breast cancer*. Breast Cancer Res, 2012. **14**(1): p. R6.

197. Usary, J., et al., *Predicting drug responsiveness in human cancers using genetically engineered mice*. Clin Cancer Res, 2013. **19**(17): p. 4889-99.
198. Scribner, K.C., F. Behbod, and W.W. Porter, *Regulation of DCIS to invasive breast cancer progression by Single-minded-2s (SIM2s)*. Oncogene, 2012.
199. Bretscher, P.A., *A two-step, two-signal model for the primary activation of precursor helper T cells*. Proc Natl Acad Sci U S A, 1999. **96**(1): p. 185-90.
200. Vonderheide, R.H. and M.J. Glennie, *Agonistic CD40 antibodies and cancer therapy*. Clin Cancer Res, 2013. **19**(5): p. 1035-43.
201. Aarts, S., et al., *The CD40-CD40L Dyad in Experimental Autoimmune Encephalomyelitis and Multiple Sclerosis*. Front Immunol, 2017. **8**: p. 1791.
202. Urbich, C., et al., *CD40 ligand inhibits endothelial cell migration by increasing production of endothelial reactive oxygen species*. Circulation, 2002. **106**(8): p. 981-6.
203. Reinders, M.E., et al., *Proangiogenic function of CD40 ligand-CD40 interactions*. J Immunol, 2003. **171**(3): p. 1534-41.
204. Deregibus, M.C., et al., *CD40-dependent activation of phosphatidylinositol 3-kinase/Akt pathway mediates endothelial cell survival and in vitro angiogenesis*. J Biol Chem, 2003. **278**(20): p. 18008-14.
205. Heimdal, J.H., et al., *Monocyte and monocyte-derived macrophage secretion of MCP-1 in co-culture with autologous malignant and benign control fragment spheroids*. Cancer Immunol Immunother, 2001. **50**(6): p. 300-6.
206. Thompson, W.L. and L.J. Van Eldik, *Inflammatory cytokines stimulate the chemokines CCL2/MCP-1 and CCL7/MCP-3 through NFkB and MAPK dependent pathways in rat astrocytes [corrected]*. Brain Res, 2009. **1287**: p. 47-57.
207. Rollins, B.J., et al., *Cytokine-activated human endothelial cells synthesize and secrete a monocyte chemoattractant, MCP-1/JE*. Am J Pathol, 1990. **136**(6): p. 1229-33.
208. Ward, J.R., et al., *Temporal interleukin-1beta secretion from primary human peripheral blood monocytes by P2X7-independent and P2X7-dependent mechanisms*. J Biol Chem, 2010. **285**(30): p. 23147-58.
209. Alfaidi, M., et al., *Neutrophil elastase promotes interleukin-1beta secretion from human coronary endothelium*. J Biol Chem, 2015. **290**(40): p. 24067-78.
210. Melichar, B., et al., *Expression of CD40 and growth-inhibitory activity of CD40 ligand in ovarian cancer cell lines*. Gynecol Oncol, 2007. **104**(3): p. 707-13.
211. Hirano, A., et al., *Inhibition of human breast carcinoma growth by a soluble recombinant human CD40 ligand*. Blood, 1999. **93**(9): p. 2999-3007.
212. Najafi, M., et al., *Macrophage polarity in cancer: A review*. J Cell Biochem, 2018.
213. Elliott, L.A., et al., *Human Tumor-Infiltrating Myeloid Cells: Phenotypic and Functional Diversity*. Front Immunol, 2017. **8**: p. 86.
214. Lin, E.Y., et al., *Colony-stimulating factor 1 promotes progression of mammary tumors to malignancy*. J Exp Med, 2001. **193**(6): p. 727-40.
215. Georgoudaki, A.M., et al., *Reprogramming Tumor-Associated Macrophages by Antibody Targeting Inhibits Cancer Progression and Metastasis*. Cell Rep, 2016. **15**(9): p. 2000-11.
216. Buhtoiarov, I.N., et al., *CD40 ligation activates murine macrophages via an IFN-gamma-dependent mechanism resulting in tumor cell destruction in vitro*. J Immunol, 2005. **174**(10): p. 6013-22.

217. Mashreghi, M., et al., *Angiogenesis biomarkers and their targeting ligands as potential targets for tumor angiogenesis*. J Cell Physiol, 2018. **233**(4): p. 2949-2965.
218. Ager, A. and M.J. May, *Understanding high endothelial venules: Lessons for cancer immunology*. Oncoimmunology, 2015. **4**(6): p. e1008791.
219. Hong, K.H., J. Ryu, and K.H. Han, *Monocyte chemoattractant protein-1-induced angiogenesis is mediated by vascular endothelial growth factor-A*. Blood, 2005. **105**(4): p. 1405-7.
220. Stamatovic, S.M., et al., *CCL2 regulates angiogenesis via activation of Ets-1 transcription factor*. J Immunol, 2006. **177**(4): p. 2651-61.
221. Leroyer, A.S., et al., *CD40 ligand+ microparticles from human atherosclerotic plaques stimulate endothelial proliferation and angiogenesis a potential mechanism for intraplaque neovascularization*. J Am Coll Cardiol, 2008. **52**(16): p. 1302-11.
222. Alabdulkareem, H., et al., *The impact of molecular subtype on breast cancer recurrence in young women treated with contemporary adjuvant therapy*. Breast J, 2018. **24**(2): p. 148-153.
223. Fung, F., et al., *Predictors of 5-year local, regional, and distant recurrent events in a population-based cohort of breast cancer patients*. Am J Surg, 2017. **213**(2): p. 418-425.
224. Denkert, C., et al., *Tumor-associated lymphocytes as an independent predictor of response to neoadjuvant chemotherapy in breast cancer*. J Clin Oncol, 2010. **28**(1): p. 105-13.
225. Ono, M., et al., *Tumor-infiltrating lymphocytes are correlated with response to neoadjuvant chemotherapy in triple-negative breast cancer*. Breast Cancer Res Treat, 2012. **132**(3): p. 793-805.
226. Miyashita, M., et al., *Tumor-infiltrating CD8+ and FOXP3+ lymphocytes in triple-negative breast cancer: its correlation with pathological complete response to neoadjuvant chemotherapy*. Breast Cancer Res Treat, 2014. **148**(3): p. 525-34.
227. Asano, Y., et al., *Prediction of Treatment Response to Neoadjuvant Chemotherapy in Breast Cancer by Subtype Using Tumor-infiltrating Lymphocytes*. Anticancer Res, 2018. **38**(4): p. 2311-2321.
228. Tham, M., et al., *Melanoma-initiating cells exploit M2 macrophage TGFbeta and arginase pathway for survival and proliferation*. Oncotarget, 2014. **5**(23): p. 12027-42.
229. Nedoszytko, B., et al., *Chemokines and cytokines network in the pathogenesis of the inflammatory skin diseases: atopic dermatitis, psoriasis and skin mastocytosis*. Postepy dermatologii i alergologii, 2014. **31**(2): p. 84-91.
230. Zhuang, H., et al., *CCL2/CCR2 axis induces hepatocellular carcinoma invasion and epithelial-mesenchymal transition in vitro through activation of the Hedgehog pathway*. Oncology reports, 2018. **39**(1): p. 21-30.
231. Soldano, S., et al., *Alternatively Activated (M2) Macrophage Phenotype Is Inducible by Endothelin-1 in Cultured Human Macrophages*. PLoS One, 2016. **11**(11): p. e0166433.
232. Carulli, M.T., et al., *Chemokine receptor CCR2 expression by systemic sclerosis fibroblasts: evidence for autocrine regulation of myofibroblast differentiation*. Arthritis Rheum, 2005. **52**(12): p. 3772-82.
233. Chen, X., et al., *CCL2/CCR2 Regulates the Tumor Microenvironment in HER-2/neu-Driven Mammary Carcinomas in Mice*. PloS one, 2016. **11**(11): p. e0165595-e0165595.
234. Bolitho, P., et al., *Apoptosis induced by the lymphocyte effector molecule perforin*. Current Opinion in Immunology, 2007. **19**(3): p. 339-347.

235. Kitanaka, C. and Y. Kuchino, *Caspase-independent programmed cell death with necrotic morphology*. Cell Death Differ, 1999. **6**(6): p. 508-15.
236. Qi, R. and X.Y. Liu, *New advance in caspase-independent programmed cell death and its potential in cancer therapy*. International journal of biomedical science : IJBS, 2006. **2**(3): p. 211-216.
237. Crist, S.A., D.L. Sprague, and T.L. Ratliff, *Nuclear factor of activated T cells (NFAT) mediates CD154 expression in megakaryocytes*. Blood, 2008. **111**(7): p. 3553-61.
238. Bakos, E., et al., *CCR2 Regulates the Immune Response by Modulating the Interconversion and Function of Effector and Regulatory T Cells*. The Journal of Immunology, 2017. **198**(12): p. 4659-4671.
239. Li, M., et al., *A role for CCL2 in both tumor progression and immunosurveillance*. Oncoimmunology, 2013. **2**(7): p. e25474.
240. Sandhu, S.K., et al., *A first-in-human, first-in-class, phase I study of carlumab (CNTO 888), a human monoclonal antibody against CC-chemokine ligand 2 in patients with solid tumors*. Cancer Chemother Pharmacol, 2013. **71**(4): p. 1041-50.
241. Lipson, E.J., et al., *Antagonists of PD-1 and PD-L1 in Cancer Treatment*. Seminars in Oncology, 2015. **42**(4): p. 587-600.
242. Emens, L.A., *Breast Cancer Immunotherapy: Facts and Hopes*. Clinical Cancer Research, 2018. **24**(3): p. 511.
243. Vonderheide, R.H., et al., *Phase I study of the CD40 agonist antibody CP-870,893 combined with carboplatin and paclitaxel in patients with advanced solid tumors*. Oncoimmunology, 2013. **2**(1): p. e23033.
244. Ruter, J., et al., *Immune modulation with weekly dosing of an agonist CD40 antibody in a phase I study of patients with advanced solid tumors*. Cancer Biol Ther, 2010. **10**(10): p. 983-93.
245. Vonderheide, R.H., et al., *Phase I study of recombinant human CD40 ligand in cancer patients*. J Clin Oncol, 2001. **19**(13): p. 3280-7.
246. Fitzgibbons, P.L., D.E. Henson, and R.V. Hutter, *Benign breast changes and the risk for subsequent breast cancer: an update of the 1985 consensus statement*. Cancer Committee of the College of American Pathologists. Arch Pathol Lab Med, 1998. **122**(12): p. 1053-5.
247. Tozbikian, G., et al., *Atypical Ductal Hyperplasia Bordering on Ductal Carcinoma In Situ*. International journal of surgical pathology, 2017. **25**(2): p. 100-107.
248. Weigelt, B., J.L. Peterse, and L.J. van 't Veer, *Breast cancer metastasis: markers and models*. Nat Rev Cancer, 2005. **5**(8): p. 591-602.
249. Welch, H.G., D.H. Gorski, and P.C. Albertsen, *Trends in Metastatic Breast and Prostate Cancer*. N Engl J Med, 2016. **374**(6): p. 596.
250. Bleyer, A. and H.G. Welch, *Effect of three decades of screening mammography on breast-cancer incidence*. N Engl J Med, 2012. **367**(21): p. 1998-2005.
251. Tai, P., et al., *Survival of patients with metastatic breast cancer: twenty-year data from two SEER registries*. BMC Cancer, 2004. **4**: p. 60.
252. Emens, L.A., M. Kok, and L.S. Ojalvo, *Targeting the programmed cell death-1 pathway in breast and ovarian cancer*. Curr Opin Obstet Gynecol, 2016. **28**(2): p. 142-7.
253. Mittendorf, E.A., et al., *Final report of the phase I/II clinical trial of the E75 (nelipepimut-S) vaccine with booster inoculations to prevent disease recurrence in high-risk breast cancer patients*. Annals of Oncology, 2014. **25**(9): p. 1735-1742.

254. Miles, D., et al., *Phase III multicenter clinical trial of the sialyl-TN (STn)-keyhole limpet hemocyanin (KLH) vaccine for metastatic breast cancer*. *Oncologist*, 2011. **16**(8): p. 1092-100.
255. Tsuyada, A., et al., *CCL2 mediates crosstalk between cancer cells and stromal fibroblasts that regulates breast cancer stem cells*. *Cancer Research*, 2012. **72**(11): p. 2768-2779.
256. Wu, A., et al., *Glioma cancer stem cells induce immunosuppressive macrophages/microglia*. *Neuro Oncol*, 2010. **12**(11): p. 1113-25.

## Appendix

### Overview of cancer and nomenclature

Under normal physiologic conditions, cellular division is regulated tightly to ensure cellular phenotypes are maintained. Cells can increase their functional mass in response to a stimulus by increasing cell number (hyperplasia) or increasing their size (hypertrophy). The regenerative capacity required of immune cells and the epithelial linings of glands and organs require a continuous ability to faithfully replicate. Controlled proliferation allows for an increase in cellular mass that appears and functions normally, and require that upon removal of a stimulus, the tissue involutes back to a normal cellular size and number.

Abnormal cellular growth is considered neoplasia if the division continues independent of the presence of a stimulus, and this abnormal growth of cells is called a neoplasm or tumor. Tumors can be benign or malignant, in which benign tumors are confined to their tumor of origin and cannot spread. A malignant tumor, or cancer, is an abnormal proliferation of cells is capable of invading beyond the margins of its tissue of origin (invasion) and growing in distant organs (metastasis). Benign and malignant describe only the invasive potential of a tumor, and are not indicators of prognosis.

## Normal breast structure and function

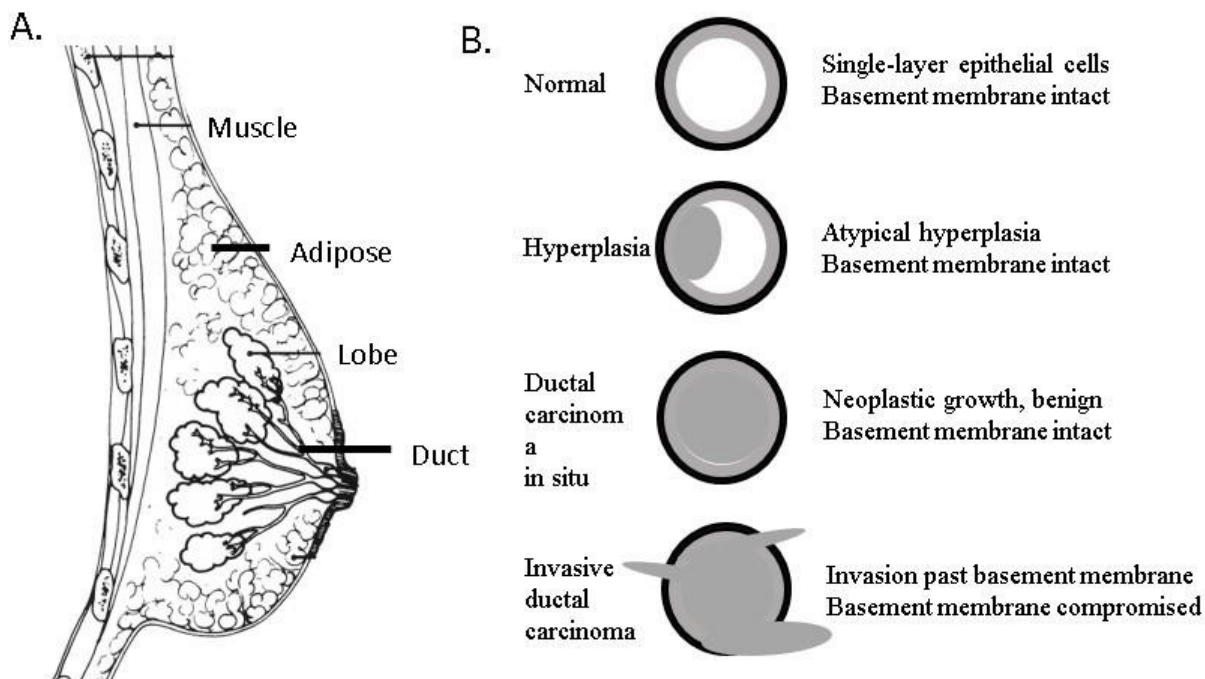


Figure 34- Normal architecture of the breast and pathogenesis of invasive ductal carcinoma.

The human breast is composed of milk-producing-glands, the lumens of which are continuous with tubular structures called ducts that carry the milk to the nipple during lactation (Fig 1A). The lobe is made up of lobules, which are made up of alveoli, which are the most basic milk-producing structure of the human breast. The ducts feed from the alveoli, merging together as they extend to the nipple. Both structures are lined with a single layer of epithelial cells and surrounded by a layer of basement membrane to which they are anchored, as well as a layer of myoepithelial cells that contract to excrete milk upon oxytocin stimulation.

It is these 2 epithelial layers (the luminal epithelium and the ductal epithelium) that most often give rise to breast cancer. Cancer that arises from the luminal epithelium is called luminal carcinoma (carcinoma being a general term for malignant neoplasm arising from epithelium),

and cancer of the ductal epithelium is ductal carcinoma. If a carcinoma has invaded, it is termed invasive; if it has not, it is termed *in situ*.

### Pathogenesis of Breast Cancer

#### **Benign diseases**

There are a number of benign pathologies of the breast that mimic the appearance of breast cancer by gross examination or mammography, but do not increase the risk of cancer. Major benign pathologies of the breast include:

- Mastitis – Inflammation of the breast as a result of acute or chronic infection; acute is often bacterial and secondary to lactation and breast feeding, and chronic can be bacterial, viral, or idiopathic (of unknown origin).
- Mammary duct ectasia – a chronic inflammatory disease that is distinct from mastitis, caused by blocked lactiferous ducts and resulting in dilated ductal spaces and periductal immune cell infiltrates. This disease can mimic carcinoma as irregular masses, but do not increase the risk of ductal carcinoma.
- Fat necrosis – trauma or ischemia (lack of oxygen to a tissue) can result in necrotic adipose cells. Neutrophils and macrophages respond to the site of injury, which over time results in calcification and fibrosis of the necrotic area. This can cause a hard mass that resembles carcinoma.
- Fibrocystic change – The most common breast disorder, a class of breast pathologies that often produce palpable lumps. These disorders are recognized by fibrous proliferation in the breast stroma, formation of cysts (a closed sphere with a simple epithelial lining), and epithelial hyperplasia.

Since these diseases mimic carcinoma, they are often biopsied and examined. Their distinct etiologies, however, are often physical or infectious in nature, rather than genetic, and do not increase the risk of carcinoma development.

### **Initiating a malignancy: hyperplasia**

Within fibrocystic changes, there are several proliferative diseases of the epithelium that increase the risk of carcinoma. These diseases, with their relative risk of developing carcinoma, include:

- Ductal hyperplasia of the usual type (DCUT), where 2 or more epithelia exist in the lining of the duct and may show nuclear atypia. Two-fold higher risk than population.
- Atypical ductal hyperplasia (ADH), where there the ductal epithelium completely involves in the ductal lumen. Four- to five-fold fold higher risk.
- Ductal carcinoma *in situ* (DCIS), where the entire ductal lumen is filled with atypical cells. Eight- to ten-fold increase in risk[246].

Cutoffs for size and fraction of atypical cells are often used to distinguish ADH from DCIS, but this distinction is controversial[247]. The increasing risk of carcinoma that is associated with each disease suggest they represent a spectrum from normal tissue to malignant carcinoma.<sup>2</sup>

DCIS is the most common form of pre-invasive breast cancer in the US, with over 50,000 cases diagnosed every year. Standard treatment for DCIS involves a combination of lumpectomy and radiation therapy [139, 140]. Yet, 10 to 35% of patients experience disease recurrence, often accompanied by invasive ductal carcinoma (IDC) [141, 142], indicating that under-treatment and over-treatment remain significant concerns in patient care. Few approaches

---

<sup>2</sup> Summary of increased risks of fibrocystic and proliferative breast disease summarized in Table 1 from Fitzgibbons, et al. 1998.

exist to evaluate prognosis of DCIS. Compared to IDC, the use of biomarkers in DCIS has not been well studied. Small or low grade lesions may still become invasive [142, 143]. Estrogen receptor (ER), Her2, Ki67, p16 and Cox2 are associated with disease recurrence but not with development of invasive breast cancer [144]. Identifying key mechanisms associated with DCIS progression could lead to better prognostic factors and tailored treatments for patients with DCIS.

### **Malignancy: early growth and invasion**

The most dangerous attribute a cancer cell is their ability to invade. Without invasion, tumors could become massive and compress nearby structures, but they would all be curable by surgical excision. It is for this reason that the definitive characteristic of a malignant cell is invasive potential. In order to move across a 2-dimensional plate or a three-dimensional scaffold, cells must make drastic changes to their shape and morphology by rearranging their cytoskeleton, which is largely composed of stiff actin filaments and microtubules.

### **Metastasis: spreading to distant organs**

Approximately 40,000 women will die from breast cancer in 2018, with over 90% of these deaths caused by metastasis [248]. Metastases can arise from lesions that are undetectable by mammography screening [249, 250]. Tumors are classified based on whether their gene expression matches the epithelium of the differentiated milk duct lumen (luminal), or the undifferentiated stem cells in the basal layer (basal). Basal tumors are often triple-negative, expressing no ER, progesterone receptor (PR), or growth factor receptor (Her2). Targeted therapies for breast cancer antagonize either ER or Her2, leaving chemotherapy as the only

treatment option for ER-/Her2- lesions. TNBC cells most resemble mammary stem cells, which possibly explains their increased tendency to metastasize [111]. Despite recent advances in immunotherapy, which has cured patients with previously untreatable malignant melanoma, trials in breast cancer have shown mixed results[113, 251-254]. Stem cells likely contribute to this resistance because they are lowly immunogenic and often senescent[255, 256]. Thus, targeting the molecular determinants of stem cells could enhance the efficacy of immune therapies. Understanding the molecular processes by which cancer stem cells arise and persist will enhance treatments for patients with incurably disseminated breast cancer.